

Aus der II. Medizinischen Klinik
der Medizinischen Fakultät Mannheim
(Direktor: Prof. Dr. med. Matthias Ebert)

Expression and function of blood receptors ROR α , REVERBA and
BMAL1 in human colorectal cancer

Inauguraldissertation
zur Erlangung des Doctor scientiarum humanarum (Dr. sc. hum.)
der
Medizinischen Fakultät Mannheim
der Ruprecht-Karls-Universität
zu
Heidelberg

vorgelegt von
Wen Wu

aus
Anhui, China
2021

Dekan: Prof. Dr. S. Goerd
Referent: Prof. Dr. M. Ebert

Für meinen Vater

CONTENTS

ABRREVIATIONS.....	1
1 Introduction.....	2
1.1 Colorectal cancer.....	2
1.1.1 <i>Epidemiology of CRC</i>	2
1.1.2 <i>Risk factors of CRC</i>	3
1.1.3 <i>Classification of CRC</i>	3
1.1.4 <i>Management of CRC</i>	4
1.1.5 <i>Role of bevacizumab in targeted therapies</i>	8
1.2 Circadian clock.....	9
1.2.1 <i>The molecular mechanism of circadian clock</i>	9
1.2.2 <i>The circadian nuclear receptors, RORα, REVERBA and BMAL1</i>	12
2 Aims of the thesis.....	16
3 Materials and methods.....	17
3.1 Materials.....	17
3.1.1 <i>Cell lines</i>	17
3.1.2 <i>Tissue samples</i>	18
3.1.3 <i>Reagents</i>	18
3.1.4 <i>Antibodies</i>	19
3.1.5 <i>Oligonucleotide primers</i>	19
3.1.6 <i>Solutions</i>	21
3.2 Methods.....	24
3.2.1 <i>Cell culture</i>	24
3.2.2 <i>Transient Transfection</i>	25
3.2.3 <i>cDNA synthesis</i>	26
3.2.4 <i>Quantitative PCR</i>	27
3.2.5 <i>Agarose gel electrophoresis</i>	28

3.2.6 RNA extraction.....	28
3.2.7 Plasmid construction.....	28
3.2.8 Cell proliferation assay.....	33
3.2.9 Western blot analysis.....	34
3.2.10 Immunohistochemistry.....	35
3.2.11 ELISA assay.....	36
3.2.12 Luciferase assay.....	37
3.2.13 Chromatin immunoprecipitation (ChIP).....	38
3.2.14 Electrophoretic Mobility Shift Assay (EMSA).....	40
3.2.15 Statistics.....	42
4 Results.....	46
4.1 ROR α is downregulated in human colorectal cancer.....	46
4.2 REVERBA is upregulated in human colorectal cancer.....	48
4.3 BMAL1 is downregulated in human colorectal cancer.....	50
4.4 Expression of ROR α , REVERBA and BMAL1 is associated with response or non-response/resistance to anti-angiogenesis treatment in mice.....	52
4.5 Expression level of ROR α , REVERBA and BMAL1 in various normal mouse tissues and in different colorectal cancer cell lines.....	54
4.6 Subcellular localization of ROR α and REVERBA in HEK293T cells.....	56
4.7 Effects of ROR α , REVERBA and BMAL1 on cell proliferation.....	56
4.8 Overexpression of REVERBA in colorectal cancer cells increases transcription of the human VEGF α gene.....	58
4.9 Overexpression of REVERBA increases human VEGF α secretion <i>in vitro</i>	61
4.10 REVERBA enhances the activity of the VEGF α gene promoter.....	63
4.11 REVERBA cooperates with BMAL1 to enhance the promoter activity of VEGF α	67
4.12 REVERBA induces resistance of colorectal cancer cells to anti-angiogenesis therapy with VEGF α -neutralizing antibody bevacizumab.....	70
4.13 Effect of REVERBA and BMAL1 on signaling pathway reporters.....	72
4.14 REVERBA binds directly to the promoter region of human VEGF α using chromatin	

immunoprecipitation assay.....	76
4.15 REVERBA binds directly to the promoter region of human VEGFa using electrophoretic mobility shift assay.....	78
5 Discussion.....	80
5.1 ROR α is associated with the clinicopathological variables concerning tumor progression.....	80
5.2 REVERBA exerts a potential mechanism to positively regulate VEGFA expression.....	82
5.3 BMAL1 is a potential marker of resistance to anti-angiogenesis treatment in CRC.....	83
6 Conclusion.....	86
7 References.....	87
8 Curriculum Vitae.....	99
9 Acknowledgements.....	101

ABBREVIATIONS

AJCC American Joint Committee on Cancer

ASRi Age-standardized incidence rate

ASRm Age-standardized mortality rate

CO Carbon monoxide

CRC Colorectal cancer

DBD DNA-binding domain

EGFR Epidermal growth factor receptor

LBD Ligand-binding domain

NO Nitric oxide

REVERBA Nuclear receptor subfamily 1, group D, member 1

ROR α Retinoic Acid Receptor-related Orphan Receptor α

RORE ROR response element

RORs Receptor-related orphan receptors

SCN Suprachiasmatic nucleus

UICC Union for International Cancer Control

VEGF Vascular endothelial growth factor

VEGF α Vascular endothelial growth factor A

WHO World Health Organization

1 Introduction

1.1 Colorectal cancer

1.1.1 Epidemiology of CRC

Colorectal cancer (CRC) is the most common gastrointestinal cancer in the world. According to the World Health Organization GLOBOCAN database, more than 1.3 million new cases were diagnosed and approximately 700,000 people died of CRC all over the world (Ferlay et al., 2010; Torre et al., 2015). In China, CRC is the fifth (8.6% of new cases) and fourth (9.0% of new cases) commonly diagnosed cancer in men and women, respectively, and CRC is the fifth (6.1% and 8.0% of estimated deaths) cause of death in both men and women (Chen et al., 2016). CRC is the third (8.6% of all new cases) most frequently diagnosed cancer and also the third (8.5% of estimated deaths) common cancer cause of death in the United States (Siegel et al., 2018).

The incidence of CRC is low at ages under 50 years, but dramatically increases with age. The median age at diagnosis for colorectal cancer is 66 years for men and 70 years for women in developed countries (Miller et al., 2016). Patients with colon cancer tend to be older at diagnosis than those with rectal cancer (median age, 70 vs 63 years, respectively) (Miller et al., 2016). Most patients with CRC are older than 50 years of age, for example, 75% of patients with rectal cancer and 80% of patients with colon cancer being older than 60 years of age at the time of diagnosis (Kuipers et al., 2015). The age-standardized incidence rate (ASR_i) of CRC is higher in males (20.6 per 100,000 individuals) than in females (14.3 per 100,000 individuals) (Kuipers et al., 2015).

In 2013, about 771,000 patients died as a result of CRC, making the disease the fourth common cause of cancer-related death after lung, liver and stomach cancer in the world (Mortality and Causes of Death, 2015). The age-standardized mortality rate

(ASRm) is almost 2-fold lower in less-developed regions (ASRm: 6.6 per 100,000) than in more-developed regions (ASRm: 11.6 per 100,000). Western Africa showed the lowest age-standardized mortality (ASRm: 3.5 and 3.0 per 100,000 men and women, respectively) in the world and Central and Eastern Europe exhibited the highest mortality (ASRm: 20.3 and 11.7 per 100,000 men and women, respectively) in the world, in both men and women (Kuipers et al., 2015). The mortality due to CRC has increased by 57% between 1990 and 2013 worldwide. Since the 1980s, in some high-income countries and countries in Europe and Asia, the mortality has been decreasing. This decrease probably be attributable to improved early detection and treatment, for example, the introduction of colonoscopy, which has significantly improved the detection and treatment of early lesions (Brenner et al., 2014).

1.1.2 Risk factors of CRC

There is no single risk factor accounting for most CRC cases (Table 1.1). The majority of CRC is sporadic and attributed to increasing age and male sex (Brenner et al., 2014). Despite older age and male sex, some following risk factors have been found: inflammatory bowel disease (Jess et al., 2012), family history of CRC (Taylor et al., 2010), obesity (Ma et al., 2013), diabetes (De Bruijn et al., 2013; Luo et al., 2012), tobacco (Liang et al., 2009), high consumption of alcohol (Fedirko et al., 2011), and high consumption of red and processed meat (Chan et al., 2011). About 2% to 5% of all CRC arise in the setting of well-defined inherited syndromes, including two most common forms of hereditary CRC (Lynch syndrome, familial adenomatous polyposis (FAP)) (Jasperson et al. 2010).

1.1.3 Classification of CRC

As shown in Table 1.2 and Table 1.3, according to the TNM staging system from the World Health Organization (WHO) (Table 1.2) , the Union for International Cancer Control (UICC) (Table 1.3) and the American Joint Committee on Cancer (AJCC), the

staging of CRC is routinely done, which provides the basis for therapeutic decisions and valuable prognostic information. But the response and outcome of therapy cannot be predicted. This is a shortcoming for patients with UICC stage II and stage III CRC in particular. The novel genetic molecular classification of CRC by CMS (consensus molecular subtypes) was reported by Guinney et al. (Guinney et al., 2015). It shows marked interconnectivity between 6 independent classification systems coalescing into 4 CMS with distinguishing features: CMS1 (MSI Immune, 14%), CMS2 (Canonical, 37%), CMS3 (Metabolic, 13%), and CMS4 (Mesenchymal, 23%). Approximately 13% of CRC show mixed features.

1.1.4 Management of CRC

Treatments used for CRC include surgery, chemotherapy, targeted therapy, and radiation therapy. For patients with non-metastasized CRC, complete surgical resection is the preferred treatment. Open laparotomy and laparoscopic resection are options available. Besides combined chemotherapy regimens, targeted drugs are used for metastatic CRC treatment. There are three main groups of targeted drugs: monoclonal antibodies against vascular endothelial growth factor A (VEGF_A) (bevacizumab), monoclonal antibodies against epidermal growth factor receptor (EGFR) (cetuximab), and small-molecule-based multi-kinase inhibitors (regorafenib) and fusion proteins that target multiple proangiogenic growth factors (afibercept) (Kuipers et al., 2015). In randomised clinical studies, addition of bevacizumab to standard chemotherapy regimens improved outcomes in bevacizumab-naive patients with metastatic CRC in the first-line and second-line settings (Hurwitz et al., 2004; Saltz, L.B., 2008).

Table 1.1 Risk and preventive factors of CRC

	Risk
Sociodemographic factors	
Older age	↑↑↑
Male sex	↑↑
Medical factors	
Family history	↑↑
Inflammatory bowel disease	↑↑
Diabetes	↑
<i>Helicobacter pylori</i> infection	(↑)
Other infections	(↑)
Large bowel endoscopy	↓↓
Hormone replacement therapy	↓
Aspirin	↓
Statins	(↓)
Lifestyle factors	
Smoking	↑
Excessive alcohol consumption	↑
Obesity	↑
Physical activity	↓
Diet factors	
High consumption of red and processed meat	↑
Fruit and vegetables	(↓)
Cereal fibre and whole grain	(↓)
Fish	(↓)
Dairy products	(↓)

↑↑↑ = very strong risk increase. ↑↑ = strong risk increase. ↑ = moderate risk increase. ↓↓ = strong risk reduction. Parentheses show probable but not fully established associations.

Table 1.2 Classification of CRC according to local invasion depth (T stage), lymph node involvement (N stage), and presence of distant metastases (M stage)

T stage	
Tx	No information about local tumor infiltration available
Tis	Tumor restricted to mucosa, no infiltration of lamina muscularis mucosae
T1	Infiltration through lamina muscularis mucosae into submucosa, no infiltration of lamina muscularis propria
T2	Infiltration into, but not beyond, lamina muscularis propria
T3	Infiltration into subserosa or non-peritonealised pericolic or perirectal tissue, or both; no infiltration of serosa or neighbouring organs
T4a	Infiltration of the serosa
T4b	Infiltration of neighbouring tissues or organs
N stage	
Nx	No information about lymph node involvement available
N0	No lymph node involvement
N1a	Cancer cells detectable in 1 regional lymph node
N1b	Cancer cells detectable in 2–3 regional lymph nodes
N1c	Tumor satellites in subserosa or pericolic perirectal fat tissue, regional lymph nodes not involved
N2a	Cancer cells detectable in 4–6 regional lymph nodes
N2b	Cancer cells detectable in 7 or greater regional lymph nodes
M stage	
Mx	No information about distant metastases available
M0	No distant metastases detectable
M1a	Metastasis to 1 distant organ or distant lymph nodes
M1b	Metastasis to more than 1 distant organ or set of distant lymph nodes or peritoneal metastasis

Table 1.3 Overall UICC stage classification of CRC

	T	N	M
Stage 0	Tis	N0	M0
Stage I	T1/T2	N0	M0
Stage II	T3/T4	N0	M0
IIA	T3	N0	M0
IIB	T4a	N0	M0
IIC	T4b	N0	M0
Stage III	Any	N+	M0
IIIA	T1–T2	N1	M0
	T1	N2a	M0
IIIB	T3–T4a	N1	M0
	T2–T3	N2a	M0
	T1–T2	N2b	M0
IIIC	T4a	N2a	M0
	T3–T4a	N2b	M0
	T4b	N1–N2	M0
Stage IV	Any	Any	M+
IVA	Any	Any	M1a
IVB	Any	Any	M1b

1.1.5 Role of bevacizumab in targeted therapies

Angiogenesis plays an important role in the growth and development of tumors (Risau, 1997), including CRC. The main pro-angiogenic factor is vascular endothelial growth factor (VEGF), and VEGF is a potent angiogenic cytokine that induces mitosis and also regulates the permeability of endothelial cells (Ranieri et al., 2006). Overexpression of VEGF in tumor tissue has been found in solid malignancies and is associated with tumor progression and poor prognosis in CRC (Lee et al., 2000; Takahashi et al., 1995). The VEGF pathway is a key regulator of angiogenesis, which has led to efforts to explore its potential for target therapy in cancer. Therefore, most of the anti-angiogenesis treatment strategies focus on inhibition of the VEGF pathway (Hicklin and Ellis, 2005).

Bevacizumab, sold under the trade name Avastin, is a recombinant humanized monoclonal antibody. It was developed against VEGF_A by binding to soluble VEGF_A, thereby preventing VEGF receptor binding, inhibiting endothelial cell proliferation and new blood vessel formation (Ranieri et al., 2006). In the first line setting, Avastin can be combined with an irinotecan-based (Hurwitz and Kabbinavar, 2005), an oxaliplatin-based (Saltz et al., 2008) chemotherapy doublet, or chemotherapy triplet (Loupakis et al., 2014). However, Avastin is only specific to human VEGF and does not bind mouse VEGF. Thus, its use of researches in animal models is limited. B20, with an unrelated sequence in its complement-determining regions, is able to bind both human and mouse VEGF (Liang et al., 2005). This property makes B20 a useful research tool as it does not share the shortcomings of the Avastin antibody, which is unable to block the function of murine VEGF (Liang et al., 2005).

Clinical studies have demonstrated that the use of bevacizumab with or without other chemotherapy drugs can decrease tumor growth and increase median survival time (Hurwitz et al., 2004; Kabbinavar et al., 2003). The median duration of progression free survival was 10.6 months in the group given irinotecan, bolus fluorouracil, and leucovorin (IFL) plus bevacizumab, as compared with 6.2 months in the group given

IFL plus placebo (Hurwitz et al., 2004). But therapy failure in patients with advanced CRC is a major obstacle to curative treatment and survival. The efficacy of antibodies which inhibit angiogenesis is often limited by yet unknown mechanisms of unresponsiveness or resistance in CRC patients. Thus, novel markers or targets are needed.

1.2 Circadian clock

1.2.1 The molecular mechanism of circadian clock

The term “circadian” is derived from a Latin word “circa diem”, which means “about a day”. The circadian clock or circadian rhythms in mammals is driven by an auto-regulatory transcriptional feedback loop mechanism that takes about a day time, 24 hours. The suprachiasmatic nucleus (SCN) serves as a circadian master clock, or an endogenous biological oscillator, which controls biochemical, physiological and behavioral rhythms, entrained by light and other external signals.

The first circadian gene, *Per*, was found in fruit flies in the 1980s (Bargiello et al., 1984; Reddy et al., 1984). Since then, the transcriptional network that drives circadian rhythms has been identified (Lowrey and Takahashi, 2004, 2011; Reppert and Weaver, 2002). The core mammalian clock is composed of many transcription factors (Figure 1.1). A ROR response element within the *BMAL1* promoter is responsive to both ROR and *Reverb*; ROR activates the transcription of *BMAL1*, whereas *Reverb* suppresses its transcription. *Clock* and *BMAL1* activate the transcription of *Per* and *Cry* genes via E-box sequences within their promoters. *Per* and *Cry* proteins form dimers and directly interact with the *Clock*–*BMAL1* heterodimers, thus suppressing their activity. This feedback loop follows a 24-hour rhythm where peak expression of the *Clock*–*BMAL1* complex is 12 hours out of phase with peak *Per* and *Cry* expression. The expression of ROR and *Reverb* also oscillates in a circadian manner, reinforcing the core circadian oscillator. It has been reported that disturbed circadian clock gene

expression and disruption of circadian rhythms correlate with tumor development and tumor progression (Filipski and Levi, 2009; Filipski et al., 2009; Sahar and Sassone-Corsi, 2009).

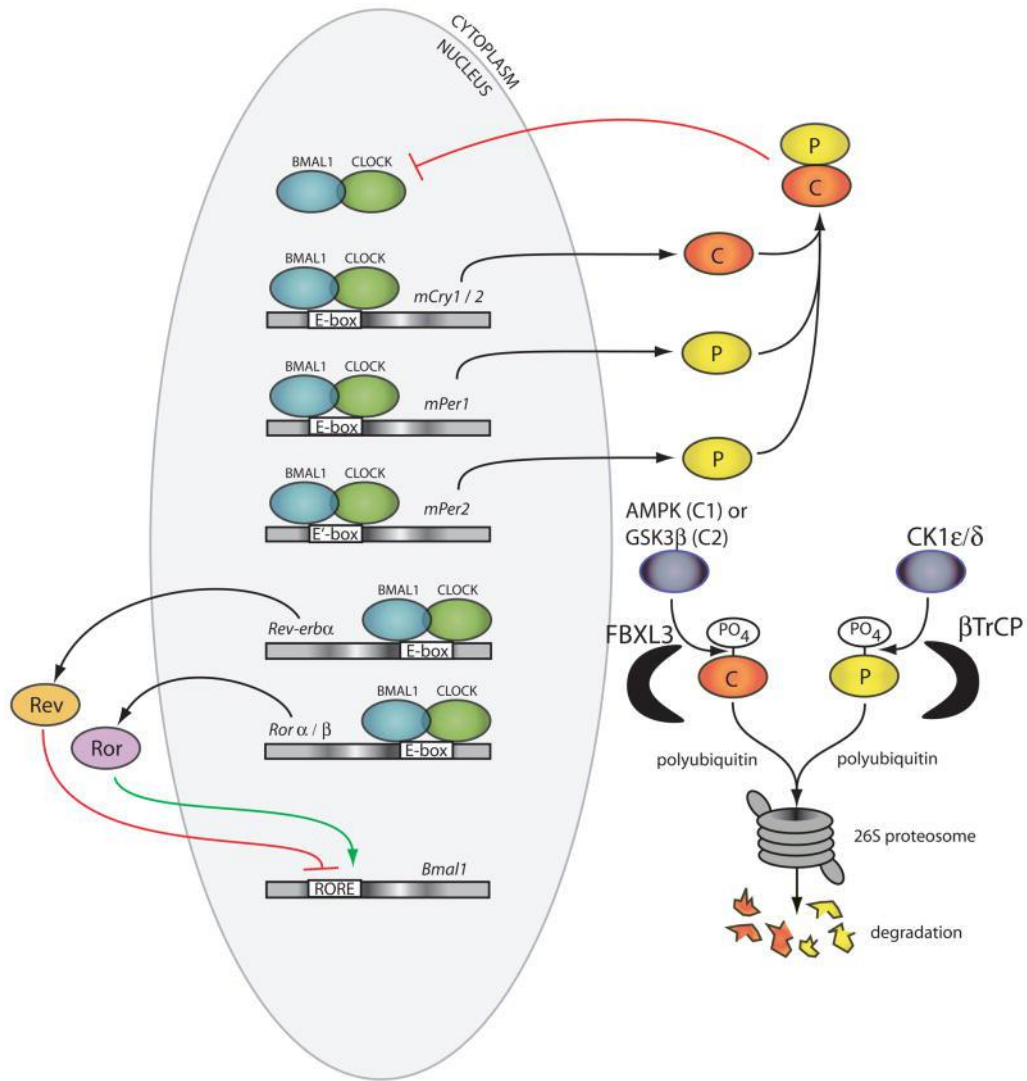


Figure 1.1 Core mammalian circadian clock gene feedback loops.

1.2.2 The circadian nuclear receptors, ROR α , REVERBA and BMAL1

The circadian nuclear receptor, ROR α (Figure 1.2), (Retinoic Acid Receptor-related Orphan Receptor α) is a member of the ROR steroid hormone receptor superfamily (Jetten, 2004). It has been reported that ROR α plays an important role in the regulation of many physiological processes including differentiation, metabolism, inflammation, transformation, and circadian clock function (Lee et al., 2010; Dzhagalov et al., 2004; Sato et al., 2004; Lau et al., 2004). However, the molecular mechanisms of ROR α in physiological processes *in vivo* remain unknown.

The circadian nuclear receptor, REVERBA (Figure 1.2), acquired its name from the genomic organization of NR1D1 (nuclear receptor subfamily 1, group D, member 1), which encodes REVERBA. REVERBA is encoded by the opposite DNA strand of the ERBA oncogene (Lazar et al., 1989; Miyajima et al., 1989; Miyajima et al., 1988), so its name is derived from reverse strand of ERBA. REVERBA can be inhibited by heme from degraded red blood cells. The functions of some heme-binding proteins are further regulated by nitric oxide (NO), and carbon monoxide (CO). REVERBA is responsive to NO and CO, which repress REVERBA-mediated transcription (Pardee et al., 2009), and is sensitive to the tissue's redox status (Gupta and Ragsdale, 2011; Marvin et al., 2009).

The receptors are ligand-regulated transcription factors which act as activators (ROR α) and repressors (REVERBA) of genes regulating circadian rhythm, metabolism, inflammation and development including angiogenesis (Delezie and Challet, 2011). REVERBA and ROR α have a conserved modular domain structure (Figure 1.2). The binding of ligands to the ligand-binding domain causes a conformational change in this domain, which mediates a cascade of downstream events. Both classes of nuclear receptors bind to a similar DNA response element, named "retinoic acid receptor-related orphan receptor-binding element" or "ROR response element" (RORE) (Forman et al., 1994), thus both nuclear receptors are often co-expressed in tissues (Smith and Muscat, 2006). Because REVERBA

represses transcription, but ROR α activates transcription, the antagonistic activities of ROR α and REVERBA are important for the regulation of target genes containing the DNA response elements that are responsive to REVERBA and ROR α (Figure 1.3) (Kojetin and Burris, 2014). It was reported that ROREs are located in the promoter regions of cell cycle-related genes, such as cyclin A, cyclin-dependent kinase (CDK) inhibitor p21WAF1/CIP1 (Schrader et al., 1996), and N-myc (Lee et al., 1984). These data suggest that ROR α and REVERBA might be involved in the regulation of cell growth and tumor progression.

BMAL1 (also known as Arntl or MOP3) is the core component of the circadian clock system in mammals and encodes a transcription factor with a basic helix-loop-helix and two PAS domains (Ikeda et al., 1997). It has been reported that BMAL1 is correlated to aging, immune disorders and cancers (Khapre et al., 2011; Sun et al., 2006; Taniguchi et al., 2009). Evidence also suggests that BMAL1 plays an important role in angiogenesis, and BMAL1 can directly binds to and activates VEGF promoter via E-box (Jensen et al., 2012).

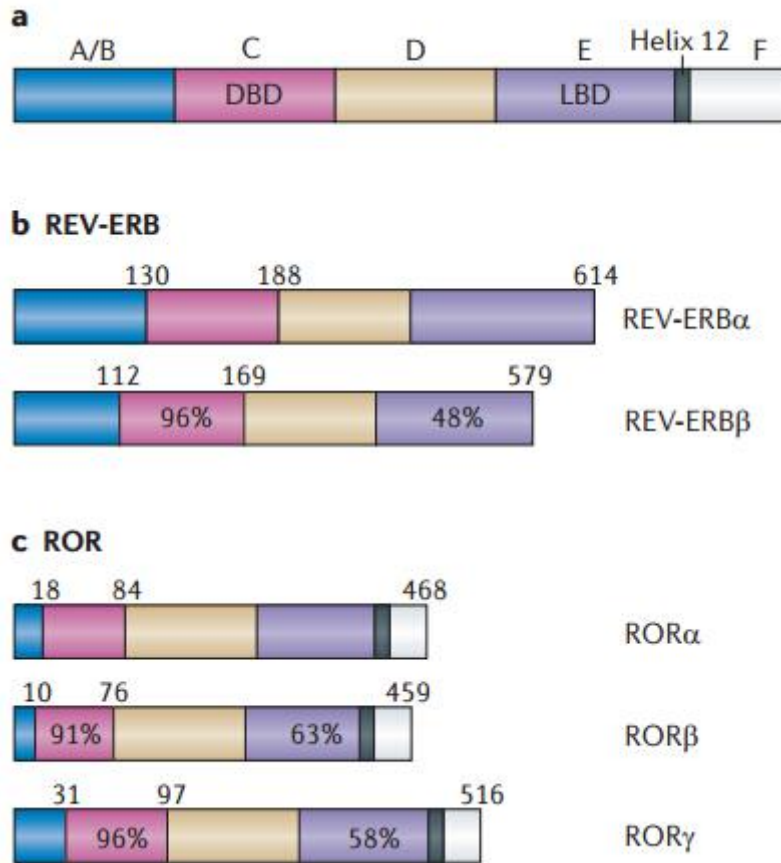


Figure 1.2 Structure of RORs and Reverbs.

(A) General structure of members of the nuclear receptor superfamily. (B) Structure of Reverbs. (C) Structure of retinoic acid receptor-related orphan receptors (RORs). A/B, C, D, E and F refer to defined regions in nuclear receptor domain structure. DBD, DNA-binding domain; LBD, ligand-binding domain. Numbers above each receptor indicate the amino acid position. Percentages represent amino acid identity within a particular domain relative to either REVERBA or ROR α .

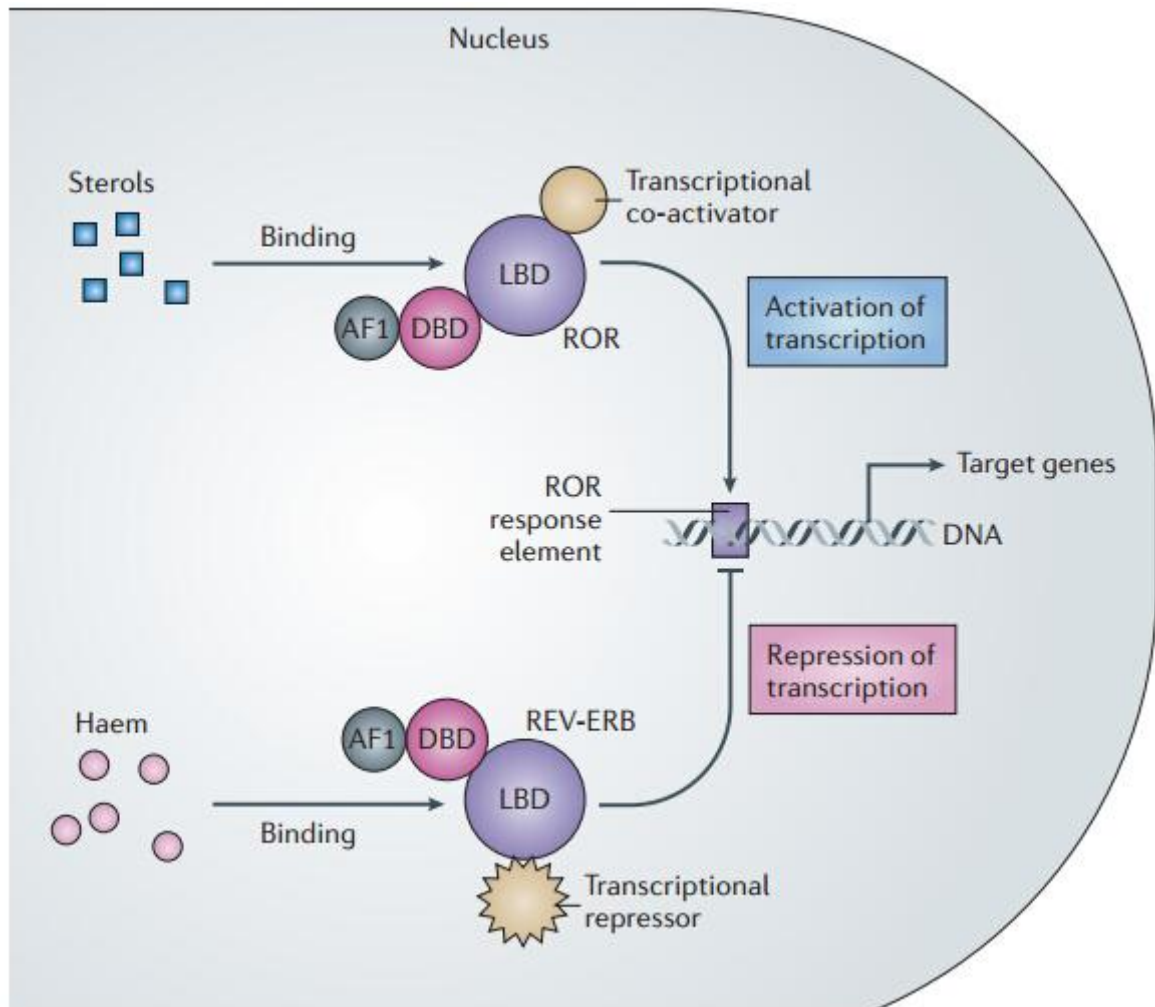


Figure 1.3 Molecular mechanism of action of RORs and Reverbs.

RORs and Reverbs are involved in transcriptional regulation and are regulated by ligands. Sterols, such as cholesterol, cholesterol sulphate and oxysterols, function as ligand for RORs, whereas heme is a ligand for Reverbs. Both classes of nuclear receptors bind to a DNA response element, ROR response element (RORE). ROR activates transcription, whereas Reverb represses transcription. AF1, activation function 1; DBD, DNA-binding domain; LBD, ligand-binding domain.

2 Aims of the thesis

The overall aim of the thesis was therefore the analysis of the expression and function of these nuclear receptors and circadian transcription factors (ROR α , REVERBA, and BMAL1) in human CRC cells and tissues. Expression and function of the transcriptional activator ROR α and its antagonist REVERBA and their downstream target BMAL1 were explored in human CRC cell lines and correlated to anti-angiogenic therapy in murine and human CRC.

The main objective of the study was to elaborate nuclear blood receptors as potential future biomarkers and/or druggable targets which may improve the response to anti-angiogenic therapy in human CRC.

3 Materials and methods

3.1 Materials

3.1.1 Cell lines

Table 3.1 and Table 3.2 show a brief overview of different cell lines used in the study.

Table 3.1 Cell lines used in the study

Cell Line	Species	Morphology	Source
HEK-293T	Human	Embryonic kidney	ATCC® CRL-3216™
SW480	Human	Epithelial cells	ATCC® CCL-228™
HCT116	Human	Epithelial cells	ATCC® CCL-247™
Caco2	Human	Epithelial cells	ATCC® HTB-37™
HT29	Human	Epithelial cells	ATCC® HTB-38™
NIH3T3	Mouse	Fibroblast cells	ATCC® CRL-1658™

Table 3.2 General information of cell lines used in the study

Cell Line	Patient Age	Patient Gender	Tissue	Disease
HEK-293T	Fetus	-	Embryonic kidney	-
SW480	50y	Male	Colon	Dukes' type B, colorectal adenocarcinoma
HCT116	Adult	Male	Colon	Colorectal carcinoma
Caco2	72y	Male	Colon	Well differentiated adenocarcinoma
HT29	44y	Female	Colon	Colorectal adenocarcinoma
NIH3T3	Embryo	-	Embryo	-

3.1.2 Tissue samples

Tissue microarrays were from Biomax US, Inc (Derwood, Maryland, USA). Each array contained 40 cases of colon tumor and 8 normal colonic tissues from autopsy as control. A total of 48 matched cases were used for IHC analysis. Clinical and pathological data of individual cancer samples were provided by the array manufacturer (Biomax).

3.1.3 Reagents

Table 3.3 shows reagents used the thesis and their manufacturer.

Table 3.3 Reagents and Manufacturer

Reagent	Manufacturer
Acrylamide(30%)	Merck KGaA, Germany
Agarose	Bio-Budget GmbH, Germany
DMEM	GIBCO, Germany
DMSO	Sigma-Aldrich GmbH, Germany
Ethanol	Merck KGaA, Germany
Ethidiumbromid	Sigma-Aldrich GmbH, Germany
Fetal bovine serum	Thermo Scientific, UK
Isopropanol	Merck KGaA, Germany
Methanol	Merck KGaA, Germany
Na ₃ VO ₄	Sigma, Germany
Newborn calf serum	Thermo Scientific, New Zealand
Non-fat dry milk powder	Carl Roth GmbH, Germany
Protease Inhibitor Cocktail Tablets	Roche Diagnostics GmbH, Germany
SDS	Carl Roth GmbH, Germany
TEMED	Sigma-Aldrich GmbH, Germany
Trypsin(0.05%, 0.25%)	Invitrogen, CA
Tween-20	Carl Roth GmbH, Germany

3.1.4 Antibodies

Table 3.4 shows antibodies used in the thesis and their manufacturer

Table 3.4 Antibodies and their Manufacturer

Antibody	Manufacturer
ROR α (sc-28612) for IHC and WB	Santa Cruz, USA
ROR α (638802) for IF	Biologend, CA
REVERBA (LS-B4487) for IHC	Life Span, USA
REVERBA (PA5-29865) for WB, CHIP and EMSA	ThermoScientific, Germany
BMAL1 (NBP2-02544) for IHC (TMA)	Novus, USA
BMAL1 (NB100-2288) for IHC (mouse)	Novus, USA
BMAL1 (H-170) for WB	Santa Cruz, USA
VEGF α (sc-152)	Santa Cruz, USA
Ki-67 (NB600-1252)	Novus, USA
β -actin (sc-69879)	Santa Cruz, USA

3.1.5 Oligonucleotide primers

As shown in Table 3.5, all human (hu-) and mouse (m-) oligonucleotide primers have been purchased from Eurofins MWG synthesis GmbH (Ebersberg, Germany).

Table 3.5 Sequence of human and mouse oligonucleotide primers

Primers	Sequence 5'-3'
huB2M Forward	TGCTGTCTCCCCACCTCTAAGT
huB2M Reverse	TCTCTGCTCCCCACCTCTAAGT
huROR α Forward	GACGCCACCTACAACATCT
huROR α Reverse	TCTGGGGAAGGCTGTATGTC
mROR α Forward	GAACACCTTGCCCAGAACAT

mROR α Reverse	AGCTGCCACATCACCTCTCT
huREVERBA Forward	CTGGGAGGATTTCTCCATGA
huREVERBA Reverse	TTCACGTTGAACAACGAAGC
mREVERBA Forward	ATGCCCATGACAAGTTAGGC
mREVERBA Reverse	GCCAAAAGGTTGTTGTCGTT
huBMAL1 Forward	GTAACCTCAGCTGCCTCGTC
huBMAL1 Reverse	TAGCTGTTGCCCTCTGGTCT
mBMAL1 Forward	CGAAGACAATGAGCCAGACA
mBMAL1 Reverse	AAATAGCTGTGCGCCCTCTGA
huVEGFa-1 Forward	AGGCCAGCACATAGGAGAGA
huVEGFa-1 Reverse	TTTCTTGCGCTTTCGTTTTT
huVEGFa-2 Forward	TGCAGATTATGCGGATCAAACC
huVEGFa-2 Reverse	TGCATTCACATTTGTTGTGCTGTA
huVEGFa Eform Forward	CCCACTGAGGAGTCCAACAT
huVEGFa Eform Reverse	AAATGCTTTCTCCGCTCTGA
huVEGFa All Forward	AGGCCAGCACATAGGAGAGA
huVEGFa All Reverse	TTTCTTGCGCTTTCGTTTTT
huVEGFR2 Forward	AGCGATGGCCTCTTCTGTAA
huVEGFR2 Reverse	ACACGACTCCATGTTGGTCA
5XhohVEGFAp2kb	ATCTCGAGGGAGGAAAGTTAGTGGCTTCCC
3HindhVEGFAp2kb	ATAAGCTTGCCCTCCGCGATCCTCCCCGCTAC
ROREv-700 ChIP Forward	GTCTGCAGGCCAGATGAGGGC
ROREv-700 ChIP Reverse	CTAGTGACTGCCGTCTGCACAC
ROREv-1500 ChIP Forward	CTGCATTCCCATTCTCAGTCCATG
ROREv-1500 ChIP Reverse	TCTCCACATCTTCCCTAAGTGCTC
Bio-RORE-700 Forward	TGTAGCTGTTTGGGAGGTCAGAAATAGGGGGTC
Bio-RORE-700 Reverse	GACCCCCTATTTCTGACCTCCCAAACAGCTACA
Bio-MutRORE-700 Forward	TGTAGCTGGGGAAATTTCCCGAAATAGGGGGTC
Bio-MutRORE-700 Reverse	GACCCCCTATTTCTGGGAAATTTCCCCAGCTACA

Comp-RORE-700 Forward	TGTAGCTGTTTGGGAGGTCAGAAATAGGGGGTC
Comp-RORE-700 Reverse	GACCCCCTATTTCTGACCTCCCAAACAGCTACA

3.1.6 Solutions

3.1.6.1 Solutions for SDS-PAGE

3.1.6.1.1 SDS lysis buffer (50 mM Tris HCl, 2% SDS, pH7.4)

0.1M Na₃VO₄

0.1M DTT

1/4 Protease Inhibitor Cocktail Tablets

3.1.6.1.2 Running buffer

SDS 10ml (10%)

dH₂O 890ml

10X stock buffer 100ml (288g Glycine, 60g Trizma base in 2L dH₂O)

3.1.6.1.3 Transfer buffer

Methanol 200ml

dH₂O 700ml

10X stock buffer 100ml (288g Glycine, 60g Trizma base in 2L dH₂O)

3.1.6.1.4 Blocking buffer

5% Non-fat dry milk powder in TBS-Tween(0.1%)

3.1.6.1.5 Separating gel

dH₂O 2.59ml
30% Acrylamide 3.5ml
1.5M Tris-HCl (pH8.8) 2.1ml
10% SDS 83µl
10%APS 42µl
TEMED 2.8µl
Total volume 8.3ml

3.1.6.1.6 Stacking Gel

dH₂O 1.53ml
30% Acrylamide 333µl
0.5M Tris-HCl (pH6.8) 625µl
10% SDS 25µl
10%APS 12.5µl
TEMED 2.5µl
Total volume 2.5ml

3.1.6.2 Solutions for ChIP

3.1.6.2.1 Protein A Agarose/Salmon Sperm DNA

One vial containing 1.5ml packed beads with 600µg sonicated salmon sperm DNA, 1.5mg BSA and approximately 4.5mg recombinant Protein A. Provided as a 50% gel slurry for a final volume of 3ml per vial. Suspended in TE buffer, pH 8.0, containing 0.05% sodium azide. Liquid suspension.

3.1.6.2.2 ChIP Dilution Buffer

Two vials, each containing 24ml of 0.01% SDS, 1.1% Triton X-100, 1.2mM EDTA, 16.7mM Tris-HCl, pH 8.1, 167mM NaCl.

3.1.6.2.3 Low Salt Immune Complex Wash Buffer

One vial containing 24ml of 0.1% SDS, 1% Triton X-100, 2mM EDTA, 20mM Tris-HCl, pH 8.1, 150mM NaCl.

3.1.6.2.4 High Salt Immune Complex Wash Buffer

One vial containing 24ml of 0.1% SDS, 1% Triton X-100, 2mM EDTA, 20mM Tris-HCl, pH 8.1, 500mM NaCl.

3.1.6.2.5 LiCl Immune Complex Wash Buffer

One vial containing 24ml of 0.25M LiCl, 1% IGEPAL-CA630, 1% deoxycholic acid (sodium salt), 1mM EDTA, 10mM Tris, pH 8.1.

3.1.6.2.6 TE Buffer

Two vials, each containing 24ml of 10mM Tris-HCl, 1mM EDTA, pH 8.0.

3.1.6.2.7 0.5M EDTA

One vial containing 250µl of 0.5M EDTA, pH 8.0.

3.1.6.2.8 5M NaCl

One vial containing 500µl of 5M NaCl.

3.1.6.2.9 1M Tris-HCl, pH 6.5

One vial containing 500µl of 1M Tris-HCl, pH 6.5.

3.1.6.2.10 SDS Lysis Buffer

One vial containing 10ml of 1% SDS, 10mM EDTA, 50mM Tris, pH 8.1.

Elution buffer

3.1.6.2.11 1% SDS, 0.1M NaHCO₃.

3.2 Methods

3.2.1 Cell culture

The NIH3T3 cell line was routinely grown in Dulbecco's Modified Eagle's Medium (DMEM) with heat-inactivated 10%(v/v) bovine calf serum, 1%(v/v) Glutamine and 1%(v/v) penicillin streptomycin. All the other cell lines such as HEK-293, SW480, HCT116, Caco-2 and HT29 were maintained in DMEM medium containing 10%(v/v) heat-inactivated fetal bovine serum (FBS), 1%(v/v) Glutamine and 1%(v/v) penicillin. All the cell lines were incubated at 37°C in a humidified incubator containing 5% CO₂. Confluent cells were washed with sterile PBS, split using Trypsin-EDTA 0.25% and seeded into new T75 flasks containing fresh medium. Normally, different cell lines were split with differing frequency dependent on cell growth characteristics. For example, NIH3T3 cells were split at 1:4 ratio bi-weekly. SW480 and Caco2 cells were

split at 1:10 ratio bi-weekly. HEK293T, HCT116 and HT29 cells were split at 1:25 ratio bi-weekly.

3.2.2 Transient Transfection

3.2.2.1 Single plasmid transient transfection

pTarget vector (Promega) was used as empty vector, and Figure 3.1 shows the general structure of pTarget vector. Full length cDNAs of human ROR α and REVERBA were cloned into pTarget mammalian expression vector and used for transient transfection. BMAL1-pCMV-SPORT6 vector were purchased from GE Dharmacon, and Figure 3.2 shows the general structure of pCMV-SPORT6 vector. ROR α -pTarget vector, REVERBA-pTarget vector, BMAL1-pCMV-SPORT6 vector, and empty pTarget vector were transfected into cell lines using TurboFect (Thermo Scientific). Cultured cells were seeded into a 6-well plate at a final cell number of 5.0×10^5 the day before transfection. Plasmids were diluted into DMEM (-/-) and mixed, followed by adding TurboFect and mixed immediately, then incubated for 20min before transfer to the cells. The cells were then incubated overnight. The exact volume of each reagent was prepared according to the instruction provided by the manufacturer.

3.2.2.2 Double plasmids transient co-transfection

Table 3.6 and Table 3.7 show dosage of each plasmid used in double plasmids transient co-transfection

Table 3.6 BMAL1+ROR α co-transfection

	BMAL1(μg)	RORα(μg)	pVEGFα-luc(μg)	pT(μg)	Total(μg)
Control	0	0	2	3	5
Group 1	1	0	2	2	5
Group 2	1	0.5	2	1.5	5

Group 3	1	1	2	1	5
Group 4	1	2	2	0	5
Group 5	0	1	2	2	5
Group 6	0.5	1	2	1.5	5
Group 7	1	1	2	1	5
Group 8	2	1	2	0	5

Table 3.7 BMAL1+REVERBA co-transfection

	BMAL1(μl)	REVERBA(μl)	pVEGFα-luc(μl)	pT(μl)	Total(μl)
Control	0	0	2	3	5
Group 1	1	0	2	2	5
Group 2	1	0.5	2	1.5	5
Group 3	1	1	2	1	5
Group 4	1	2	2	0	5
Group 5	0	1	2	2	5
Group 6	0.5	1	2	1.5	5
Group 7	1	1	2	1	5
Group 8	2	1	2	0	5

3.2.3 cDNA synthesis

For cDNA synthesis, the Verso cDNA Synthesis Kit (Thermo Scientific) was used. It supplies all the reagents to generate high yields of full-length cDNA from all RNA types. Reaction mix preparation is listed:

Reagent	Volume(μl)	Final Concentration
5X cDNA synthesis buffer	4	1X
dNTP Mix	2	500 μ M each
Anchored Oligo dT primers	1	
RT Enhancer	0.5	

Verso Enzyme Mix	0.5	
Template (RNA)	12	1µg
Total volume	20	

Reverse transcription cycling program is as follow:

	Temp(°C)	Time	Number of cycles
cDNA synthesis	42°C	30min	1 cycle
Inactivation	95°C	2min	1 cycle

3.2.4 Quantitative PCR

Quantitative PCR was performed on the StepOnePlus™ Real-Time PCR System (Thermo Scientific) using the Power SYBR™ Green PCR Master Mix (Thermo Scientific). For normal quantification, cDNA was diluted 1:2. PCR protocol and mastermix were identical in both experiments and are listed in Tables 3.8 and 3.9.

Table 3.8 Standard protocol for the qPCR master mix of one 10µl reaction

qPCR Mastermix	
Reagent	Volume(µl)
2X Master Mix	5
Forward primer	1
Reverse primer	1
H ₂ O	2
cDNA	1

Table 3.9 Standard protocol used for qPCR-reactions at the StepOnePlus™ Real-Time PCR System

qPCR protocol		
Repeat	Temp(°C)	Time

1X	95	10min
40X	95	15s
	60	1min
Hold	4	

3.2.5 Agarose gel electrophoresis

For DNA products, 2% (in TAE) agarose gels were used in this work. Appropriate amount of agarose was boiled in TAE buffer. Gels were cast and 2 drop ethidiumbromide was added and mixed. Gels were run in a chamber filled with TAE buffer at 120V for 30min.

3.2.6 RNA extraction

The peqGOLD Total RNA Kit (Pepqlab) was used for extraction of RNA from cell lysate. It provides a rapid and easy method for the isolation of up to 100µg of total RNA from eukaryotic and tissue.

3.2.7 Plasmid construction

3.2.7.1 Design primer for fly-in PCR

Forward and Revers primer were designed with requested restriction enzyme sites flanking the insert.

3.2.7.2 Fly-in PCR set up

The DNA template was amplified from blood cell. The DNA template was diluted 10-20ng/µl, PCR program is listed:

Repeat	Temp(°C)	Time(sec)
--------	----------	-----------

1X	94	300
35X	94	30
	60	60
	72	240
1X	72	120
Hold	4	

3.2.7.3 Gel purification of fly-in PCR insert

An 2% agarose gel in 1X TAE buffer with wide comb (>20µl per well) was prepared, DNA loading buffer was added to whole PCR reaction and the PCR reaction was run in gel. Correct size of PCR product was checked and correct band was cut with a clean scalpel under a UV-transilluminator. PCR fragment was immediately purified with Gel Extraction Kit (Qiagen) according to the manufacturer's instructions. A minimal volume of 20µl of DNA was eluted. DNA concentration was measured with Nanodrop device (Thermo).

3.2.7.4 Topoisomerise fly-in PCR insert into TOPO AT-cloning vector

TOPO reaction is listed:

Reagent	Volume(µl)
Fresh purified linear PCR product	4
Salt Solution	1
Linear TOPO vector	1
Total volume	6

TOPO reaction was incubated for 10min at room temperature. 1µl of the TOPO reaction was immediately transformed into competent TOPO10 bacteria (Invitrogen). Colonies was incubated for overnight on selection agar plates.

3.2.7.5 Colony PCR

The white colonies from agar plates was picked with sterile yellow tips and was put into 50µl LB medium in a 1.5 ml sterile tube. Colony LB fluid was incubated for 1h at 37°C in a mix machine (Thermo) under rotation, then set up PCR program:

Repeat	Temp(°C)	Time(sec)
1X	94	300
35X	94	30
	60	60
	72	240
1X	72	120
Hold	4	/

3.2.7.6 Plasmid minipreparation

The PCR reaction was loaded into an agarose gel and plasmid minipreps was made from colonies that was positive for a band of the correct size.

3.2.7.7 Preparative restriction of recipient vector

5µg of pGL3 plasmid (Figure 3.3) was used for double digest, the reaction is listed:

pVEGFa-pGL3 reporter plasmid reaction:

Reagent	Volume(µl)
pVEGFa DNA	6
XHoi	2
HindIII	2
Buffer2.1	2
H ₂ O	8

Reagent	Volume(µl)
pGL3 plasmid	10
XHoi	2
HindIII	2
Buffer2.1	2
H ₂ O	4

BMAL1-pGL3 reporter plasmid reaction:

Reagent	Volume(μ l)
BMAL1 DNA	2
KpnI	2
SacI	2
Buffer1.1	2
H ₂ O	12

Reagent	Volume(μ l)
pGL3 plasmid	10
KpnI	2
SacI	2
Buffer1.1	2
H ₂ O	4

The reaction was incubated for 1h at 37°C.

3.2.7.8 Preparative gel electrophoresis of linearized recipient vector

An 2% agarose gel in 1X TAE buffer with wide comb (>20 μ l per well) was prepared, DNA loading buffer was added into reaction to purify and cut DNA easily. Gel was run for good separation of the linearized vector. The correct band was cut with a clean scalpel under a UV-transilluminator. PCR fragment was immediately purified with Gel Extraction Kit (Qiagen) according to the manufacturer's instructions. DNA concentration was measured with Nanodrop device (Thermo).

3.2.7.9 Preparative restriction of fly in PCR insert from the donor TOPO-vector

An 2% agarose gel in 1X TAE buffer with wide comb (>20 μ l per well) was prepared, DNA loading buffer was added into reaction to purify and cut DNA easily. Gel was run for good separation of the linearized TOPO donor vector. The correct band was cut with a clean scalpel under a UV-transilluminator. PCR fragment was immediately purified with Gel Extraction Kit (Qiagen) according to the manufacturer's instructions. DNA concentration was measured with Nanodrop device (Thermo).

3.2.7.10 Ligation of linear recipient vector and purified fly in PCR insert

Ligase reaction (Promega) is listed:

Reagent	Volume(μ l)
T4 Ligase	1
T4 Ligase buffer	1
Vector	4
Insert	4

The reaction was incubated for 16h at 11°C.

3.2.7.11 Transformation

5 μ l of the ligation reaction was transformed to the competent TOPO 10 bacteria (Invitrogen). Transformation was proceeded according to manufacturer's protocol (Invitrogen).

3.2.7.12 Colony orientation PCR

The single colonies from agar plates was picked with sterile tips and was put into 50 μ l LB medium in a 1.5 ml sterile tube. Colony LB fluid was incubated for 1h at 37°C in a mix machine (Thermo) under rotation, then set up PCR program:

Repeat	Temp(°C)	Time(sec)
1X	94	300
35X	94	30
	55	60
	72	240
1X	72	120
Hold	4	

3.2.7.13 Plasmid minipreparation

The PCR reaction was loaded into an agarose gel and plasmid minipreps was made

from colonies that was positive for a band of the correct size.

3.2.7.14 Send plasmid for DNA sequencing

The plasmid was sent to GATC company for DNA sequencing to make sure that correct plasmid was gotten. Then plasmid maxipreparation was done according to the manufacturer's protocol (Qiagen). Finally, DNA concentration was measured and the plasmid was used for transfection.

3.2.8 Cell proliferation assay

To measure the influence of ROR α and Rev-erba overexpression on proliferation of cells, MTT assay was conducted. Cells were seeded into a 6-well plate at a final cell number of 5×10^5 the day before transfection. Then the cells were transfected with ROR α -pTarget vector, NR1D1-pTarget vector, and empty pTarget vector, separately. The following day, cells were seeded into a 96-well plate in triplicates, with 2×10^3 or 4×10^3 of the cells per well and were incubated for 24 hours for hemin treatment. The next day, fresh medium was exchanged and the chemical was directly added into the medium with different concentrations. MTT assay was performed after 24, 96, 120, 144, 168 hours. For this purpose, 10 μ l MTT solution was added into each well. Cells were incubated for 4 hours at 37°C with 5% CO₂ and humidity. After 4 hours, 100 μ l MTT lysis buffer were added. The plate was further incubated overnight in the incubator, and the optical density (OD) of the wells was determined using an automated plate reader at a test wavelength of 570nm and a reference wavelength of 630nm.

3.2.9 Western blot analysis

3.2.9.1 Protein isolation

Cells were washed once with 1X PBS and lysed in 150µl SDS lysis buffer with proteinase inhibitors by scraping cells from 6 well plates with a cell scraper. Protein extracts were incubated on ice for 20min before sonication for 20s (10 times) and centrifuged for 10min at 12,000 rpm at 4°C to remove cell debris. The supernatant was then used to quantify total protein concentration for further experiments.

The concentration of the protein was measured using the BCA Protein Assay Reagent (Thermo Scientific™). In a 96-well plate, 10µl of each of the BSA standard dilutions were added following the order from A to I in duplicate, which was necessary to calculate the BSA protein standard curve. 10µl of the protein sample (diluted 1 to 5) were added in duplicates into the 96-well plate. 200µl of BCA working reagent was added to each well. Then, the plate was put on a plate shaker for 30s, and incubated at 37°C for 30min. The absorbance was measured at 570nm using an ELISA-Reader (Tecan). Protein concentrations were calculated as an average value of duplicate counts and compared to the BSA standard curve.

3.2.9.2 Running gels

The separating gel was prepared and inserted into a gel chamber, covered with isopropanol to avoid dehydration and the reaction with oxygen from the air. After polymerization, the isopropanol was washed out, followed by pouring the prepared stacking gel into the chamber. The gel comb was inserted to generate the gel slots. 1.5µg/µl of protein was diluted in dH₂O to achieve a total volume of 80µl and mixed with 20µl SDS loading buffer and heated for 10min at 99°C. 20µl of samples were loaded into the gel slots of the stacking gel according to the size of the gel comb. The gels were run at 30mA constant current for about 1h until the protein was fully separated and used for Western blotting afterwards.

3.2.9.3 Protein blotting

Western blotting is applied to transfer protein from gels onto a nitrocellulose membrane. Materials were pre-wet in transfer buffer and placed in the following order: case (clear side), sponge, Whatman paper, membrane, gel, Whatman paper, sponge, case (black side). This system was inserted into transfer cassettes and placed into a standard tank system filled with transfer buffer. The transfer step was run at 100V constant voltage and 4°C for 60min. Then, the nitrocellulose membrane was put into Ponceau solution for 5min and was trimmed. After blocking the membrane with 5% non-fat dry milk powder in TPBS to avoid unspecific background binding, the membrane was incubated with primary antibody solution at 4°C overnight on a shaker. The following day, the membrane was washed with TPBS for 5min 3 times, and then incubated with secondary antibody solution for 90min. After 3 times washing with TPBS, chemiluminescence was detected with Luminol solution using a Lumi-imager device.

3.2.10 Immunohistochemistry

The microarrays were dewaxed and rehydrated using a “Staining Street” with 6min each step in the following sequence: HistoClear (Xylo), 96%EtOH, 80% EtOH, 70%EtOH, and finally in dH₂O for 2min. The microarrays were inserted into a glass holder in a black plastic box containing 2.5ml Vectastain stock which was diluted in 250ml dH₂O, and heated in a microwave at 900W for 2min, 180W for 10min, and cooled down on the bench for 30min. The microarrays were then washed with 1X PBS 3 times for 2min, and then endogenous peroxidase was quenched in 3% H₂O₂ in H₂O for 15min at RT to avoid endogenous enzymatic reactions, followed by washing with 1X PBS 3 times for 2min. The slides were then put into a humid chamber. Blocking reagent consisted of 5% normal goat (RORa) or horse (NR1D1) serum (Sigma). Then, 50µl serum in 1ml 1% BSA and 1X PBS was added, and slides were incubated at RT for 1h with a parafilm covered to avoid drying. The primary RORa

(AVIVA Systems Biology) and NR1D1 (LifeSpan BioSciences, Inc) antibody (1:100) were then added, and incubated overnight at 4 °C . The next day, the slides were washed with 1X PBS 3 times for 2min. The biotinylated anti-goat or anti-horse secondary antibody was pipetted onto the slides, and the sections were incubated at RT for 1h in the humid chamber. ABC mixture which was prepared using 2.5ml 1X PBS, 1 drop of A and 1drop of B, was then added for 30min at RT. DAB mixture was prepared with 2.5ml dH₂O, 1 drop of DAB buffer, 2 drop DAB substrate and 1 drop H₂O₂, and was then transferred on the slides, for 1-5min until the color turned brown. The reaction was stopped by washing in dH₂O, 3 times for 1min, and the slides were counterstained in Hematoxylin for 10min, followed by removal of excess dye under tap water. The slides were dehydrated in the “Staining Street”, with 3min for each step, following the sequence: 70%EtOH, 80EtOH, 96%EtOH, HistoClear (Xylo). Then 1 drop of mounting medium was added on the slide, and the section was covered with a cover slip.

3.2.11 ELISA assay

3.2.11.1 Plate preparation

The Capture Antibody was diluted to the working concentration in PBS without carrier protein. Immediately coat a 96-well microplate with 100µl per well of the diluted Capture Antibody. Seal the plate and incubate overnight at room temperature. Each well was aspirated and was washed with Wash Buffer. The process was repeated two times for a total of three washes. The plate was washed by filling each well with Wash Buffer (400µl). Complete removal of liquid at each step is essential for good performance. After the last wash, remaining Wash Buffer was removed by inverting the plate and blotting it against clean paper towels. The plates were blocked by adding 300µl Reagent Diluent to each well, and the plates were incubated at room temperature for a minimum of 1 hour. The plates were washed with Wash Buffer again.

3.2.11.2 Assay procedure

100µl of sample or standards in Reagent Diluent, or an appropriate diluent was added into each well. The plates were covered with an adhesive strip and were incubated at room temperature for 2h. The plates were washed with 400µl Wash Buffer. 100µl of the Detection Antibody, diluted in Reagent Diluent, was added into each well. The plates were covered with a new adhesive strip and were incubated at room temperature for 2h. The plates were washed with 400µl Wash Buffer. 100µl of the working dilution of Streptavidin-HRP was added into each well. The plates were covered with a new adhesive strip and were incubated at room temperature for 20min (Avoid placing the plate in direct light). The plates were washed with 400µl Wash Buffer.

100µl of Substrate Solution was added into each well. The plates were covered with a new adhesive strip and were incubated at room temperature for 20min (Avoid placing the plate in direct light). 50µl of Stop Solution was added into each well. The plates were gently tapped to ensure thorough mixing. The optical density of each well was determined immediately using a microplate reader set to 450nm. If wavelength correction is available, set to 540 nm or 570 nm. If wavelength correction is not available, subtract readings at 540 nm or 570 nm from the readings at 450 nm. This subtraction will correct for optical imperfections in the plate. Readings made directly at 450 nm without correction may be higher and less accurate.

3.2.12 Luciferase assay

One day before transfection, cells were seeded into 6-well plates containing DMEM supplemented with 10% fetal bovine serum. Cells were transfected with 2µg of reporter plasmids and 2µg of expression plasmids, using TurboFect Transfection Reagent (Thermo Scientific) according to the manufacturer's instructions. The total amount of DNA/well was adjusted by adding pTarget vector (Promega). At 48h after

transfection, cell extracts were prepared with use of 100µl of cell lysis buffer (Promega). The plates were shaken for 10min. 10µl of the extracts were taken for assays of luciferase activity and 10µl of the extracts were taken for protein concentration measurement. The Ratio of luciferase activity to protein concentration in each sample served as a measure of normalized luciferase activity.

3.2.13 Chromatin immunoprecipitation (ChIP)

Chromatin immunoprecipitation Assay Kit (EMD Millipore Corporation, CA, USA) were used as recommended by the manufactures.

3.2.13.1 Cross-linking and sonication of cells

After 2×10^6 cells were stimulate or treated on a 10cm dish, 37% formaldehyde was directly added into culture medium to a final concentration of 1% for 10min at 37°C. After 10min, medium was removed as much as possible, and cells was washed twice by ice cold PBS containing protease inhibitors. Cells were scraped into two 15ml tubes. Cell suspension was centrifuged at 2000rpm at 4°C for 4min, supernatant was removed. Cell pellets were resuspended in 200µl SDS Lysis Buffer for 10min on ice. DNA was sheared to lengths between 200 and 2000 basepairs on ice. Sonication condition was 200s (100 times). 8µl 5M NaCl was added into suspension for 4h at 65°C.

3.2.13.2 Linking of antibodies to Protein A Agarose/Salmon Sperm DNA

Suspension was centrifuged for 10min at 13,000 rpm at 4°C, and the supernatant was transferred to a new 2ml-microcentrifuge tube. The pellet was discarded. The supernatant was diluted 10-fold in ChIP Dilution Buffer, for example, 1800µl ChIP Dilution Buffer was added to 200µl sonicated cell supernatant for a final volume of 2ml in each immunoprecipitation condition. Diluted cell supernatant was pre-cleared with

75µl of Protein A Agarose/Salmon Sperm DNA for 30min at 4°C with agitation. Immunoprecipitation antibody was added to the 2ml supernatant fraction and incubate overnight at 4°C with rotation. For a negative control, a no-antibody immunoprecipitation was performed by incubating the supernatant fraction with 60µl of Protein A Agarose/Salmon Sperm DNA for 1h at 4°C with rotation. After overnight incubation, 60µl Protein A Agarose/Salmon Sperm DNA was added to 2ml supernatant fraction for 1h at 4°C with rotation. Agarose was pelleted by gentle centrifuge (700 to 1000 rpm for 1min at 4°C). The supernatant was carefully removed. The protein A agarose/antibody/histone complex was washed for 5min on a rotating platform with 1ml of each of the buffers listed in the orders as given below:

- a) Low Salt Immune Complex Wash Buffer, one wash
- b) High Salt Immune Complex Wash Buffer, one wash
- c) LiCl Immune Complex Wash Buffer, one wash
- d) TE Buffer, two washes

3.2.13.3 PCR protocol to amplify DNA that was bound to the immunoprecipitated histone

Elution buffer (1% SDS, 0.1M NaHCO₃) was prepared freshly. The histone complex was eluted from the antibody by adding 250µl elution buffer to the pelleted protein A agarose/antibody/histone complex. The histone complex was vortexed briefly to mix and was incubated at room temperature for 15min with rotation. The agarose was spinet down and the supernatant fraction (eluate) was carefully transferred to another tube and elution step was repeated. The eluates were combined together (total volume was about 500µl). 20µl 5M NaCl was added to the combined eluates (500µl) and histone-DNA crosslinks was reversed by heating at 65°C for 4h. 10µl of 0.5M EDTA, 20µl 1M Tris-HCl, pH6.5 and 2µl of 10 mg/ml Proteinase K were added to the combined elutes and the mix was incubated for 1h at 45°C. Recover DNA by QIAGEN Kit.

3.2.14 Electrophoretic Mobility Shift Assay (EMSA)

Electrophoretic Mobility Shift Assay Kit (Pierce Biotechnology, IL, USA) were used as recommended by the manufactures.

3.2.14.1 Prepare and pre-run gel

A native 6% polyacrylamide gel in 0.5X TBE was prepared. The gel was placed in the electrophoresis unit and was clamped to obtain a seal. The inner chamber was filled with 0.5X TBE to a height several millimeters above the top of the wells. The outside of the tank was filled with 0.5X TBE to just above the bottom of the wells, which reduces heat during electrophoresis. The gel was pre-electrophoresed for 60min. 100V was applied for an 8 x 8 x 0.1cm gel.

3.2.14.2 Prepare and perform binding reactions

Binding reactions was incubated at room temperature for 20min. 5 μ l of 5X Loading Buffer was added to each 20 μ l binding reaction. Do not vortex or mix vigorously.

3.2.14.3 Electrophorese binding reactions

20 μ l of each sample was loaded onto the polyacrylamide gel. The current was set to 100V for an 8 x 8 x 0.1cm gel. The samples were electrophoresed until the bromophenol blue dye has migrated approximately 2/3 to 3/4 down the length of the gel.

3.2.14.4 Electrophoretic transfer of binding reactions to nylon membrane

Nylon membrane was soaked in 0.5X TBE for at least 10min. The membrane was transferred at 380mA (~100V) for 30min.

3.2.14.5 Crosslink transferred DNA to membrane

The membrane was crosslinked at 120mJ/cm² using a commercial UV-light crosslinking instrument equipped with a 254nm bulbs.

3.2.14.6 Detect biotin-labeled DNA by chemiluminescence

20ml of Blocking Buffer was added to membrane and the membrane was incubated for 15min with gentle shaking. Conjugate/blocking buffer solution was prepared by adding 66.7µl Stabilized Streptavidin-Horseradish Peroxidase Conjugate to 20ml Blocking Buffer (1:300 dilution). Blocking Buffer was decanted from the membrane. The membrane was replaced with the conjugate/blocking buffer solution and was incubated for 15min with gentle shaking. 1X wash buffer solution was prepared by adding 40ml of 4X Wash Buffer to 120ml of ultrapure water. The membrane was transferred to a new container and was rinsed briefly with 20ml of 1X wash buffer solution. The membrane was washed four times for 5min each in 20ml of 1X wash buffer solution with gentle shaking. The membrane was transferred to a new container and 30ml of Substrate Equilibration Buffer was added. The membrane was incubated for 5min with gentle shaking. Substrate Working Solution was prepared by adding 6ml Luminol/Enhancer Solution to 6ml Stable Peroxide Solution. The membrane was removed from the Substrate Equilibration Buffer and was placed in a clean container. The Substrate Working Solution was poured onto the membrane and the membrane was incubated in the substrate solution for 5min without shaking. The membrane was removed from the Working Solution and was exposed to an appropriately equipped CCD camera.

3.2.15 Statistics

Data are reported as Means \pm Standard Deviation of the mean (SD). GraphPad Prism 5.0 was used to analyze the difference between experimental groups by one-way ANOVA. Individual comparisons were made using two-tailed Student t-test, when significant differences were found. The significant level was set at *p-value* < 0.05.

pTarget vector

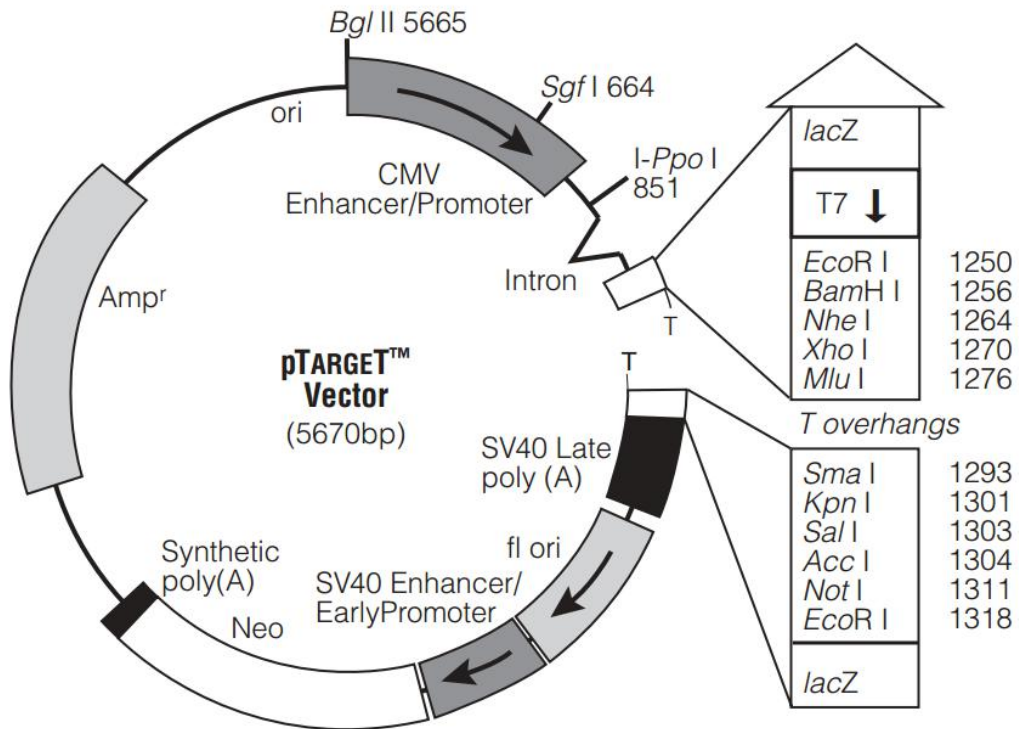


Figure 3.1 Vectorcard of pTarget as provided by the manufacturer (Promega).

The plasmid pTarget was obtained from Promega. pTarget contains an ampicillin resistance for selection of stable cell lines.

pCMV-SPORT6 vector

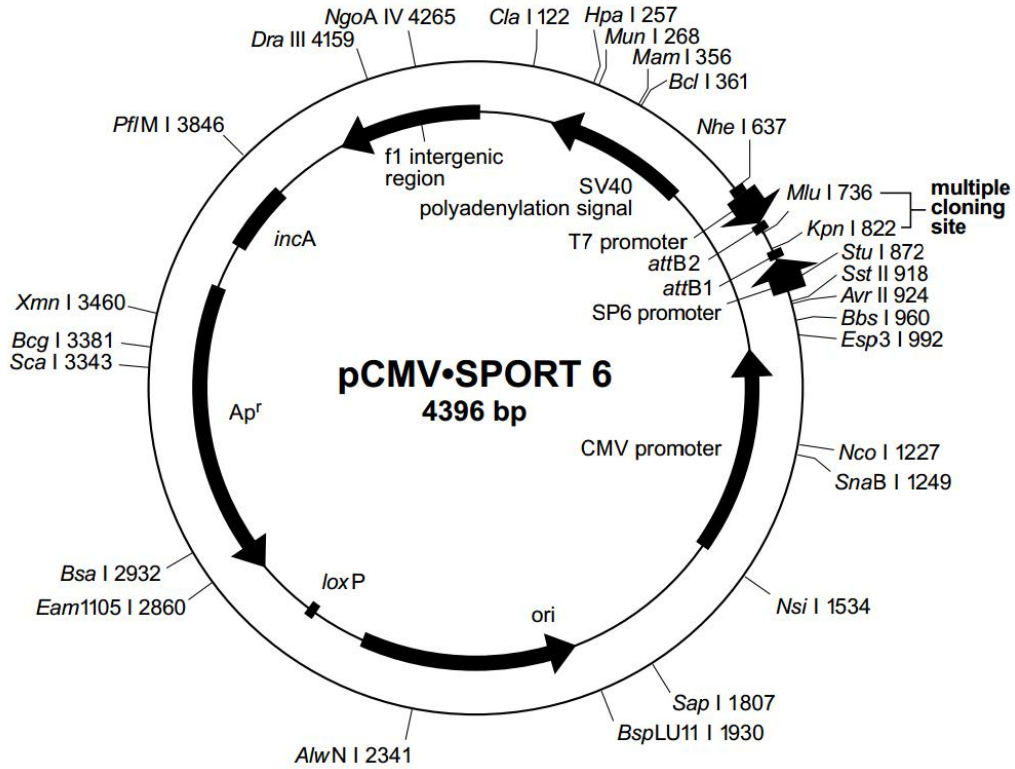


Figure 3.2 Map of Gateway™ pCMV SPORT6 plasmid as provided by the manufacturer (GE Dharmacon).

pGL3 luciferase reporter vector

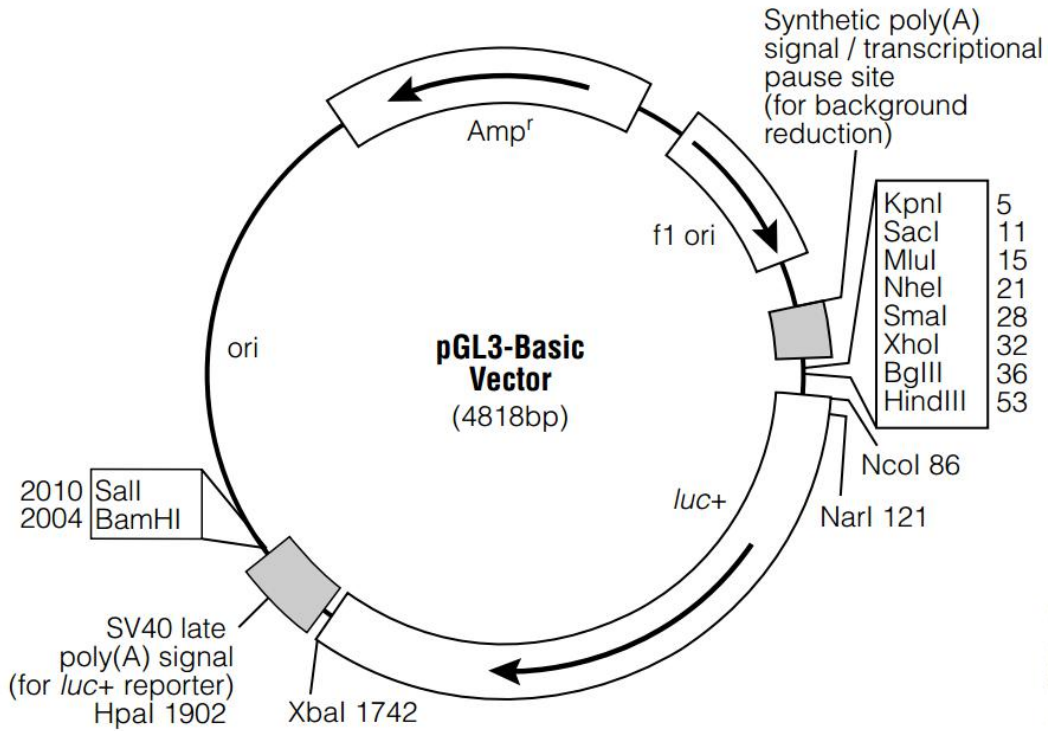


Figure 3.3 pGL3 plasmid circle map and sequence reference point as provided by the manufacturer (Promega).

4 Results

4.1 ROR α is downregulated in human colorectal cancer

To examine the potential relationships between ROR α and clinicopathological of human colorectal cancer, expression of ROR α in 40 colorectal cancer samples and 8 normal colon tissues was analyzed by IHC staining of tissue microarray. There was no significant correlation between expression levels of ROR α in tumor tissues and gender or age. The expression level of ROR α was significantly decreased in cancer tissue compared with normal colonic tissue (Figure 4.1). As shown in Figure 4.1A, in the normal colon mucosa, staining of ROR α was mainly in the nuclei of the cells. As shown in Figure 4.1B, in the colorectal cancer tissue sample, staining of ROR α was much lower than in the normal colon mucosa. In Figure 4.1C, low expression of ROR α significantly correlated with important clinicopathological variables concerning tumor progression such as histological differentiation and tumor stage. The expression of ROR α in colorectal cancer tissue at different tumor grades showed significant lower levels than in normal tissue samples. Meanwhile, the expression of ROR α in colorectal cancer tissue at different tumor stages according to the TNM staging system also significant lower levels than in normal tissue samples.

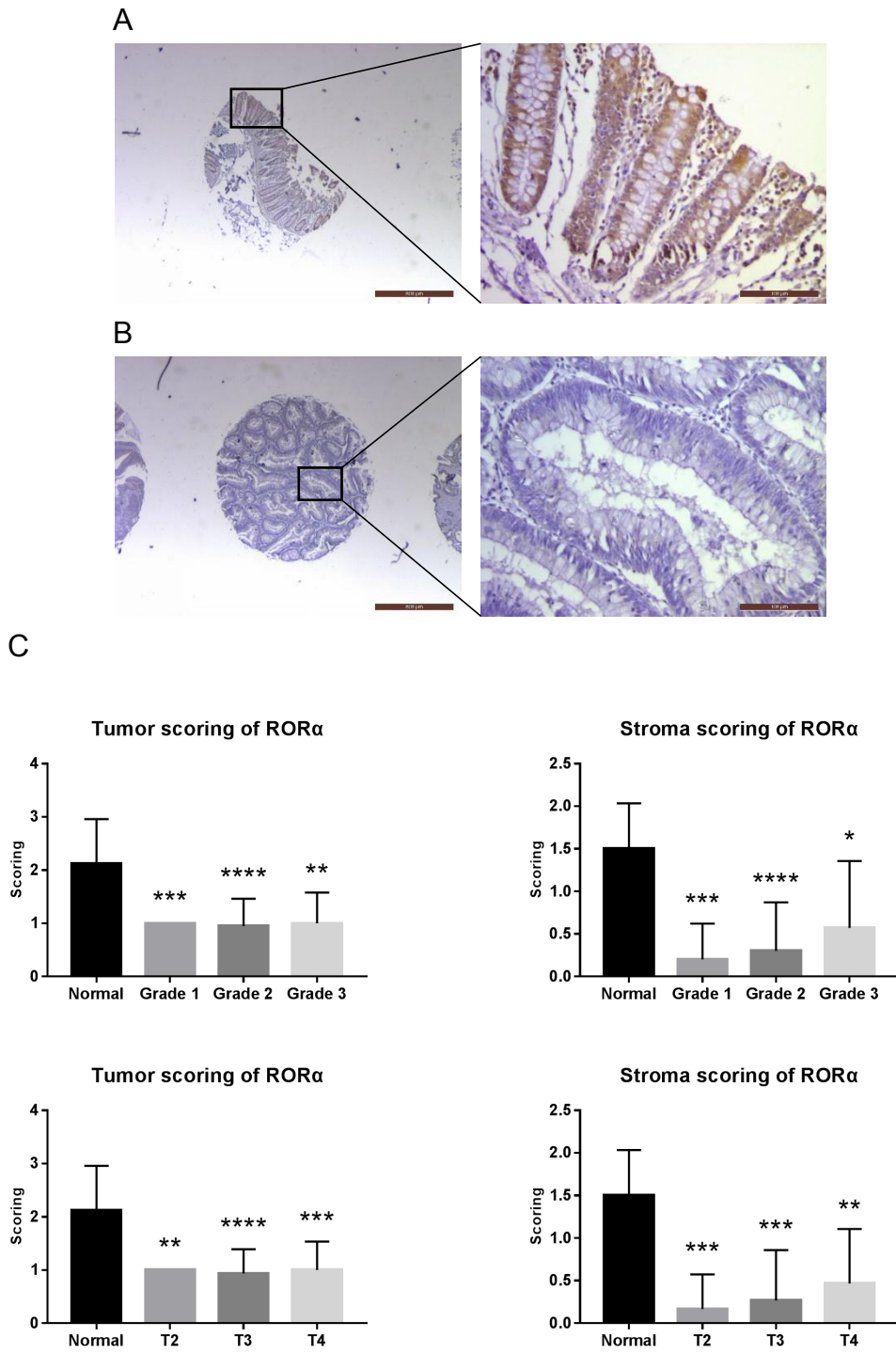


Figure 4.1 RORα was downregulated in human colorectal cancer.

(A-B) IHC of colon cancer tissue arrays showing the expression of RORα in human (A) normal colon tissues (n=8) and (B) colorectal cancer tissues (n=40). Bar size: left: 800µm; right: 100µm. (C) The expression of RORα at different tumor grade and TNM staging in tumor and stroma cells, respectively. IHC-analysis scores were: 0 = negative, 1 = weak positive, 2 = moderate positive, 3 = strong positive. Grade 1, well differentiated; Grade 2, moderate differentiation; Grade 3, poor differentiation; Grade 4, undifferentiated. T2, T3, T4 refer to tumor stage according to the TNM staging system. Data are presented as the mean ± S.D. * $p < 0.05$, ** $p < 0.01$, *** $p < 0.001$, **** $p < 0.0001$, vs. Normal.

4.2 REVERBA is upregulated in human colorectal cancer

To examine the potential relationships between REVERBA and clinicopathological of human colorectal cancer, expression of REVERBA in 40 colorectal cancer samples and 8 normal colon tissues was analyzed by IHC staining of tissue microarray. There was no significant correlation between expression levels of REVERBA in tumor tissues and gender or age. The expression level of REVERBA was significantly increased in cancer tissue compared with normal colonic tissue (Figure 4.2). As shown in Figure 4.2A, in the normal colon mucosa, staining of REVERBA was mainly in the nuclei of the cells. As shown in Figure 4.2B, in the colorectal cancer tissue sample, staining of REVERBA was much higher than in the normal colon mucosa. As shown in Figure 4.2C, high expression of REVERBA in cancer cells significantly correlated with important clinicopathological variables concerning tumor progression such as histological differentiation and tumor stage. The expression of REVERBA in colorectal cancer tissue at different tumor grades showed significant higher levels than in normal tissue samples. The expression of REVERBA in colorectal cancer tissue at different tumor stages according to the TNM staging system also showed significant higher levels than in normal tissue samples. However, there was no significant correlation between expression of REVERBA in stroma cells and different tumor grade or tumor stage.

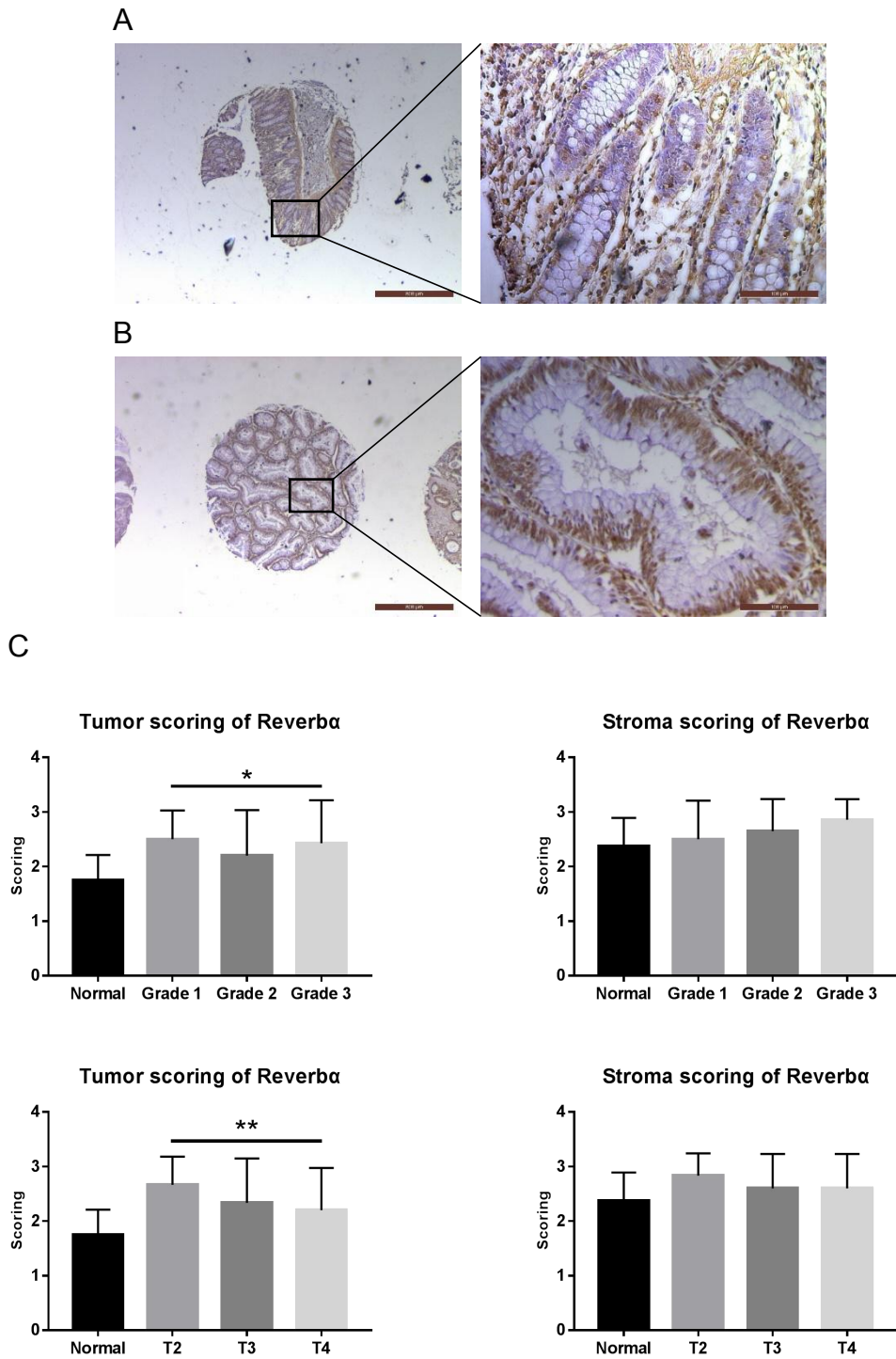


Figure 4.2 REVERBA was upregulated in human colorectal cancer.

(A-B) IHC of colon cancer tissue arrays showing the expression of REVERBA in human (A) normal colon tissues (n=8) and (B) colorectal cancer tissues (n=40). Bar size: left: 800µm; right: 100µm. (C) The expression of REVERBA at different tumor grade and TNM staging in tumor and stroma cells, respectively. IHC-analysis scores were: 0 = negative, 1 = weak positive, 2 = moderate positive, 3 = strong positive. Grade 1, well differentiated; Grade 2, moderate differentiation; Grade 3, poor differentiation; Grade 4, undifferentiated. T2, T3, T4 refer to tumor stage according to the TNM staging system. Data are presented as the mean ± S.D. * $p < 0.05$, ** $p < 0.01$, vs. Normal.

4.3 BMAL1 is downregulated in human colorectal cancer

To examine the potential relationships between BMAL1 and parameters of human colorectal cancer, expression of BMAL1 in 40 colorectal cancer samples and 8 normal colon tissues was analyzed by IHC staining of tissue microarray. There was no significant correlation between expression levels of BMAL1 in tumor tissues and gender or age. The expression level of BMAL1 was significantly decreased in cancer tissue compared with normal colonic tissue (Figure 4.3). As shown in Figure 4.3A, in the normal colon mucosa, staining of BMAL1 was mainly in the nuclei of the cells. As shown in Figure 4.3B, in the colorectal cancer tissue sample, staining of BMAL1 was much lower than in the normal colon mucosa. Further analysis in Figure 4.3C revealed that the expression of BMAL1 showed a decreased trend with advanced tumor grade and tumor stage. The expression of BMAL1 was significantly lower at grade 3 in both cancer cells and stroma cells. Meanwhile, the expression of BMAL1 was significantly lower at T3 tumor stage in both cancer cells and stroma cells.

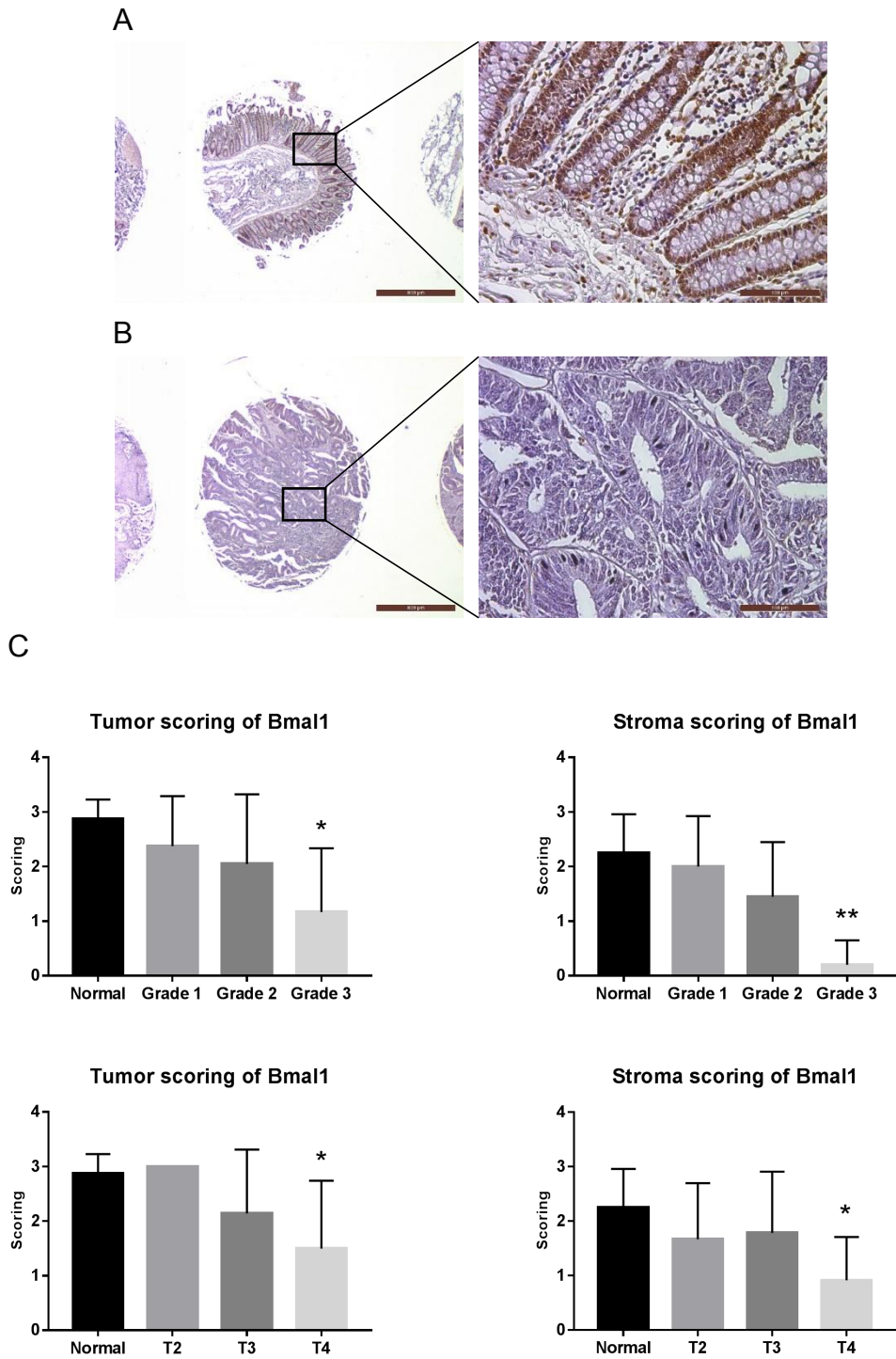


Figure 4.3 BMAL1 was downregulated in human colorectal cancer.

(A-B) IHC of colon cancer tissue arrays showing the expression of BMAL1 in human (A) normal colon tissues (n=8) and (B) colorectal cancer tissues (n=40). Bar size: left: 800µm; right: 100µm. (C) The expression of BMAL1 at different tumor grade and TNM staging in tumor and stroma cells, respectively. IHC-analysis scores were: 0 = negative, 1 = weak positive, 2 = moderate positive, 3 = strong positive. Grade 1, well differentiated; Grade 2, moderate differentiation; Grade 3, poor differentiation; Grade 4, undifferentiated. T2, T3, T4 refer to tumor stage according to the TNM staging system. Data are presented as the mean ± S.D. * $p < 0.05$, ** $p < 0.01$, vs. Normal.

4.4 Expression of ROR α , REVERBA and BMAL1 is associated with response or non-response/resistance to anti-angiogenesis treatment in mice

To evaluate the relationship between expression of nuclear receptors in responder (response to anti-angiogenesis treatment) or non-responder (no response or resistance to anti-angiogenesis treatment) mice, expression of ROR α , REVERBA and BMAL1 in 4 responder and 4 non-responder mice in the same tissue area were analyzed by IHC staining, respectively (Figure 4.4). Ki67 was used as control to confirm responder or non-responder characteristics. Usually, non-responder mice exhibited a high level of cell proliferation, so high expression of Ki67 was observed (Figure 4.4 A). Responder mice had a relative low level of cell proliferation, so low expression of Ki67 was observed (Figure 4.4 B). As shown in Figure 4.4, in non-responder mice tissue, expression of BMAL1 was significantly higher than in responder mice tissue, and expression of REVERBA was higher than in responder mice tissue as well ($p=0.0584$). Conversely, expression of ROR α showed no difference between non-responder and responder animals..

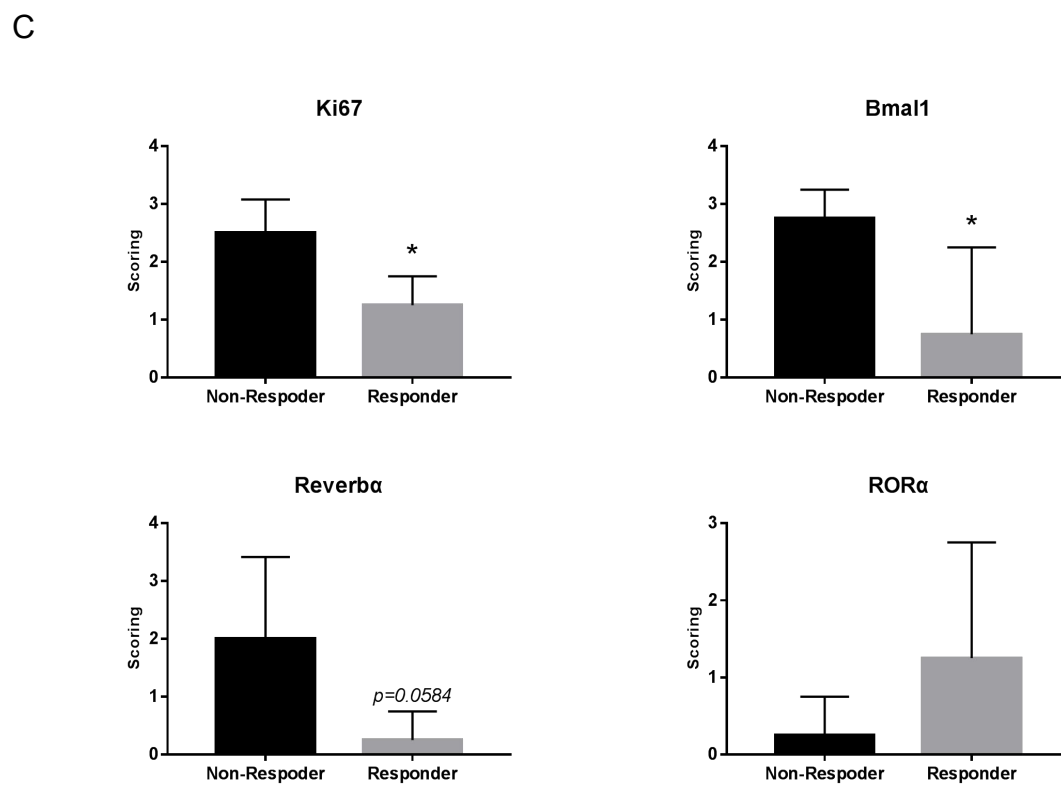
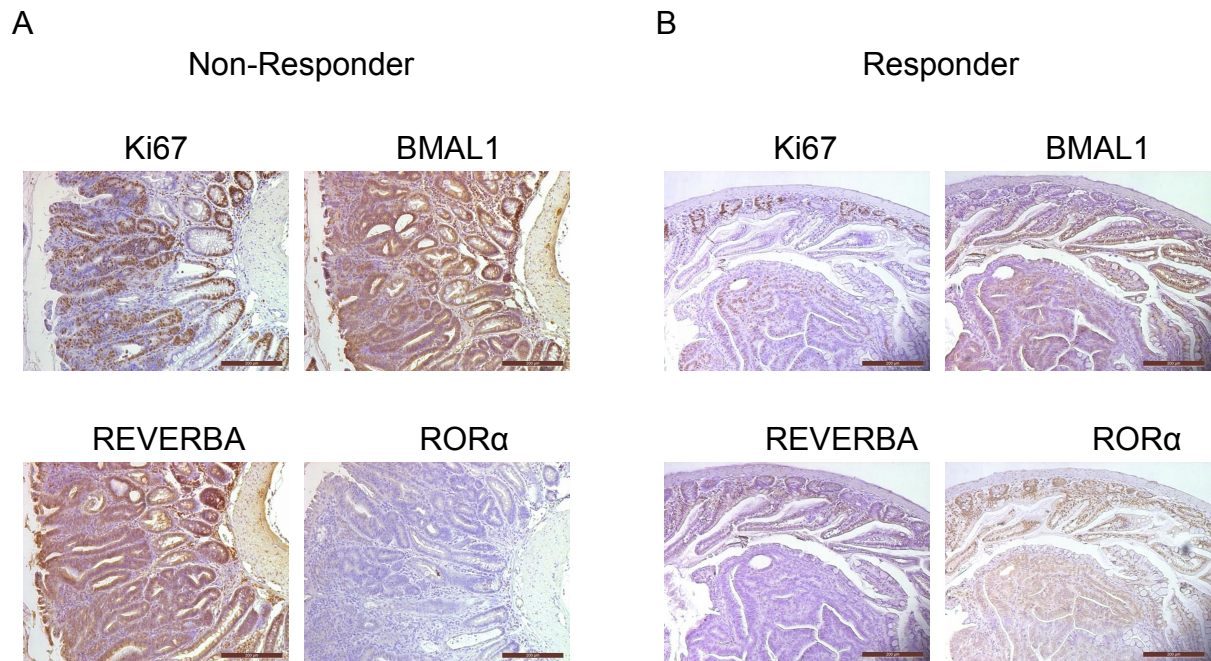


Figure 4.4 Expression of RORα, REVERBA and BMAL1 in non-responder and responder mouse intestine tissue.

(A-B) Expression of Ki67, RORα, REVERBA and BMAL1 in (A) non-responder and (B) responder mouse intestine tissue (n=4 per group). Photomicrographs were taken at the same tissue area. (C) Quantitative analyses of (A) and (B). IHC-analysis scores were: 0 = negative, 1 = weak positive, 2 = moderate positive, 3 = strong positive. Data are presented as the mean ± S.D. * $p<0.05$, vs. Non-Responder.

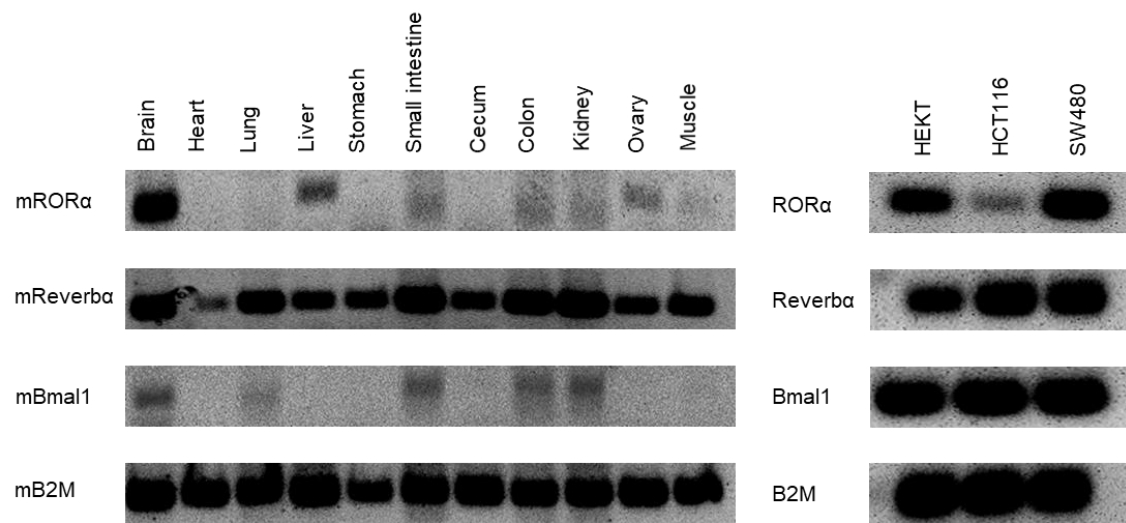
4.5 Expression level of ROR α , REVERBA and BMAL1 in various normal mouse tissues and in different colorectal cancer cell lines

To detect whether ROR α , REVERBA and BMAL1 was expressed in normal mouse tissues, reverse transcription-polymerase chain reaction (RT-PCR), and western blot (WB) (Figure 4.5) were conducted.

Using RT-PCR and the mouse primers for ROR α , REVERBA and BMAL1, it was shown that the mouse ROR α gene was only transcribed in mouse brain, and was low transcribed in, for example, liver, small intestine, colon, kidney and ovary, however, mouse ROR α gene could not be detected in heart, lung, stomach, cecum or muscle (Figure 4.5A). It was also shown that the mouse ROR α gene was lower transcribed in HCT116 cells compared with SW480 cells (Figure 4.5A). Similar results also were observed in BMAL1. It was shown that the BMAL1 gene was low transcribed in some of the mouse tissue samples, for example, brain, lung, small intestine, colon and kidney, however, mouse BMAL1 gene could not be detected in heart, liver, stomach, cecum, ovary or muscle (Figure 4.5A). Mouse BMAL1 gene was transcribed in all of these three cell lines (Figure 4.5A). On the contrary, mouse REVERBA gene was transcribed in all of these mouse tissue samples as well as in all of these cell lines (Figure 4.5A).

Using WB and corresponding antibodies, ROR α and BMAL1 showed high expression in mouse organs, but REVERBA only showed weak expression in mouse brain and heart and could not be detected in the other organ samples (Figure 4.5B). As for cell lines, ROR α and BMAL1 were expressed, but REVERBA was undetectable in all of these three cell lines (Figure 4.5B).

A



B

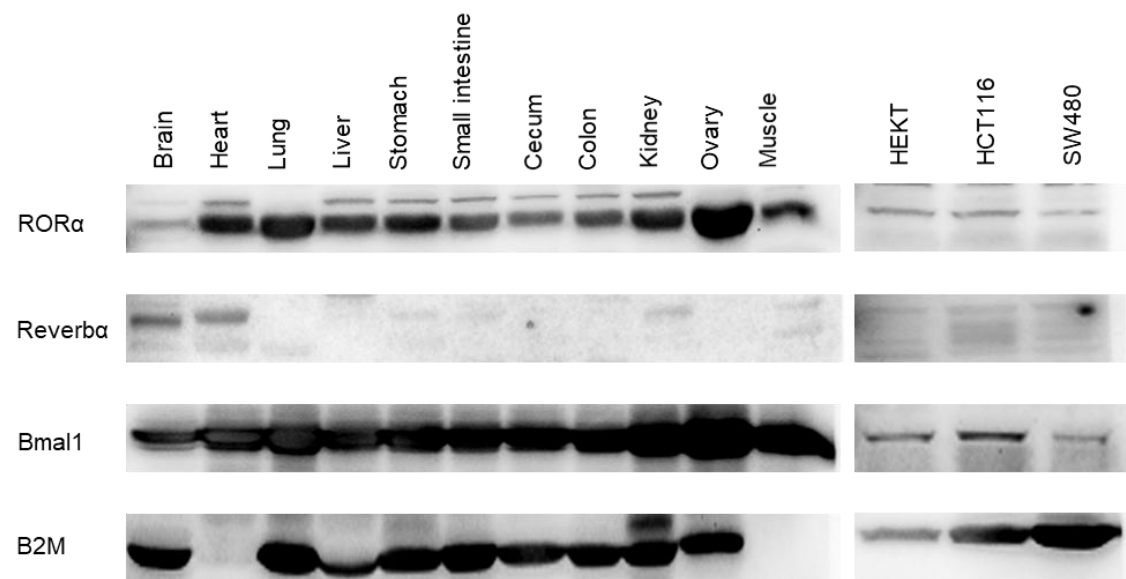


Figure 4.5 Expression of ROR α , REVERBA and BMAL1 in mouse organs and in different colorectal cancer cell lines.

(A) mRNA expression of ROR α , REVERBA and BMAL1 in mouse organs (brain, heart, lung, liver, stomach, small intestine, cecum, colon, kidney, ovary, muscle) and in different cell lines (HEK293T, HCT116, SW480). RNA was collected from mouse organs and cells, and cDNA was synthesized for PCR amplification. (B) protein expression of ROR α , REVERBA and BMAL1 in mouse organs (brain, heart, lung, liver, stomach, small intestine, cecum, colon, kidney, ovary, muscle) and in different cell lines (HEK293T, HCT116, SW480). Protein lysis was collected from mouse organs and cells, and ROR α , REVERBA and BMAL1 antibodies were used to detect corresponding protein expression.

4.6 Subcellular localization of ROR α and REVERBA in HEK293T cells

To reveal the distribution of ROR α and REVERBA *in vitro*, immunofluorescence (IF) was performed. As shown in Figure 4.6, HEK293T cells were stained for immunofluorescence microscopy, and red staining of ROR α and REVERBA mainly located within the nuclei of the cells..

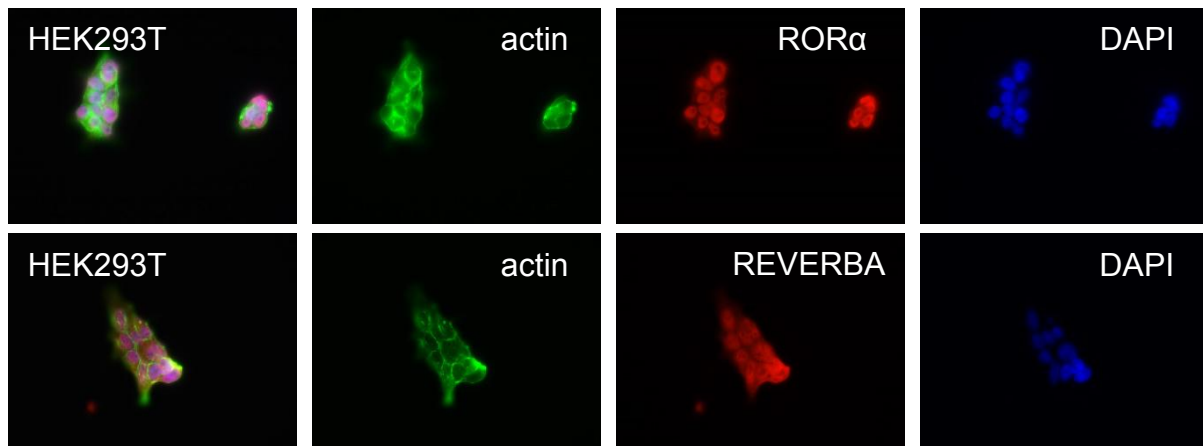


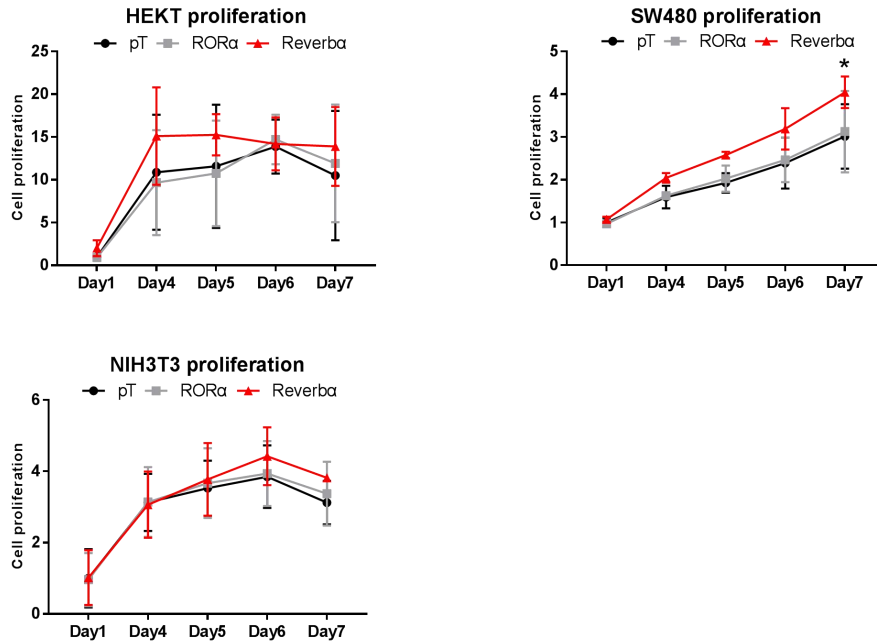
Figure 4.6 Subcellular localization of ROR α and REVERBA in HEK293T cells.

HEK293T cells were stained for immunofluorescence microscopy to detect distribution of ROR α and REVERBA. Green = actin, red = ROR α or REVERBA, blue = nuclei.

4.7 Effects of ROR α , REVERBA and BMAL1 on cell proliferation

To measure the effects of overexpression of ROR α , REVERBA and BMAL1 on the proliferation of HEK293T, HCT116 and SW480 cell, MTT assay was conducted (Figure 4.7). A significant increase in SW480 cell proliferation was observed in REVERBA-overexpressing cells compared with the empty-vector control cells. However, the growth rate of REVERBA-overexpressing HEK293T and HCT116 cells was not significantly changed (Figure 4.7A). Similarly, the growth rates of ROR α -overexpressing (Figure 4.7A) and BMAL1-overexpressing were not altered either (Figure 4.7B).

A



B

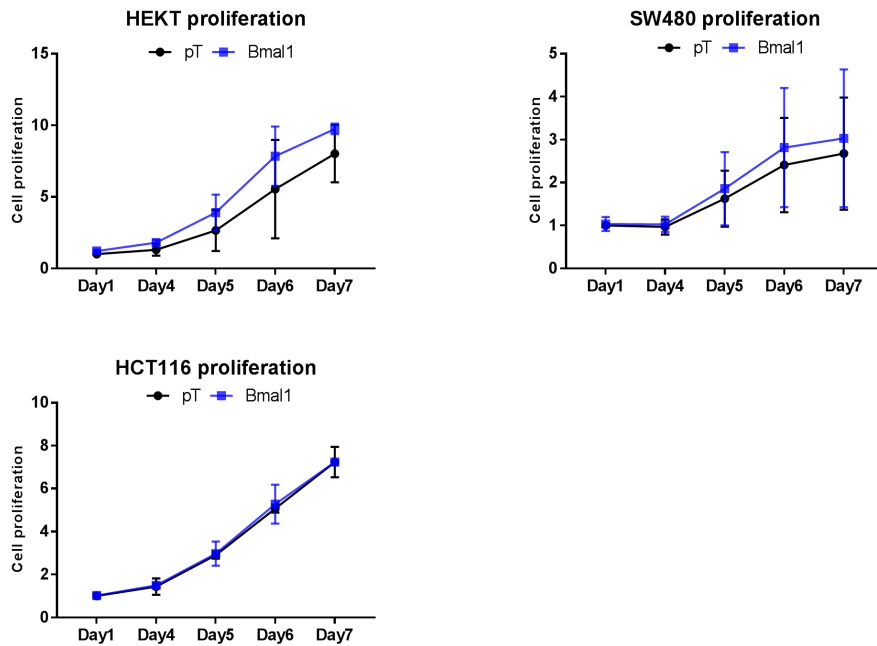


Figure 4.7 Effects of ROR α , REVERBA and BMAL1 on cell proliferation.

(A) MTT results of proliferation assay in cells (HEK293T, SW480 and NIH3T3) transfected with ROR α and REVERBA compared to cells transfected with p-Target vector. (B) MTT results of proliferation assay in cells (HEK293T, SW480 and NIH3T3) transfected with BMAL1 compared to cells transfected with p-Target vector. Proliferation ratio was measured at time point 24h, 96h, 120h, 144h, and 168h by MTT assays. O.D. values from assay were calculated as fold \pm S.D. (n=3). * p <0.05, vs. pT group.

4.8 Overexpression of REVERBA in colorectal cancer cells increases transcription of the human VEGFa gene.

To explore the effect of REVERBA on the activity of the human VEGFa gene transcription in colorectal cancer cells, real-time semiquantitative PCR (qPCR) was performed in HCKT and SW480 cells (Figure 4.8 and Figure 4.9).

HEK293T cells with overexpressed REVERBA (Figure 4.8A), BMAL1 expression was repressed (Figure 4.8B), consistent with the existing literature (Lowrey and Takahashi, 2011). 4 different human VEGFa primers (huVEGFa-1, huVEGFa-2, huVEGFa Eform and huVEGFa All) were used to evaluate the human VEGFa gene transcription level. Figure 4.8C and Figure 4.8D showed a trend for a reduced expression of huVEGFa-1 and huVEGFa-2 in presence of overexpressed REVERBA. Figure 4.8E and Figure 4.8F showed a significant decrease of the amplicons detected by the primers of huVEGFa Eform and huVEGFa All in presence of overexpressed REVERBA compared with the empty-vector control cells.

In SW480 cells overexpressing REVERBA (Figure 4.9A), only a trend for reduced BMAL1 expression was observed (Figure 4.9B). The same human VEGFa primers were used to evaluate the human VEGFa gene transcription level. Figure 4.9C and Figure 4.9F showed an increase trend of amplicon detection by the primers of huVEGFa-1 and huVEGFa All in presence of overexpressed REVERBA. Figure 4.9D and Figure 4.9E display a significant increase of huVEGFa-2 and huVEGFa Eform amplicons in presence of overexpressed Reverba compared with the empty-vector control cells.

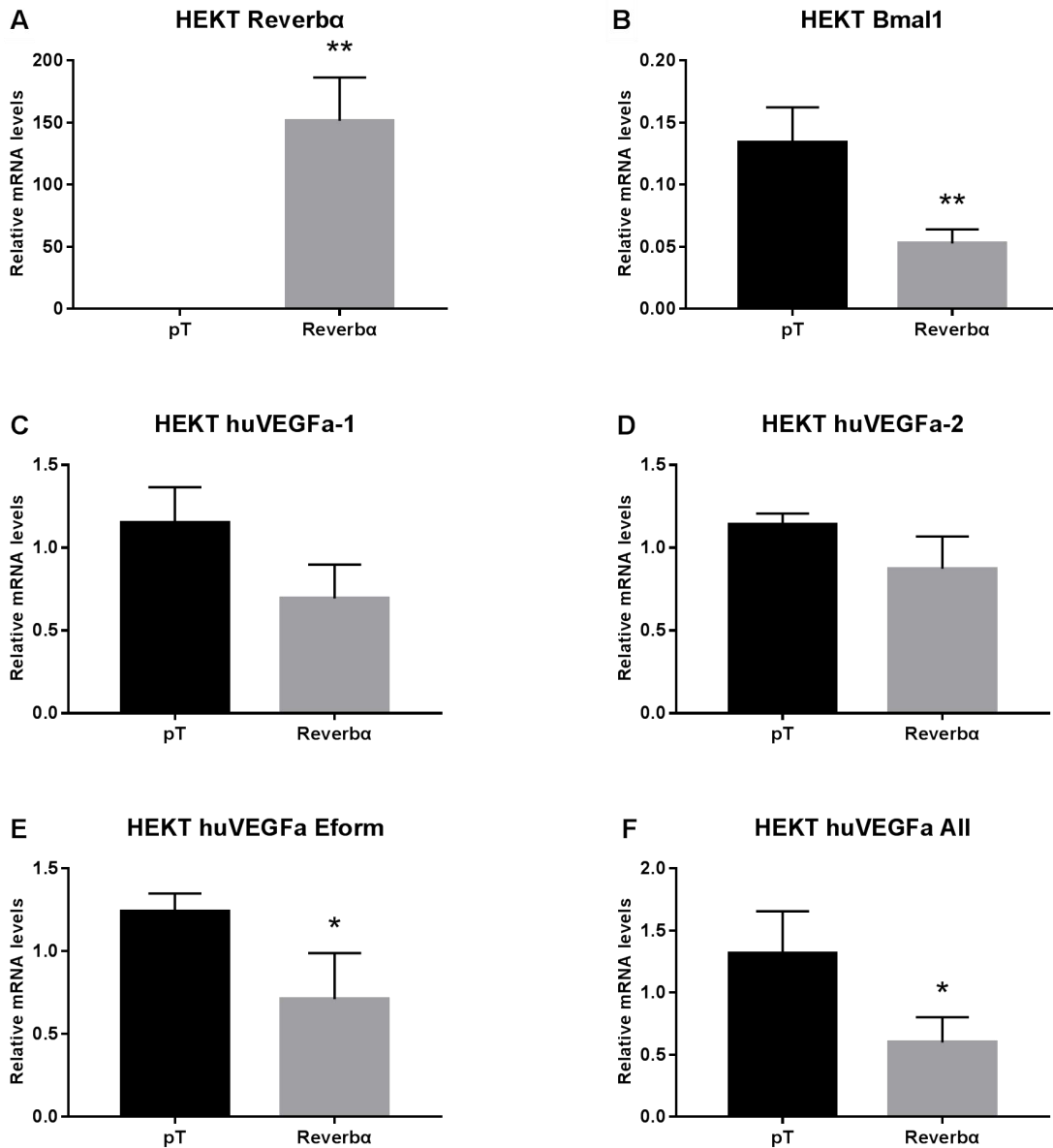


Figure 4.8 Effects of REVERBA on mRNA expression of BMAL1 and human VEGFa in HEK293T cells.

(A) Transfection efficiency of REVERBA in HEK293T cells. (B) Effects of REVERBA on mRNA expression of BMAL1 in HEK293T cells. (C-F) Effects of REVERBA on mRNA expression of human VEGFa. 4 different human VEGFa primers ((C) huVEGFa-1, (D) huVEGFa-2, (E) huVEGFa Eform and (F) huVEGFa All) were designed to detect mRNA expression of human VEGFa. RNA was collected after REVERBA transfection of HEK293T for 48h and cDNA was synthesized for qPCR analysis. Data are presented as the mean \pm S.D. (n=3). * p <0.05, ** p <0.01, vs. pT group.

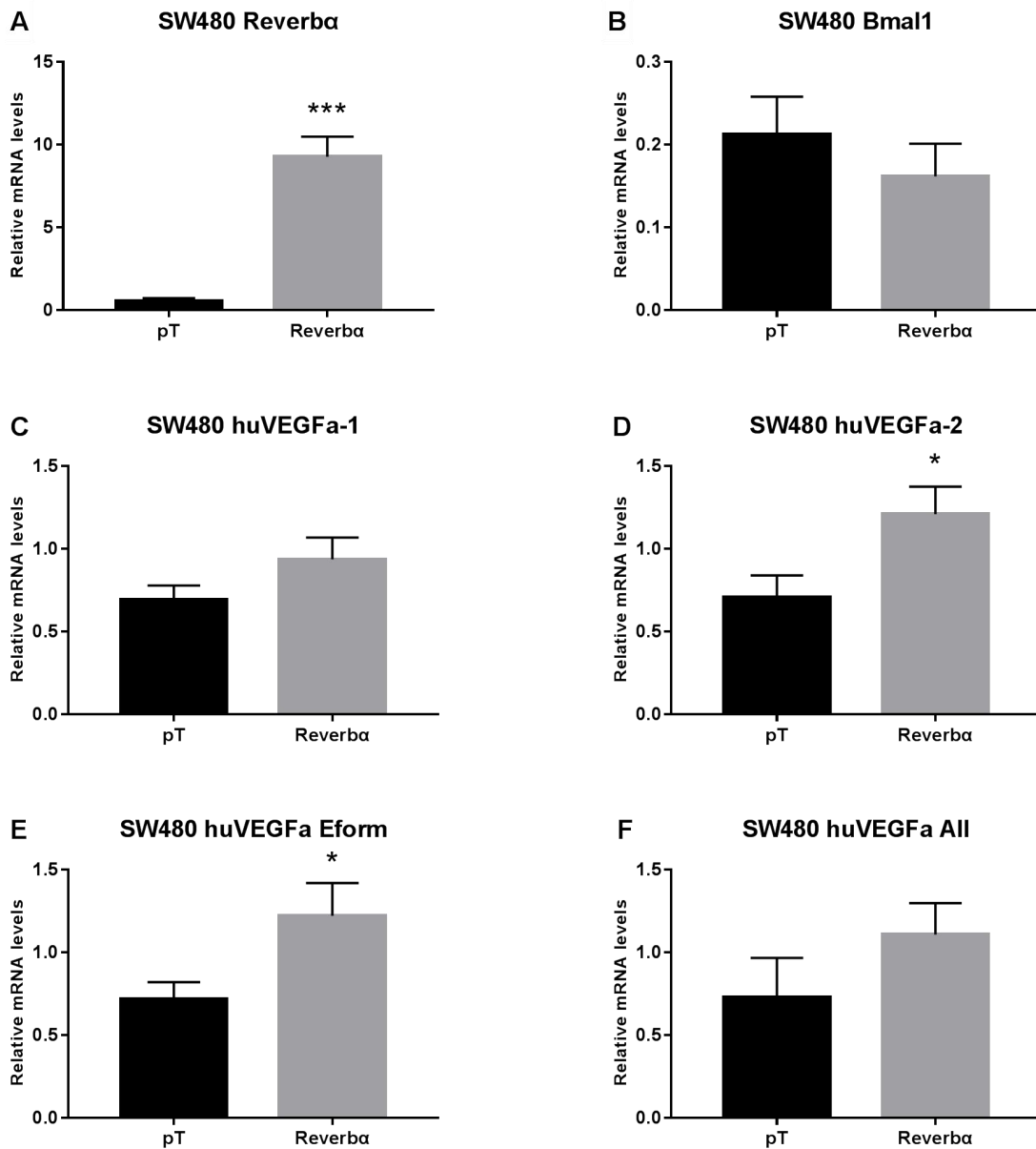


Figure 4.9 Effects of REVERBA on mRNA expression of BMAL1 and human VEGFa in SW480 cells.

(A) Transfection efficiency of REVERBA in SW480 cells. (B) Effects of REVERBA on mRNA expression of BMAL1 in SW480 cells. (C-F) Effects of REVERBA on mRNA expression of human VEGFa. 4 different human VEGFa primers ((C) huVEGFa-1, (D) huVEGFa-2, (E) huVEGFa Eform and (F) huVEGFa All) were designed to detect mRNA expression of human VEGFa. RNA was collected after REVERBA transfection of SW480 for 48h and cDNA was synthesized for qPCR analysis. Data are presented as the mean \pm S.D. (n=3). * p <0.05, *** p <0.001, vs. pT group.

4.9 Overexpression of REVERBA increases human VEGFa secretion *in vitro*

Because the mRNA levels of the human VEGFa gene showed an increase in colorectal cancer cells by upon overexpression of REVERBA, we explored the effect of REVERBA on the secretion of human VEGFa in colorectal cancer cells (SW480, HCT116, HT29 and CaCo2) by ELISA (Figure 4.10).

As shown in Figure 4.10A, VEGFa content in conditioned medium collected from HEK293T cells transfected with REVERBA plasmid for 48h exhibited a significant increase compared with the empty-vector control cells. VEGFa content in HEK293T cells transfected with REVERBA plasmid for 48h was 304.58 ± 45.03 pg/ml and VEGFa content in the control group was 164.62 ± 20.63 pg/ml.

Overexpressed REVERBA also increased VEGFa content in SW480 cells as shown in Figure 4.10B. VEGFa content in SW480 cells transfected with REVERBA plasmid for 48h was 82.12 ± 5.82 pg/ml and VEGFa content in the control group was 54.00 ± 9.35 pg/ml.

However, VEGFa content already had a high secretion baseline in HCT116, HT29 and CaCo2 cells compared with HEK293T and SW480 cells. As shown in Figure 4.10C, Figure 4.10D, and Figure 4.10E, VEGFa content in HCT116, HT29 and CaCo2 transfected with empty-vector was 518.95 ± 25.92 pg/ml, 994.52 ± 257.51 pg/ml, and 317.54 ± 36.46 pg/ml, respectively. VEGFa content in HCT116, HT29 and CaCo2 transfected with REVERBA also had a high secretion level and the amount was 554.48 ± 94.74 pg/ml, 935.21 ± 189.97 pg/ml, and 336.68 ± 39.90 pg/ml. But there was no significant difference between these two groups.

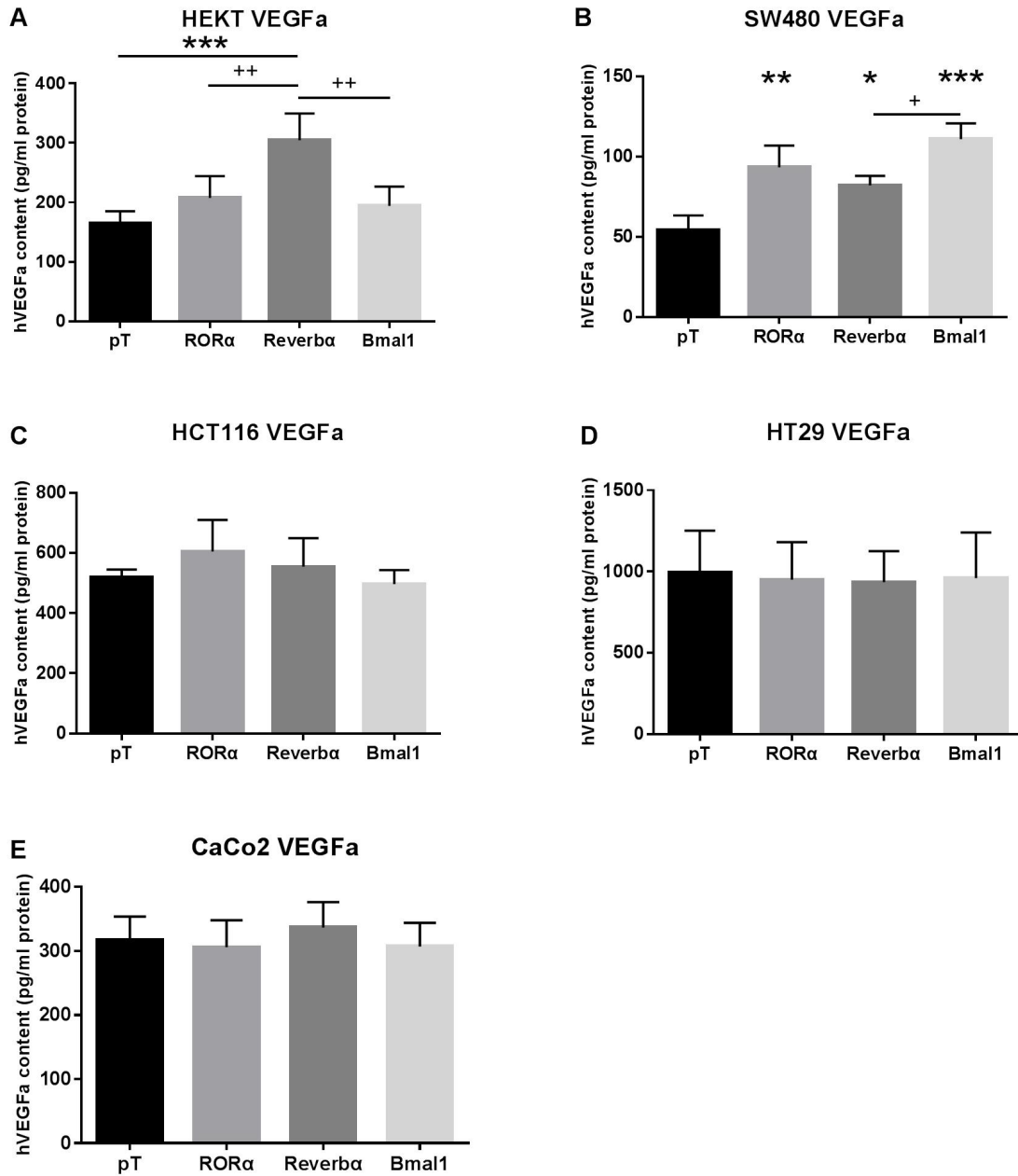


Figure 4.10 Effects of RORα, REVERBA and BMAL1 on human VEGFa protein secretion levels. (A-E) Cell culture medium was collected after RORα, REVERBA and BMAL1 transfection for 48h. The human VEGFa concentrations in cell culture medium ((A) HEK293T, (B) SW480, (C) HCT116, (D) HT29 and (E) CaCo2) were determined by an ELISA. The VEGFa concentration in cell culture medium is expressed in pg/ml. Data are presented as the mean ± S.D. (n=3). * $p < 0.05$, ** $p < 0.01$, *** $p < 0.001$, vs. pT group. + $p < 0.05$, ++ $p < 0.01$, vs. corresponding group.

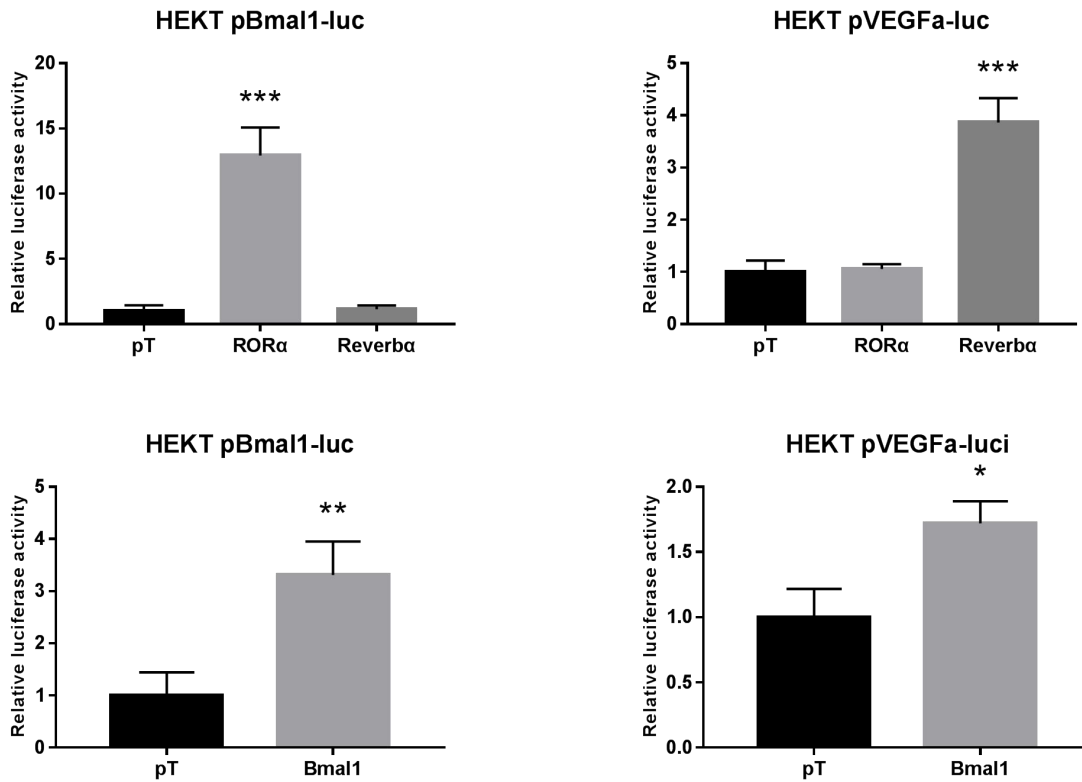
4.10 REVERBA enhances the activity of the VEGFa gene promoter

To examine whether REVERBA regulates transcription of the VEGFa gene, luciferase assay was performed *in vitro*, using VEGFa promoter reporter constructs (pVEGFa-luc). BMAL1 promoter reporter constructs (pBMAL1-luc) were used as a positive control read-out for ROR α and BMAL1 activities. We conducted co-transfection of ROR α , REVERBA or BMAL1 with pBMAL1-luc or pVEGFa-luc in HEK293T, SW480 and HCT116 cells, respectively, and examined the expression of ROR α , REVERBA and VEGFa (dimer and monomer) by WB (Figure 4.11, Figure 4.12, and Figure 4.13).

As shown in Figure 4.11A, Figure 4.12A, and Figure 4.13A, pBMAL1-luc was used as a positive control reporter for verifying the transfection efficiency of ROR α and BMAL1, according to the literature (Lowrey and Takahashi, 2011). Co-transfection of pBMAL1-luc reporter with ROR α or BMAL1, resulted in a significant increase in the transcriptional activity. Co-transfection of pVEGFa-luc reporter with BMAL1 resulted in a significant increase in the transcriptional activity, result in accordance with the existing literature (Lasse et al., 2012). However, co-transfection of pVEGFa-luc reporter with ROR α , failed to increase transcriptional activity, suggesting that ROR α has no effect on the promoter activity of VEGFa.

Notably, co-transfection of pVEGFa-luc reporter with REVERBA, instead resulted in a significant increase in the transcriptional activity, suggesting that REVERBA regulates transcription of VEGFa by activating the promoter activity of VEGFa.

A



B

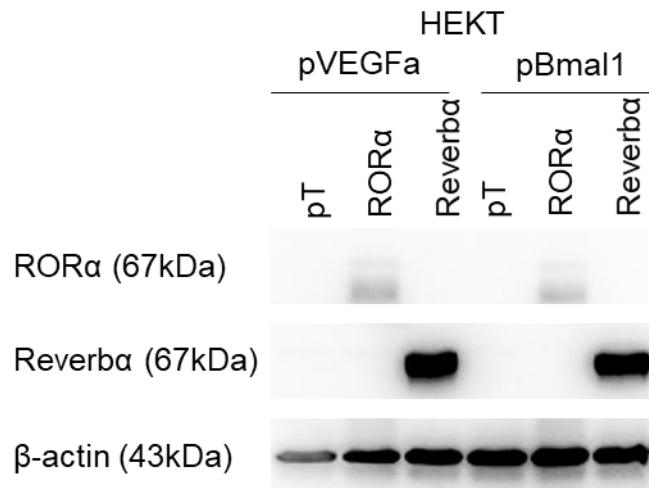
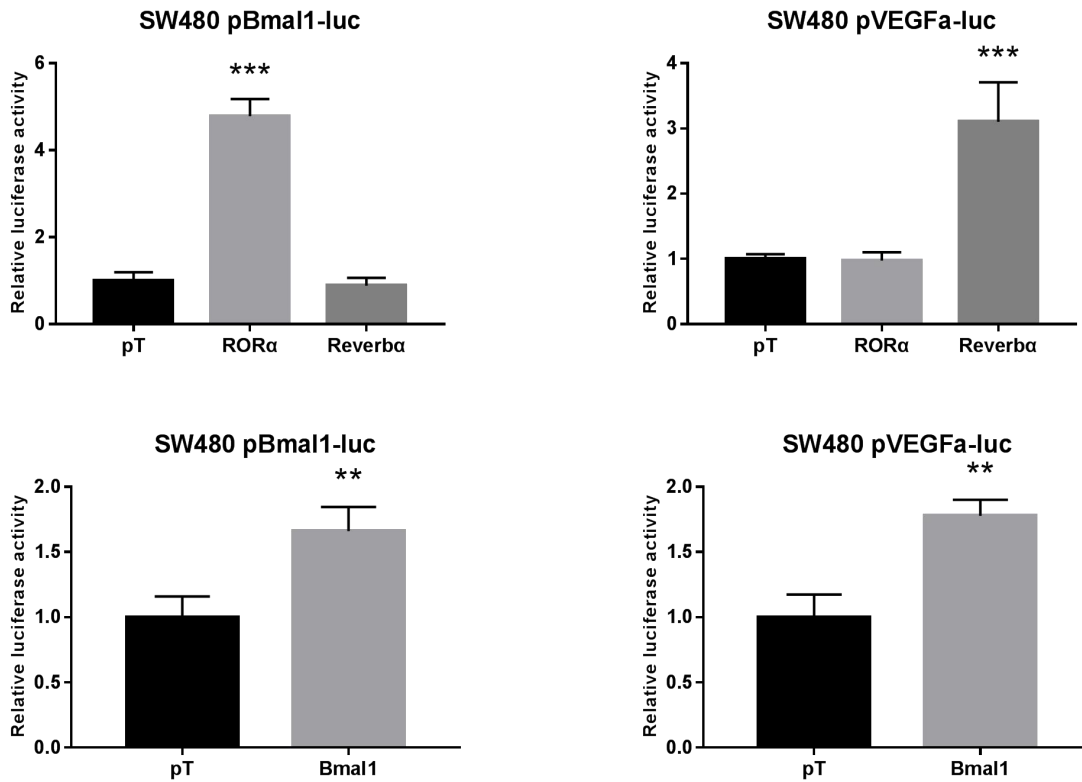


Figure 4.11 Transcriptional regulation of human VEGFa and BMAL1 genes by RORα, REVERBA and BMAL1 in HEK293T cells.

(A) pBMAL1 or pVEGFa luciferase plasmid were transfected together with pT, RORα, REVERBA or BMAL1, respectively, in HEK293T cells. The relative luciferase activity was measured 48h later. (B) The expression of RORα, REVERBA was detected by Western blot using β-actin as the control. Data are presented as the fold ± S.D. (n=3). * $p < 0.05$, ** $p < 0.01$, *** $p < 0.001$, vs. pT group.

A



B

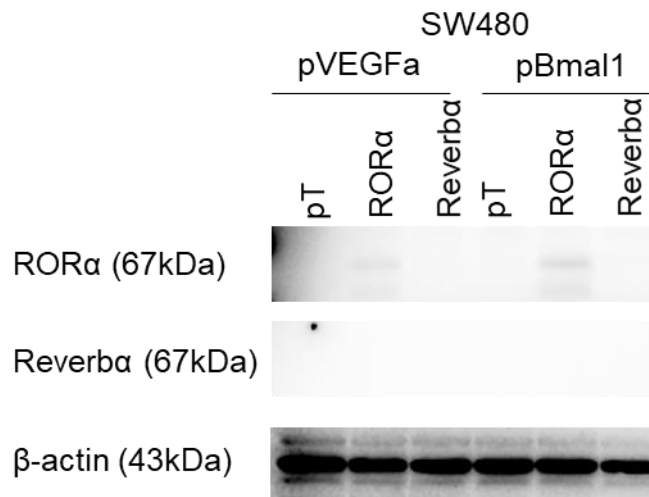
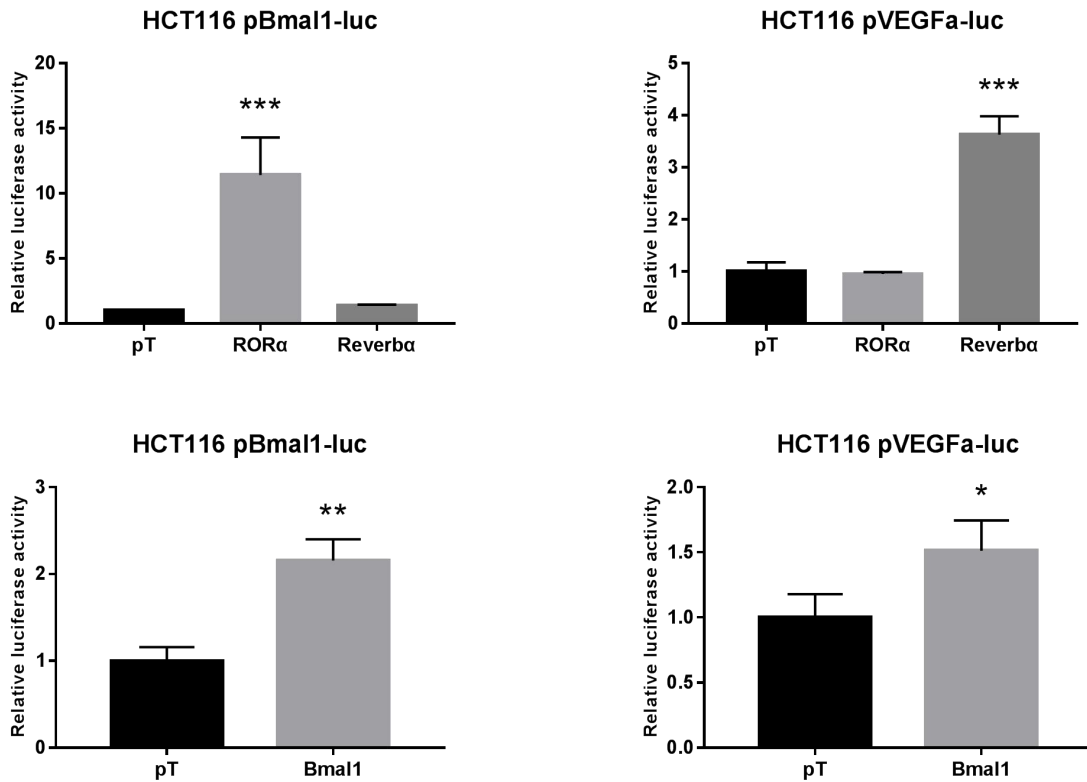


Figure 4.12 Transcriptional regulation of human VEGFa and BMAL1 genes by ROR α , REVERBA and BMAL1 in SW480 cells.

(A) pBMAL1 or pVEGFa luciferase plasmid were transfected together with pT, ROR α , REVERBA or BMAL1, respectively, in SW480 cells. The relative luciferase activity was measured 48h later. (B) The expression of ROR α , REVERBA was detected by Western blot using β -actin as the control. Data are presented as the fold \pm S.D. (n=3). ** p <0.01, *** p <0.001, vs. pT group.

A



B

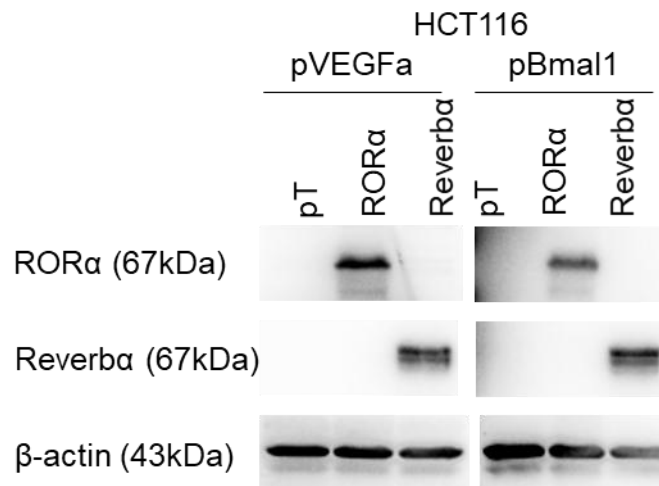


Figure 4.13 Transcriptional regulation of human VEGFa and BMAL1 genes by ROR α , REVERBA and BMAL1 in HCT116 cells.

(A) pBMAL1 or pVEGFa luciferase plasmid were transfected together with pT, ROR α , REVERBA or BMAL1, respectively, in HCT116 cells. The relative luciferase activity was measured 48h later. (B) The expression of ROR α , REVERBA was detected by Western blot using β -actin as the control. Data are presented as the fold \pm S.D. (n=3). * p <0.05, ** p <0.01, *** p <0.001, vs. pT group.

4.11 REVERBA cooperates with BMAL1 to enhance the promoter activity of VEGFa

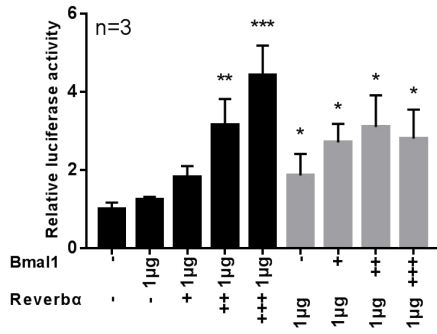
It has reported that BMAL1 directly binds to and activates the VEGFa promoter via E-boxes. In accordance, we showed that REVERBA regulates the transcription of VEGFa by activating the promoter activity of VEGFa. To evaluate the possible contribution of REVERBA to BMAL1-mediated activation on the promoter of VEGFa, 3 cell lines (HEK293T, SW480, and HCT116) were co-transfected with 1 μ g of BMAL1 together with increasing amounts (0.5 μ g, 1 μ g, 2 μ g) of REVERBA or with 1 μ g of REVERBA together with increasing amounts (0.5 μ g, 1 μ g, 2 μ g) of BMAL1, respectively (Figure 4.14).

As shown in Figure 4.14, an increased activation of the promoter of VEGFa was observed with the increased amount of REVERBA, but not with the increased amount of BMAL1, suggesting that REVERBA cooperates with BMAL1 to enhance the promoter activity of VEGFa. Hence, REVERBA might have a direct effect on the promoter activity of VEGFa.

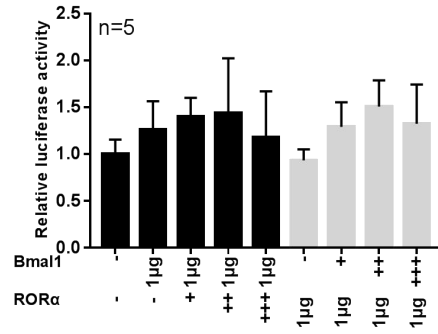
Because ROR α directly activates BMAL1 transcription, contribution of ROR α to BMAL1-mediated activation on the promoter of VEGFa was also evaluated. As shown in Figure 4.14, co-transfection of the pVEGFa-luc reporter with both ROR α and BMAL1 failed to increase the promoter activity of VEGFa, suggesting that ROR α is not cooperating with BMAL1.

A

HEKT Reverba+Bmal1 co-transfection pVEGFa-luc

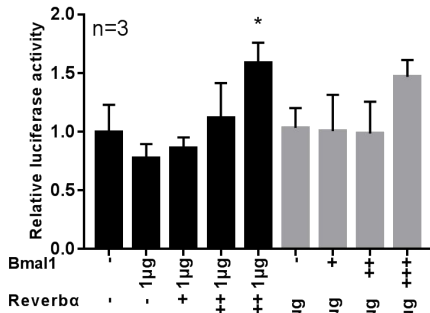


HEKT RORα+Bmal1 co-transfection pVEGFa-luc

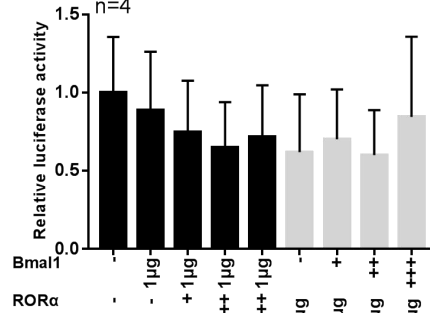


B

SW480 Reverba+Bmal1 co-transfection pVEGFa-luc

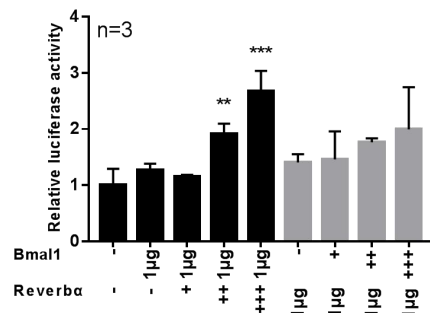


SW480 RORα+Bmal1 co-transfection pVEGFa-luc



C

HCT116 Reverba+Bmal1 co-transfection pVEGFa-luc



HCT116 RORα+Bmal1 co-transfection pVEGFa-luc

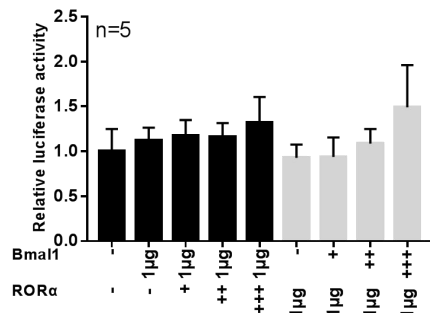


Figure 4.14 Transcriptional regulation of pVEGFa-luc reporter activity by BMAL1 and REVERBA co-transfection or by BMAL1 and RORα co-transfection.

(A) HEK293T, (B) SW480, and (C) HCT116 cells were co-transfected with BMAL1 (1µg) together with increasing amounts (+ = 0.5µg, ++ = 1µg, and +++ = 2µg) of REVERBA and reversely. Similarly, (A) HEK293T, (B) SW480, and (C) HCT116 cells were co-transfected with BMAL1 (1µg) together with increasing amounts (+ = 0.5µg, ++ = 1µg, and +++ = 2µg) of RORα and reversely. The pVEGFa-luc reporter was transfected in all of the above groups. The total plasmid amount of each well was

balanced with pT plasmid. The luciferase activity was measured and analyzed as above. Data are presented as the fold \pm S.D. (n=3-5). * p <0.05, ** p <0.01, *** p <0.001, vs. control.

4.12 REVERBA induces resistance of colorectal cancer cells to anti-angiogenesis therapy with VEGFa-neutralizing antibody bevacizumab

To evaluate the effect of ROR α , REVERBA and BMAL1 on the cellular response to the anti-angiogenesis treatment, 3 cell lines (HEK293T, SW480, and HCT116) were co-transfected with pVEGFa-luc reporter together with ROR α , REVERBA or BMAL1 plasmid, followed by incubation in conditioned medium (CM) in presence or absence of the VEGFa-neutralizing Ab (B20, murinized Beva). Thereafter, the promoter activity of VEGFa was measured by luciferase assay (Figure 4.15).

As shown in Figure 4.15, cells transfected with REVERBA without CM stimulation exhibited an increase of 3.05 ± 0.91 -fold, 2.80 ± 0.44 -fold, and 12.26 ± 2.61 -fold of the promoter activity of VEGFa compared with the empty-vector control group. These data from the 3 cell lines (HEK293T, SW480, and HCT116) suggested that REVERBA exerts a positive effect on the VEGFa promoter activity, in line with previous results (Figure 4.11, Figure 4.12, Figure 4.13 and Figure 4.14).

To further investigate whether CM affects the VEGFa promoter activity, CM was used to stimulate the cells. Under these conditions, REVERBA significantly increased VEGFa promoter activity by 5.70 ± 2.29 -fold, 5.63 ± 0.69 -fold, and 17.77 ± 5.06 -fold compared to empty-vector control group. This effect was evident in all 3 cell lines (HEK293T, SW480, and HCT116), suggesting that CM containing secreted growth factors including VEGFA itself stimulated the VEGFa promoter activity in presence of REVERBA.

B20 was added into CM to neutralize VEGFa, and the result showed that a significant decrease of 3.96 ± 2.33 -fold, 4.66 ± 0.91 -fold, and 14.97 ± 3.82 -fold in the VEGFa promoter activity compared to the CM stimulation group was observed. However, the VEGFa promoter activity was still higher than in the DMEM (starvation medium) control group, suggesting that REVERBA conferred resistance to anti-angiogenesis treatment (by B20) in presence of CM, harboring VEGFA and other growth factors.

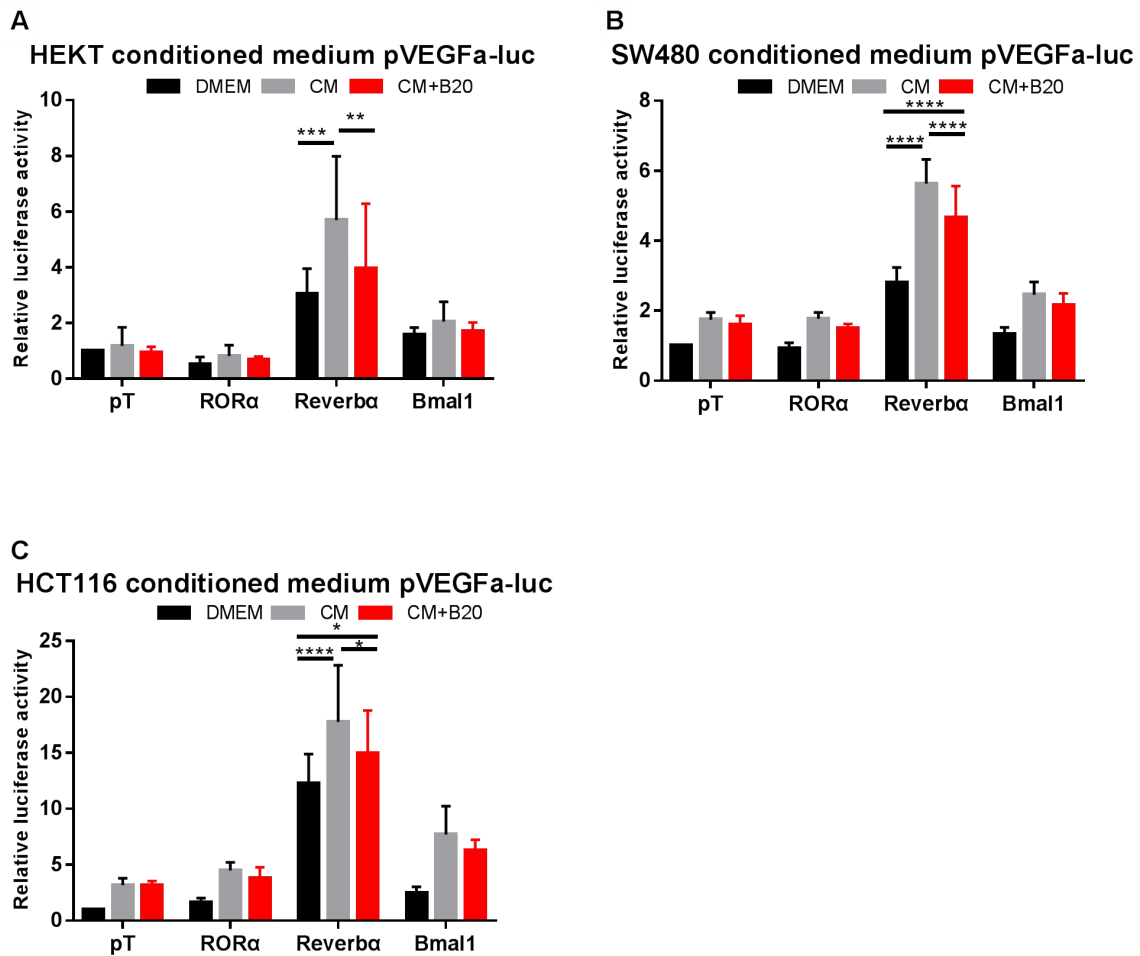


Figure 4.15 Transcriptional regulation of pVEGF α -luc reporter activity by conditioned medium and anti-VEGF α therapy.

(A) HEK293T, (B) SW480, and (C) HCT116 cells were transfected with ROR α , REVERBA and BMAL1 for 24h, followed by starvation for 24h in serum-free basal medium (DMEM -/-) before re-stimulation with conditioned medium (CM) in presence or absence of B20 (at 10 μ g/ml) for 24h, respectively. The luciferase activity was measured and analyzed. Data are presented as the fold \pm S.D. (HEK293T: n=7; SW480: n=8; HCT116: n=8). * p <0.05, ** p <0.01, *** p <0.001, **** p <0.0001 vs. pT DMEM.

4.13 Effect of REVERBA and BMAL1 on signaling pathway reporters

To evaluate the effect of REVERBA and BMAL1 on different signaling pathways, 4 different signaling pathway reporters were used to detect hypoxia (SRE-luc), metabolic (PPRE-luc), Ras (SRE-luc), and Wnt (TOPflash-luc) signaling pathways. 3 cell lines (HEK293T, SW480, and HCT116) were transfected with luciferase reporters together with REVERBA or BMAL1, followed by starvation before restimulation with conditioned medium (CM) in presence or absence of B20 (at 10 $\mu\text{g/ml}$), respectively. The luciferase activity of reporters was measured and analyzed.

As shown in Figure 4.16, Figure 4.17, and Figure 4.18, cells transfected with REVERBA showed an increased luciferase signal in most signaling pathway reporters, especially in HCT116 cells. While B20 was used to block VEGFa, a decreased luciferase signal was observed, especially in HCT116 cells.

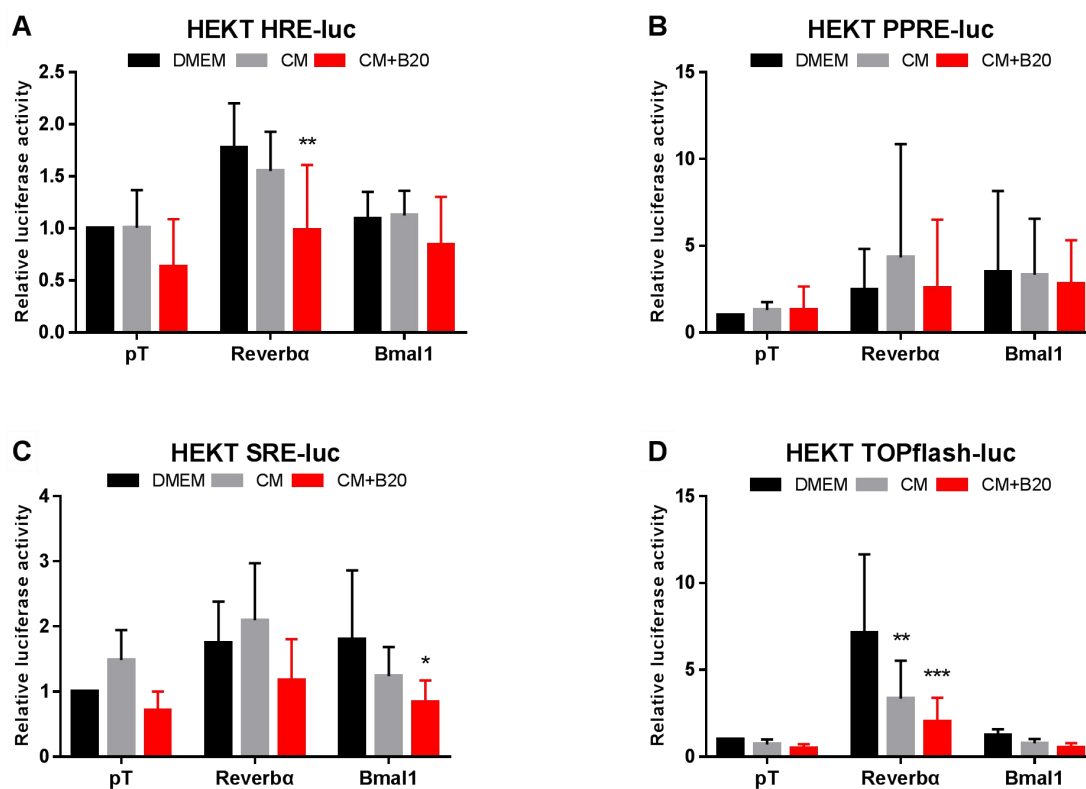


Figure 4.16 Transcriptional regulation of HRE-luc reporter, PPRE-luc reporter, SRE-luc reporter and TOPflash-luc reporter activities by conditioned medium and anti-VEGFa therapy in HEK293T cells.

HEK293T cells were transfected with luciferase reporter together with REVERBA or BMAL1 for 24h, followed by starvation for 24h by serum-free DMEM *-/-* before restimulation with conditioned medium (CM) in presence or absence of B20 (at 10 μ g/ml) for 24h, respectively. The luciferase activity of (A) HRE-luc reporter, (B) PPRE-luc reporter, (C) SRE-luc reporter, and (D) TOPflash-luc reporter was measured and analyzed. Data are presented as the fold \pm S.D. (n=5). * p <0.05, ** p <0.01, *** p <0.001, vs. pT DMEM.

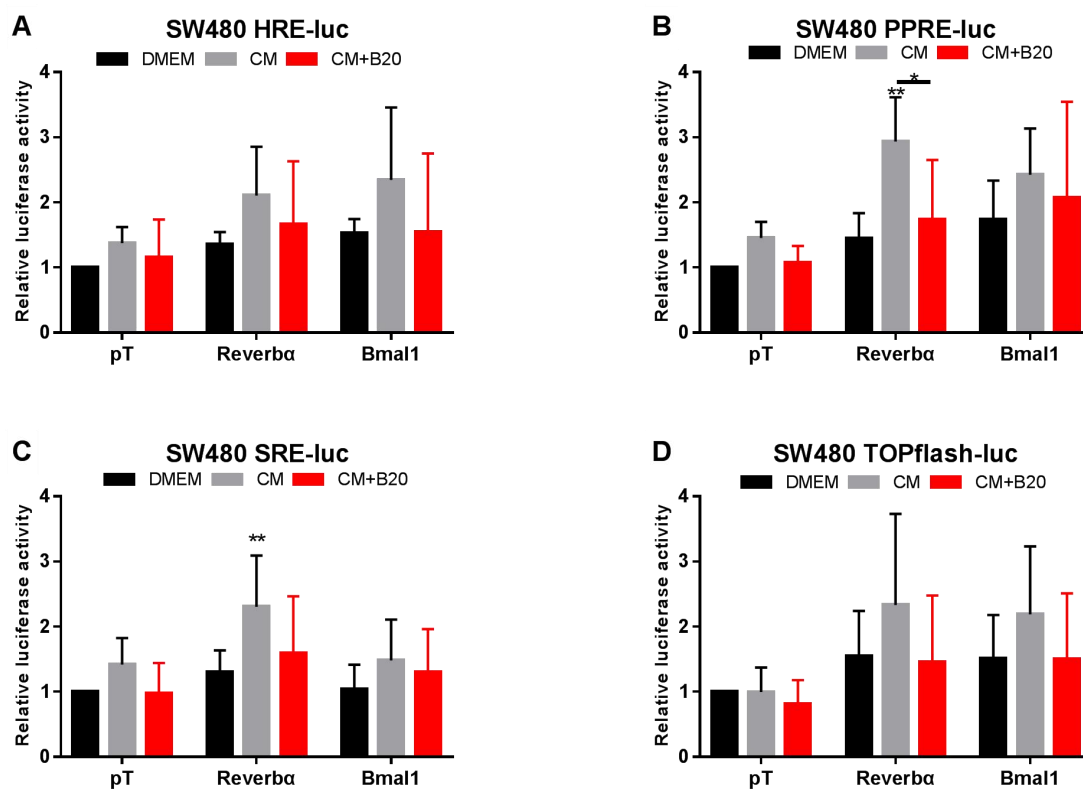


Figure 4.17 Transcriptional regulation of HRE-luc reporter, PPRE-luc reporter, SRE-luc reporter and TOPflash-luc reporter activities by conditioned medium and anti-VEGF α therapy in SW480 cells.

SW480 cells were transfected with luciferase reporter together with REVERBA or BMAL1 for 24h, followed by starvation for 24h by serum-free DMEM $-/-$ before restimulation with conditioned medium (CM) in presence or absence of B20 (at 10 μ g/ml) for 24h, respectively. The luciferase activity of (A) HRE-luc reporter, (B) PPRE-luc reporter, (C) SRE-luc reporter, and (D) TOPflash-luc reporter was measured and analyzed. Data are presented as the fold \pm S.D. (n=6). * p <0.05, ** p <0.01, vs. pT DMEM.

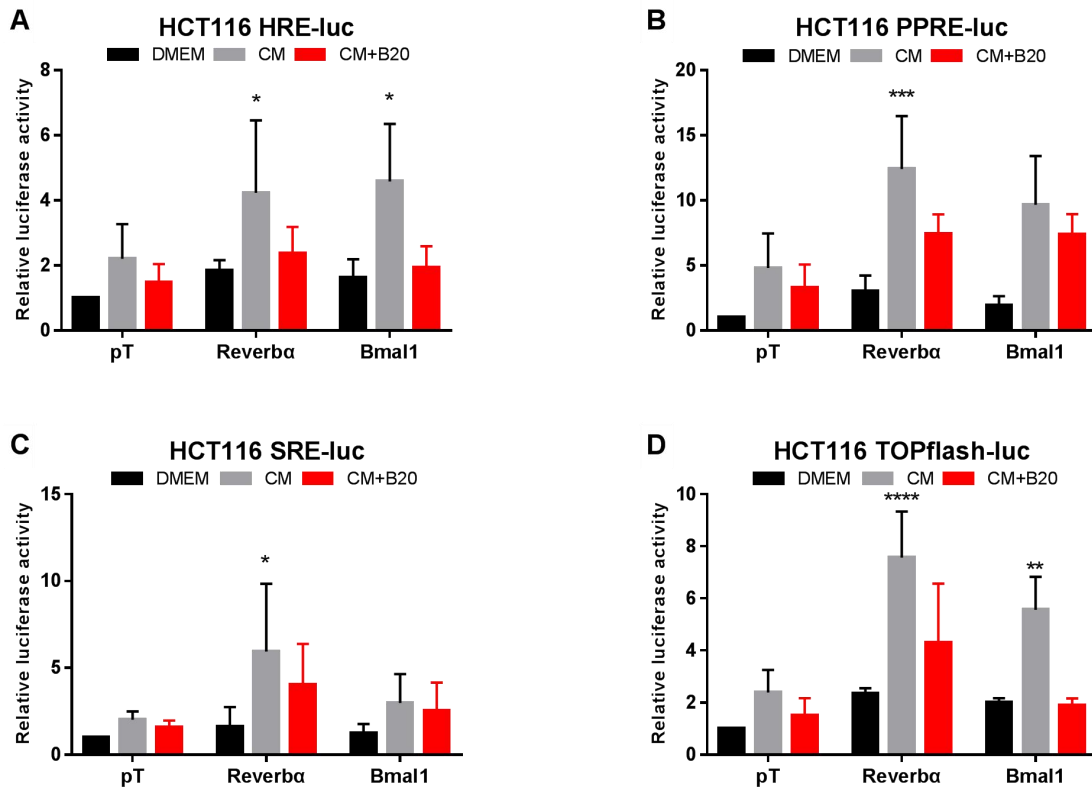


Figure 4.18 Transcriptional regulation of HRE-luc reporter, PPRE-luc reporter, SRE-luc reporter and TOPflash-luc reporter activities by conditioned medium and anti-VEGF α therapy in HCT116 cells.

HCT116 cells were transfected with luciferase reporter together with REVERBA or BMAL1 for 24h, followed by starvation for 24h by serum-free DMEM $-/-$ before restimulation with conditioned medium (CM) in presence or absence of B20 (at 10 μ g/ml) for 24h, respectively. The luciferase activity of (A) HRE-luc reporter, (B) PPRE-luc reporter, (C) SRE-luc reporter, and (D) TOPflash-luc reporter was measured and analyzed. Data are presented as the fold \pm S.D. (n=3). * p <0.05, ** p <0.01, vs. pT DMEM.

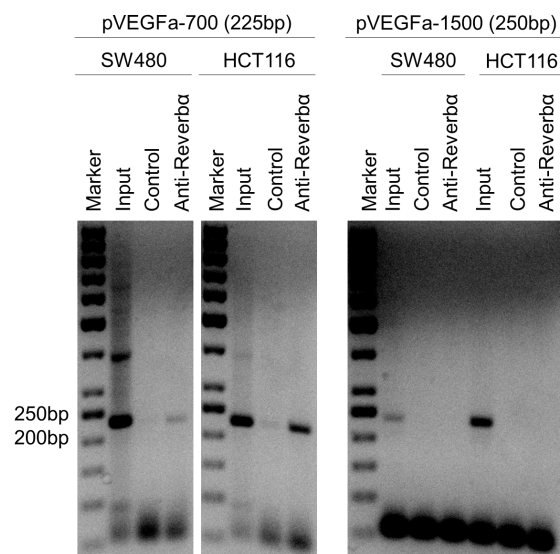
4.14 REVERBA binds directly to the promoter region of human VEGFa using chromatin immunoprecipitation assay

To confirm whether REVERBA binds directly to the promoter region of human VEGFa, nuclear extract from SW480 and HCT116 cells transfected with REVERBA for 48h was applied to a chromatin immunoprecipitation (ChIP) assay and quantified by real-time PCR (Figure 4.19).

As shown in Figure 4.19A, 2 primers (pVEGFa-700 and pVEGFa-1500) were designed to detect the binding of REVERBA to the human VEGFa promoter region. The -700kB RORE DNA-element in the proximal human VEGFa promoter was co-precipitated by anti-REVERBA antibody. On the other hand, the -1500kB RORE DNA-element in the proximal human VEGFa promoter failed to be enriched by anti-REVERBA antibody. These data revealed that REVERBA binds to the -700kB RORE DNA-element in the proximal human VEGFa promoter.

Furthermore, real-time PCR was performed to quantify the enrichment of the -700kB RORE DNA-element and the -1500kB RORE DNA-element, respectively. As shown in Figure 4.19B, the -700kB RORE DNA-element was significantly enriched in both SW480 and HCT116 cells using anti-REVERBA antibody, however, the -1500kB RORE DNA-element showed no significant increase in neither SW480 nor HCT116 cells. The fold enrichment of the -700kB RORE DNA-element was 1.76 ± 0.58 -fold and 2.01 ± 0.30 -fold compared to 0.61 ± 0.17 -fold and 0.51 ± 0.08 -fold in the control group in SW480 and HCT116 cells, respectively, suggesting that REVERBA binds directly to the promoter region of human VEGFa.

A



B

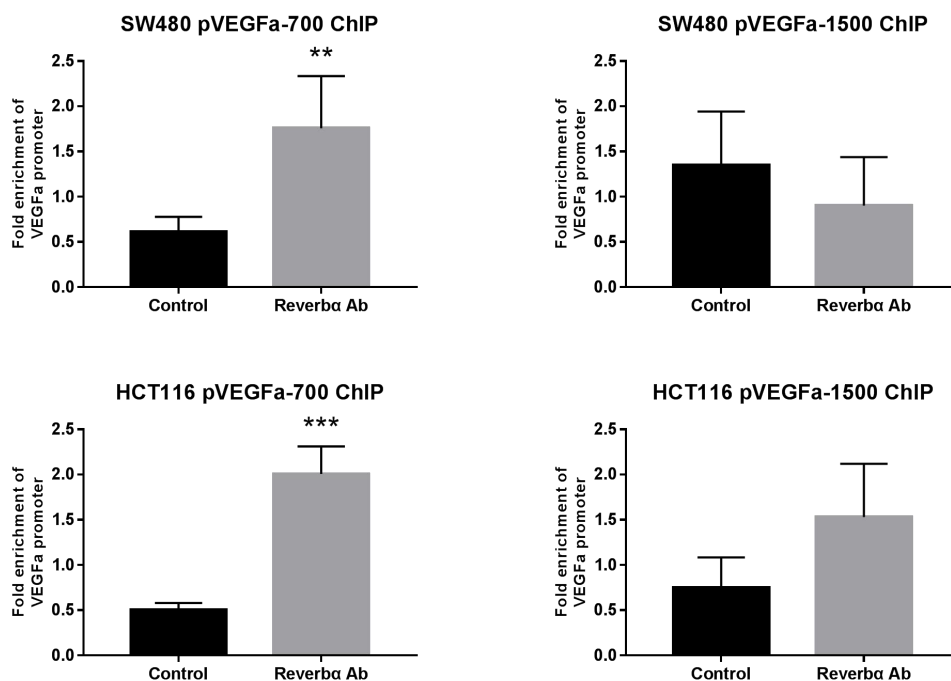


Figure 4.19 ChIP results showing REVERBA binding to the -700kB RORE DNA-element in the proximal human VEGFA promoter.

ChIP assay was performed using anti-REVERBA antibody. The co-precipitated DNA was amplified using pVEGFa-700 or pVEGFa-1500 primers targeting the VEGFa promoter. (A) Gels picture showing SW480 and HCT116 cells transfected with REVERBA for 48h, followed by ChIP procedure, before amplification of co-precipitated DNA. (B) qPCR analysis showing enrichment of VEGFa promoter DNA. SW480 and HCT116 cells transfected with REVERBA for 48h, followed by ChIP procedure, real-time qPCR was performed using co-precipitated DNA. Data are presented as the fold \pm S.D. (SW480 pVEGFa-700: n=5; SW480 pVEGFa-1500: n=3; HCT116: n=4). ** p <0.01, *** p <0.001, vs. control.

4.15 REVERBA binds directly to the promoter region of human VEGFa using electrophoretic mobility shift assay

To further confirm whether REVERBA binds directly to the promoter region of human VEGFa, electrophoretic mobility shift assay (EMSA) was performed (Figure 4.20). HEK293T, SW480, and HCT116 cells were transfected with REVERBA for 48h, and nuclear extracts were incubated with biotin (Saltz et al.)-labelled oligonucleotide (Bio-RORE-700) from the human VEGFa promoter and an excess of unlabeled competitor oligonucleotides (Comp-RORE-700 = wild type; Bio-MutRORE-700 = mutant) and a biotin-labelled oligonucleotide with a mutant RORE-700.

As shown in Figure 4.20A and Figure 4.20B, increased protein binding to the -700kB RORE DNA-element was visible in nuclear extracts from REVERBA-transfected compared to empty-vector-transfected HEK293T cells. And the binding complex was competed by an excess of unlabeled oligonucleotides.

As shown in Figure 4.20C and Figure 4.20D, increased protein binding to the -700kB RORE DNA-element, though weak, was also observed in SW480 cells. Binding intensity was increased in REVERBA-transfected cells compared to empty-vector-transfected SW480 cells.

Similar results were found in HCT116 cell. As shown in Figure 4.20E and Figure 4.20F, increased protein binding to the -700kB RORE DNA-element was observed in REVERBA-transfected cells compared to empty-vector-transfected HCT116 cells.

These data demonstrated that REVERBA binds directly to the promoter region of human VEGFa.

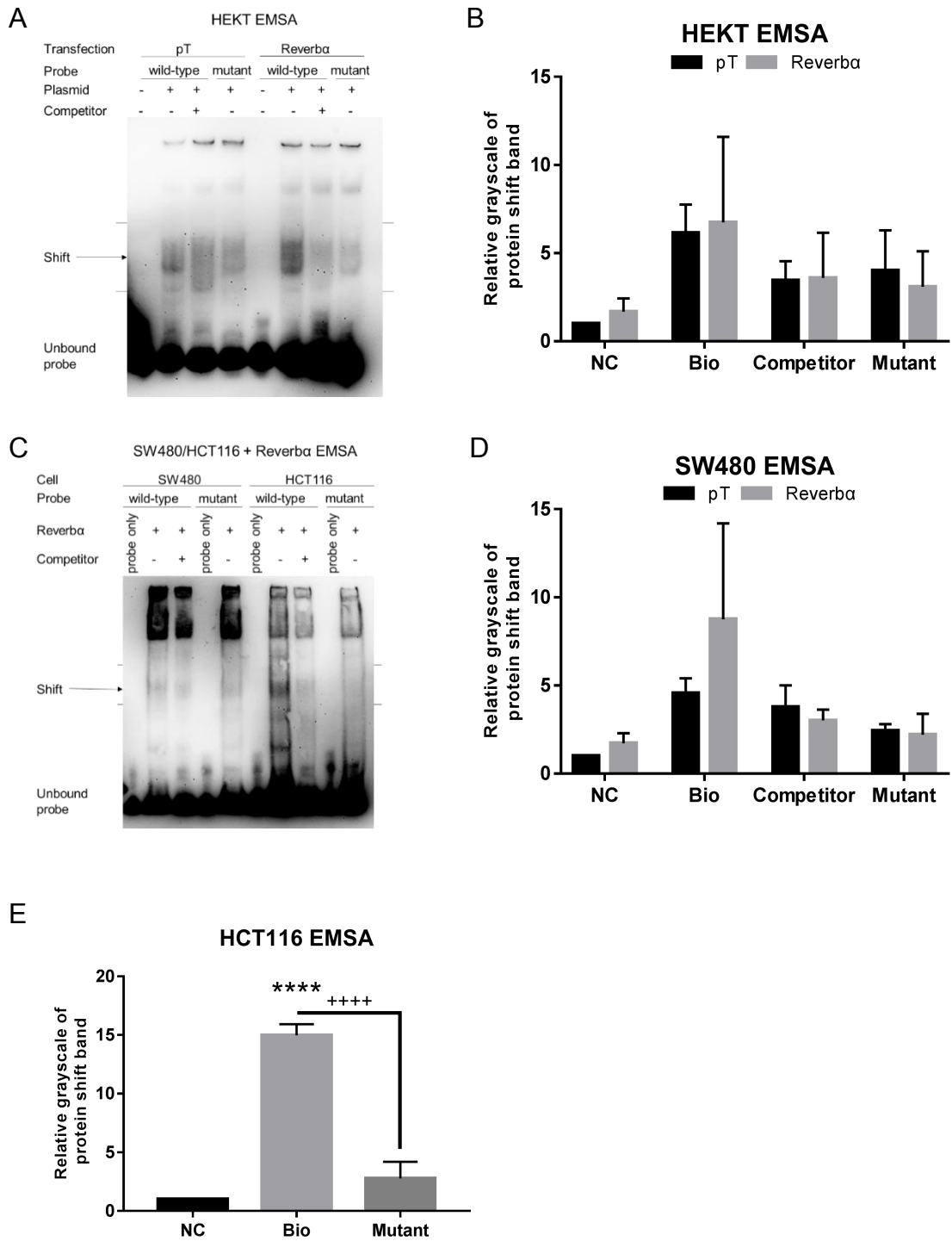


Figure 4.20 EMSA results showing REVERBA binding to the -700kB RORE DNA-element in the proximal human VEGFA promoter.

EMSA with nuclear extracts of (A) HEK293T, (C) SW480 and HCT116 cells transfected with pT or REVERBA. An -700kB RORE DNA-element in the VEGFa promoter was synthesized as a wild-type probe. The mutant probe has same sequence except that REVERBA binding site was mutated. REVERBA binding specificity was proved by competition with non labeled probe. (B), (D), and (E) showing relative gray scale of protein shift band. Data are presented as the fold \pm S.D. (HEK293T, SW480: n=3; HCT116: n=4). **** $p < 0.0001$, vs. NC, ++++ $p < 0.0001$, vs. Mutant.

5 Discussion

Therapy failure in patients with advanced CRC is a major obstacle to curative treatment and improved survival. The efficacy of antibodies which inhibit angiogenesis is often limited by yet unknown mechanisms of unresponsiveness or resistance in CRC patients. Thus, novel markers or targets are needed. The nuclear transcription factors receptors (ROR α , REVERBA and BMAL1) are potential new players within these metabolic signaling pathways, whose expression and/or activities are altered in CRC.

5.1 ROR α is associated with the clinicopathological variables concerning tumor progression

There are three ROR family members (RORs) including ROR α (Becker-Andre et al., 1993), ROR β (Andre et al., 1998b) and ROR γ (He et al., 1998). RORs contain a structural architecture that is typical of nuclear receptors (Jetten and Joo, 2006). Figure 1.2c shows the four major functional domains of RORs: an amino-terminal (A/B) domain, a DNA-binding domain (DBD), a hinge domain, and a ligand-binding domain (LBD). The DBD consists of two highly conserved zinc finger motifs involved in the recognition of ROR-response elements (ROREs) which harbour the consensus motif AGGTCA preceded by an AT-rich sequence (Andre et al., 1998a; Carlberg et al., 1994).

The binding of ligands to a region called the LBD causes a conformational change, which results in a cascade of downstream events (Kojetin and Burris, 2014). RORs and Reverbs share multiple target genes and have overlapping in functions including regulation of circadian rhythm, metabolism homeostasis and immune function (Burris, 2008; Duez and Staels, 2009; Jetten, 2009; Jetten et al., 2013). The LBDs of nuclear receptors (RORs and Reverbs) play a role in ligand binding, nuclear localization, receptor dimerization, contain a transactivation function, and provide an interface for

the interaction with co-activators and co-repressors. The LBDs of RORs are moderately conserved; the LBD of ROR α exhibits, respectively, a 63% and 58% identity with the LBDs of ROR β and ROR γ (Jetten, 2004; Jetten et al., 2001).

Recent studies suggest that ROR α may be a tumor suppressor candidate. ROR α is down-regulated in various tumors such as esophageal cancer, colon cancer, liver cancer, pancreatic cancer, cervical cancer, breast cancer, prostate cancer, ovarian cancer, head and neck cancer, bladder cancer, and leukemia (Du and Xu, 2012). Compared with normal breast tissue, ROR α expression was down-regulated or decreased in breast cancer, while restoring ROR α expression inhibited breast cancer cell proliferation and invasion in vitro and in vivo, suggesting that ROR α is a tumor suppressor gene and therapeutic target for breast cancer (Du and Xu, 2012). ROR α and its target genes are down-regulated in human CRC, and decreased expression of ROR α and its target genes promotes proliferation and migration of CRC cells and angiogenesis, while activation of ROR α inhibits proliferation and migration of CRC cells and angiogenesis, which suggests that low expression of ROR α marks tumor progression and may be detrimental for clinical performance of colon cancer patients. (Xiao et al., 2015). One possible explanation is that ROR α attenuates the Wnt/ β -catenin signaling pathway in CRC (Lee et al., 2010), proposing ROR α as a key regulator of cancer cell proliferation (Shin et al., 2014). In our present study, we found that ROR α is significantly downregulated in human CRC tissues, which is associated with the clinicopathological variables concerning tumor progression such as histological de-differentiation and tumor stage. These findings indicate that ROR α may serve as a biomarker regarding prognosis of CRC. We also found that expression of ROR α shows a higher trend in mice responding to anti-angiogenesis treatment compared to that in non-responding animals. However only 4 responder and 4 non-responder mice were used, thus, more samples will be required to confirm in the future.

5.2 REVERBA exerts a potential mechanism to positively regulate VEGFA expression.

REVERBA, also known as NR1D1 (nuclear receptor subfamily 1, group D, member 1), is a protein which is encoded by the NR1D1 gene in humans (Lazar et al., 1990). Figure 1.2b shows the four major functional domains of Reverbs: an amino-terminal (A/B) domain, a DBD, a hinge domain, and an LBD. Thus, REVERBA has similar binding specificities for ROREs as the RORs (Giguere et al., 1995). REVERBA act as transcriptional repressor (Cho et al., 2012; Yin et al., 2010), thus it is able to inhibit ROR-mediated transcriptional activation by competing with ROR α for binding to the ROREs (Austin et al., 1998; Bois-Joyeux et al., 2000). In terms of regulation of the circadian clock system, Rev-erba also targets a large number of genes involved in metabolism and cell survival (Bugge et al., 2012; Cho et al., 2012; Duez and Staels, 2009; Yang et al., 2006). In addition, Sengupta et al. have shown that REVERBA is regulated by oxidative stress and inflammation (Yang et al., 2014).

Recent studies suggest that REVERBA plays an important role in cancer. The expression level of REVERBA is correlated with a poor prognosis of breast cancer (Chin et al., 2006; Davis et al., 2007). In agreement with these data, REVERBA enhances the survival of breast cancer cells by upregulating several genes in the de novo fatty acid synthase network associated with aerobic glycolysis (Taylor et al., 2010). Kourtidis et al. demonstrated that breast cancer cells are genetically preprogrammed to depend on NR1D1 for the energy production necessary for survival (Kourtidis et al., 2010).

However, the role of REVERBA in responding to the anti-angiogenesis treatment in CRC is not known. In our present study, we found that REVERBA is upregulated in human CRC and is associated with the clinicopathological variables concerning tumor progression such as tumor grade and tumor stage. REVERBA shows a trend for higher expression in tissues of non-responder mice than in responder mice, which indicates that REVERBA is associated with anti-angiogenesis treatment in CRC. To

explore the effect of REVERBA on the activity of the human VEGFa gene transcription in CRC cells, qPCR was performed in HEK293T and SW480 cells, and we found overexpression of REVERBA in CRC cells increases human VEGFa transcriptional expression. Next, we explored the effect of REVERBA on the secretion of human VEGFa protein from CRC cells, and found overexpression of REVERBA increases human VEGFa secretion *in vitro*. To examine whether REVERBA regulates the transcription of human VEGFa mRNA, luciferase assay was performed *in vitro*, and we found REVERBA enhances the promoter activity of VEGFa. ChIP and EMSA were further performed, and we found REVERBA binds directly to the promoter region of human VEGFa. Based on these data, we may explain why REVERBA induced resistance of colorectal cancer cells and/or tissues to anti-angiogenesis treatment.

5.3 BMAL1 is a potential marker of resistance to anti-angiogenesis treatment in CRC

BMAL1 is protein that in humans is encoded by the ARNTL gene, also known as MOP3. ROR α and REVERBA, respectively, activate and repress transcription of the BMAL1 gene, which encodes a transcription factor that is important in the regulation of the circadian rhythm system, by competing for ROREs in the promoter region of the BMAL1 gene (Akashi and Takumi, 2005; Guillaumond et al., 2005; Ikeda and Nomura, 1997; Triqueneaux et al., 2004).

Disruption of the circadian clock system, e.g. by mutation or sleep deprivation, would not only affect the physiological homeostasis, but also leads to various diseases, such as cancer (Jensen and Cao, 2013). BMAL1 has been reported to play an important role in the tumorigenesis, such as regulation of cell proliferation, cell cycle, and cell invasion (Geyfman et al., 2012; Jung et al., 2013; Mullenders et al., 2009; Sahar and Sassone-Corsi, 2007). Zeng et al. (Zeng et al., 2010) reported that BMAL1 regulates tumor cell apoptosis, and down-regulation of BMAL1 accelerates the development of tumors and may influence the response to anti-cancer drugs in mouse CRC. Zeng et

al. (Zeng et al., 2014) then revealed that overexpression of BMAL1 is able to inhibit CRC cell proliferation and increase CRC sensitivity to oxaliplatin in colorectal cancer cell lines and in a mouse CRC model. Moreover, the overall survival of CRC patients with high BMAL1 levels in their primary tumors is significantly longer than that of patients with low BMAL1 levels. In addition, recent studies demonstrate that BMAL1 also regulate VEGF-dependent angiogenesis. Jensen et al. (Jensen et al., 2012) reported that that BMAL1 directly binds to and activates the VEGF promoter via E-boxes, and knockdown of BMAL1 directly reduced VEGF promoter activity.

In our present study, we found that BMAL1 is downregulated in human CRC and is associated with the clinicopathological variables concerning tumor progression such as tumor grade and tumor stage. Expression of BMAL1 was found to be reduced in tissues from responder mice compared with non-responder mice, which suggests BMAL1 failure to respond to anti-angiogenesis treatment in CRC. Since BMAL1 directly binds to and activates the VEGF promoter via E-boxes (Jensen et al., 2012). In the current thesis, as shown in Figure 5.1, we found REVERBA also binds to and activates the VEGF promoter via a predicted novel RORE, which means that both BMAL1 and REVERBA are able to bind to the proximal promotor of the VEGFa gene and up-regulate VEGFa expression. Notably, REVERBA also represses BMAL1, which means, on one hand, REVERBA up-regulates VEGFa by binding to p-VEGFa, on the other hand, REVERBA represses VEGFa by inhibiting BMAL1-induced VEGFa up-regulation. Thus, co-transfection was performed to find which is the main factor in determining VEGFa expression levels. The higher dose of REVERBA enforced activation of BMAL1 on VEGFa. However, increasing the amounts of BMAL1 had no effect on VEGF promoter activation. In sum, these data proposed that increased expression of REVERBA in CRC may overtake Bmal1-driven positive regulation of VEGFa gene expression, leading to a vicious circle that cannot be disrupted by VEGFa-neutralizing antibody.

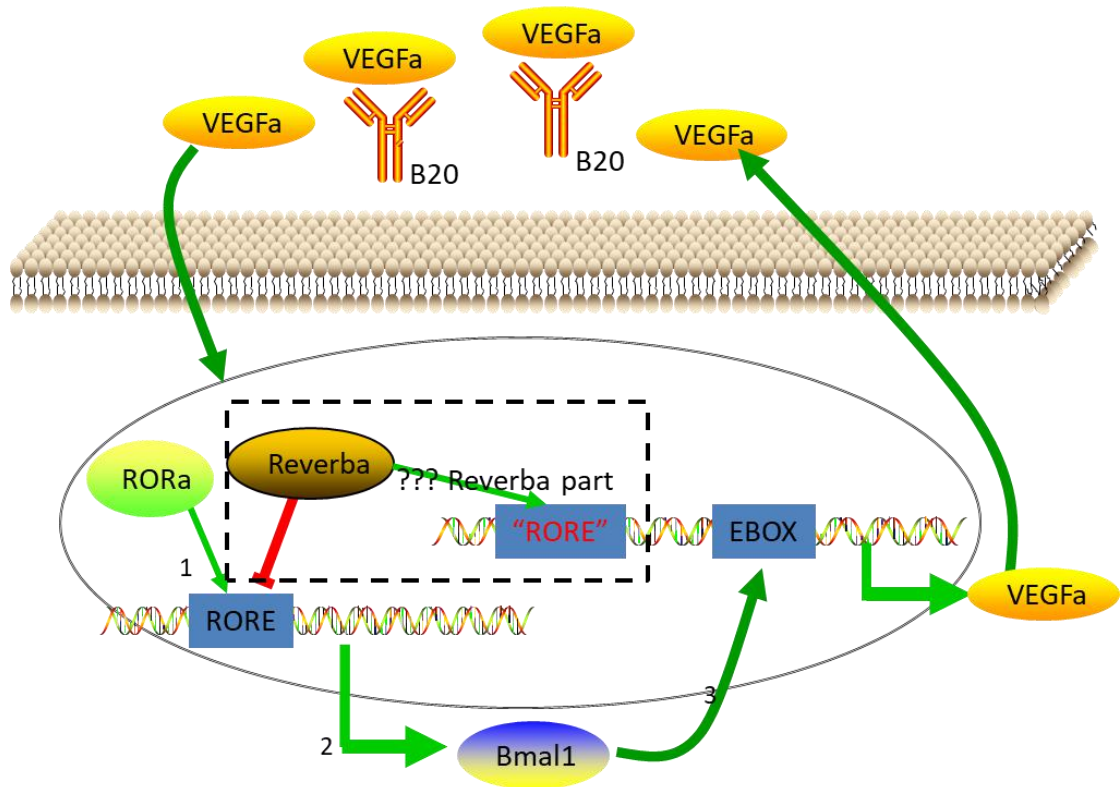


Figure 5.1 Schematic figure of our findings

1=ROR α binds to the RORE in the BMAL1 promoter, 2=ROR α activates BMAL1 transcription, 3=BMAL1 binds to the E-box in the VEGFa promoter, ???=REVERBA activates VEGFa transcription by binding to a novel predicted RORE in the human VEGFA promoter. We suggest that these transcriptional activation mechanisms promote a feed-forward cycle which cannot be disrupted by VEGFA-neutralizing antibody, thus establishing resistance to anti-angiogenic treatment in CRC.

6 Conclusion

In the present study, we found that ROR α is downregulated in CRC, BMAL1 is downregulated in CRC as well, however REVERBA is upregulated in CRC. We demonstrated that the expression of ROR α , REVERBA and BMAL1 is associated with the preclinical response to anti-angiogenesis treatment in mice, and evinced the expression level of ROR α , REVERBA and BMAL1 in various normal mouse tissues and in different colorectal cancer cell lines. Furthermore, we demonstrated that REVERBA increases the proliferation of colorectal cancer cells, and that overexpression of REVERBA in colorectal cancer cells increases human VEGFa transcriptional expression and VEGFa secretion *in vitro*. We also demonstrated that REVERBA enhances the VEGFa promoter activity by binding directly to the promoter region of the human VEGFa gene, and that REVERBA induced resistance of colorectal cancer to anti-angiogenesis treatment by activation of oncogenic signaling pathways (Ras, Wnt).

7 References

Akashi, M., and Takumi, T. (2005). The orphan nuclear receptor RORalpha regulates circadian transcription of the mammalian core-clock BMAL1. *Nat Struct Mol Biol* 12, 441-448.

Andre, E., Conquet, F., Steinmayr, M., Stratton, S.C., Porciatti, V., and Becker-Andre, M. (1998a). Disruption of retinoid-related orphan receptor beta changes circadian behavior, causes retinal degeneration and leads to vacillans phenotype in mice. *EMBO J* 17, 3867-3877.

Andre, E., Gawlas, K., and Becker-Andre, M. (1998b). A novel isoform of the orphan nuclear receptor RORbeta is specifically expressed in pineal gland and retina. *Gene* 216, 277-283.

Austin, S., Medvedev, A., Yan, Z.H., Adachi, H., Hirose, T., and Jetten, A.M. (1998). Induction of the nuclear orphan receptor RORgamma during adipocyte differentiation of D1 and 3T3-L1 cells. *Cell Growth Differ* 9, 267-276.

Bargiello, T.A., Jackson, F.R., and Young, M.W. (1984). Restoration of circadian behavioural rhythms by gene transfer in *Drosophila*. *Nature* 312, 752-754.

Becker-Andre, M., Andre, E., and DeLamarter, J.F. (1993). Identification of nuclear receptor mRNAs by RT-PCR amplification of conserved zinc-finger motif sequences. *Biochem Biophys Res Commun* 194, 1371-1379.

Bois-Joyeux, B., Chauvet, C., Nacer-Cherif, H., Bergeret, W., Mazure, N., Giguere, V., Laudet, V., and Danan, J.L. (2000). Modulation of the far-upstream enhancer of the rat alpha-fetoprotein gene by members of the ROR alpha, Rev-erb alpha, and Rev-erb beta groups of monomeric orphan nuclear receptors. *DNA Cell Biol* 19, 589-599.

Brenner, H., Kloor, M., and Pox, C.P. (2014). Colorectal cancer. *The Lancet* 383,

1490-1502.

Bugge, A., Feng, D., Everett, L.J., Briggs, E.R., Mullican, S.E., Wang, F., Jager, J., and Lazar, M.A. (2012). Rev-erbalpha and Rev-erbbeta coordinately protect the circadian clock and normal metabolic function. *Genes Dev* 26, 657-667.

Burris, T.P. (2008). Nuclear hormone receptors for heme: REV-ERBalpha and REV-ERBbeta are ligand-regulated components of the mammalian clock. *Mol Endocrinol* 22, 1509-1520.

Carlberg, C., Hooft van Huijsduijnen, R., Staple, J.K., DeLamarter, J.F., and Becker-Andre, M. (1994). RZR_s, a new family of retinoid-related orphan receptors that function as both monomers and homodimers. *Mol Endocrinol* 8, 757-770.

Chan, D.S., Lau, R., Aune, D., Vieira, R., Greenwood, D.C., Kampman, E., and Norat, T. (2011). Red and processed meat and colorectal cancer incidence: meta-analysis of prospective studies. *PLoS One* 6, e20456.

Chen, W., Zheng, R., Baade, P.D., Zhang, S., Zeng, H., Bray, F., Jemal, A., Yu, X.Q., and He, J. (2016). Cancer statistics in China, 2015. *CA Cancer J Clin* 66, 115-132.

Chin, K., DeVries, S., Fridlyand, J., Spellman, P.T., Roydasgupta, R., Kuo, W.L., Lapuk, A., Neve, R.M., Qian, Z., Ryder, T., *et al.* (2006). Genomic and transcriptional aberrations linked to breast cancer pathophysiologies. *Cancer Cell* 10, 529-541.

Cho, H., Zhao, X., Hatori, M., Yu, R.T., Barish, G.D., Lam, M.T., Chong, L.W., DiTacchio, L., Atkins, A.R., Glass, C.K., *et al.* (2012). Regulation of circadian behaviour and metabolism by REV-ERB-alpha and REV-ERB-beta. *Nature* 485, 123-127.

Davis, L.M., Harris, C., Tang, L., Doherty, P., Hraber, P., Sakai, Y., Bocklage, T., Doeden, K., Hall, B., Alsobrook, J., *et al.* (2007). Amplification patterns of three

genomic regions predict distant recurrence in breast carcinoma. *J Mol Diagn* 9, 327-336.

De Bruijn, K.M., Arends, L.R., Hansen, B.E., Leeflang, S., Ruiter, R., and van Eijck, C.H. (2013). Systematic review and meta-analysis of the association between diabetes mellitus and incidence and mortality in breast and colorectal cancer. *Br J Surg* 100, 1421-1429.

Delezie, J., and Challet, E. (2011). Interactions between metabolism and circadian clocks: reciprocal disturbances. *Ann N Y Acad Sci* 1243, 30-46.

Du, J., and Xu, R. (2012). RORalpha, a potential tumor suppressor and therapeutic target of breast cancer. *Int J Mol Sci* 13, 15755-15766.

Duez, H., and Staels, B. (2009). Rev-erb-alpha: an integrator of circadian rhythms and metabolism. *J Appl Physiol* (1985) 107, 1972-1980.

Dzhagalov, I., Giguere, V., He, Y.W. (2004). Lymphocyte development and function in the absence of retinoic acid-related orphan receptor alpha. *J Immunol* 173, 2952–2959.

Fedirko, V., Tramacere, I., Bagnardi, V., Rota, M., Scotti, L., Islami, F., Negri, E., Straif, K., Romieu, I., La Vecchia, C., *et al.* (2011). Alcohol drinking and colorectal cancer risk: an overall and dose-response meta-analysis of published studies. *Ann Oncol* 22, 1958-1972.

Ferlay, J., Shin, H.R., Bray, F., Forman, D., Mathers, C., and Parkin, D.M. (2010). Estimates of worldwide burden of cancer in 2008: GLOBOCAN 2008. *Int J Cancer* 127, 2893-2917.

Filipski, E., and Levi, F. (2009). Circadian disruption in experimental cancer processes. *Integr Cancer Ther* 8, 298-302.

Filipski, E., Subramanian, P., Carriere, J., Guettier, C., Barbason, H., and Levi, F. (2009). Circadian disruption accelerates liver carcinogenesis in mice. *Mutat Res* 680, 95-105.

Forman, B.M., Chen, J., Blumberg, B., Kliewer, S.A., Henshaw, R., Ong, E.S., and Evans, R.M. (1994). Cross-talk among ROR alpha 1 and the Rev-erb family of orphan nuclear receptors. *Mol Endocrinol* 8, 1253-1261.

Geyfman, M., Kumar, V., Liu, Q., Ruiz, R., Gordon, W., Espitia, F., Cam, E., Millar, S.E., Smyth, P., Ihler, A., *et al.* (2012). Brain and muscle Arnt-like protein-1 (BMAL1) controls circadian cell proliferation and susceptibility to UVB-induced DNA damage in the epidermis. *Proc Natl Acad Sci U S A* 109, 11758-11763.

Giguere, V., Beatty, B., Squire, J., Copeland, N.G., and Jenkins, N.A. (1995). The orphan nuclear receptor ROR alpha (RORA) maps to a conserved region of homology on human chromosome 15q21-q22 and mouse chromosome 9. *Genomics* 28, 596-598.

Guillaumond, F., Dardente, H., Giguere, V., and Cermakian, N. (2005). Differential control of BMAL1 circadian transcription by REV-ERB and ROR nuclear receptors. *J Biol Rhythms* 20, 391-403.

Gupta, N., and Ragsdale, S.W. (2011). Thiol-disulfide redox dependence of heme binding and heme ligand switching in nuclear hormone receptor rev-erb{beta}. *J Biol Chem* 286, 4392-4403.

He, Y.W., Deftos, M.L., Ojala, E.W., and Bevan, M.J. (1998). RORgamma t, a novel isoform of an orphan receptor, negatively regulates Fas ligand expression and IL-2 production in T cells. *Immunity* 9, 797-806.

Hicklin, D.J., and Ellis, L.M. (2005). Role of the vascular endothelial growth factor pathway in tumor growth and angiogenesis. *J Clin Oncol* 23, 1011-1027.

Hurwitz, H., Fehrenbacher, L., Novotny, W., Cartwright, T., Hainsworth, J., Heim, W., Berlin, J., Baron, A., Griffing, S., Holmgren, E., *et al.* (2004). Bevacizumab plus irinotecan, fluorouracil, and leucovorin for metastatic colorectal cancer. *N Engl J Med* 350, 2335-2342.

Hurwitz, H., and Kabbinavar, F. (2005). Bevacizumab combined with standard fluoropyrimidine-based chemotherapy regimens to treat colorectal cancer. *Oncology* 69 Suppl 3, 17-24.

Ikeda, M., and Nomura, M. (1997). cDNA cloning and tissue-specific expression of a novel basic helix-loop-helix/PAS protein (BMAL1) and identification of alternatively spliced variants with alternative translation initiation site usage. *Biochem Biophys Res Commun* 233, 258-264.

Jasperson K.W., Tuohy T.M., Neklason D.W., Burt R.W. (2010). Hereditary and familial colon cancer. *Gastroenterology* 138, 2044-2058.

Jensen, L.D., and Cao, Y. (2013). Clock controls angiogenesis. *Cell Cycle* 12, 405-408.

Jensen, L.D., Cao, Z., Nakamura, M., Yang, Y., Brautigam, L., Andersson, P., Zhang, Y., Wahlberg, E., Lanne, T., Hosaka, K., *et al.* (2012). Opposing effects of circadian clock genes BMAL1 and period2 in regulation of VEGF-dependent angiogenesis in developing zebrafish. *Cell Rep* 2, 231-241.

Jess, T., Rungoe, C., and Peyrin-Biroulet, L. (2012). Risk of colorectal cancer in patients with ulcerative colitis: a meta-analysis of population-based cohort studies. *Clin Gastroenterol Hepatol* 10, 639-645.

Jetten, A.M. (2004). Recent advances in the mechanisms of action and physiological functions of the retinoid-related orphan receptors (RORs). *Curr Drug Targets Inflamm Allergy* 3, 395-412.

Jetten, A.M. (2009). Retinoid-related orphan receptors (RORs): critical roles in development, immunity, circadian rhythm, and cellular metabolism. *Nucl Recept Signal* 7, e003.

Jetten, A.M., and Joo, J.H. (2006). Retinoid-related Orphan Receptors (RORs): Roles in Cellular Differentiation and Development. *Adv Dev Biol* 16, 313-355.

Jetten, A.M., Kang, H.S., and Takeda, Y. (2013). Retinoic acid-related orphan receptors alpha and gamma: key regulators of lipid/glucose metabolism, inflammation, and insulin sensitivity. *Front Endocrinol (Lausanne)* 4, 1.

Jetten, A.M., Kurebayashi, S., and Ueda, E. (2001). The ROR nuclear orphan receptor subfamily: critical regulators of multiple biological processes. *Prog Nucleic Acid Res Mol Biol* 69, 205-247.

Jung, C.H., Kim, E.M., Park, J.K., Hwang, S.G., Moon, S.K., Kim, W.J., and Um, H.D. (2013). BMAL1 suppresses cancer cell invasion by blocking the phosphoinositide 3-kinase-Akt-MMP-2 signaling pathway. *Oncol Rep* 29, 2109-2113.

Kabbinavar, F., Hurwitz, H.I., Fehrenbacher, L., Meropol, N.J., Novotny, W.F., Lieberman, G., Griffing, S., and Bergsland, E. (2003). Phase II, randomized trial comparing bevacizumab plus fluorouracil (FU)/leucovorin (LV) with FU/LV alone in patients with metastatic colorectal cancer. *J Clin Oncol* 21, 60-65.

Khapre, R.V., Kondratova, A.A., Susova, O., and Kondratov, R.V. (2011). Circadian clock protein BMAL1 regulates cellular senescence in vivo. *Cell Cycle* 10, 4162-4169.

Kojetin, D.J., and Burris, T.P. (2014). REV-ERB and ROR nuclear receptors as drug targets. *Nat Rev Drug Discov* 13, 197-216.

Kourtidis, A., Jain, R., Carkner, R.D., Eifert, C., Brosnan, M.J., and Conklin, D.S. (2010). An RNA interference screen identifies metabolic regulators NR1D1 and PBP

as novel survival factors for breast cancer cells with the ERBB2 signature. *Cancer Res* 70, 1783-1792.

Kuipers, E.J., Grady, W.M., Lieberman, D., Seufferlein, T., Sung, J.J., Boelens, P.G., van de Velde, C.J., and Watanabe, T. (2015). Colorectal cancer. *Nat Rev Dis Primers* 1, 15065.

Lau, P., Nixon, S.J., Parton, R.G., and Muscat, G.E. (2004). RORalpha regulates the expression of genes involved in lipid homeostasis in skeletal muscle cells: caveolin-3 and CPT-1 are direct targets of ROR. *J Biol Chem* 279, 36828-36840.

Lazar, M.A., Hodin, R.A., Darling, D.S., and Chin, W.W. (1989). A novel member of the thyroid/steroid hormone receptor family is encoded by the opposite strand of the rat c-erbA alpha transcriptional unit. *Mol Cell Biol* 9, 1128-1136.

Lazar, M.A., Jones, K.E., and Chin, W.W. (1990). Isolation of a cDNA encoding human Rev-ErbA alpha: transcription from the noncoding DNA strand of a thyroid hormone receptor gene results in a related protein that does not bind thyroid hormone. *DNA Cell Biol* 9, 77-83.

Lee, J.C., Chow, N.H., Wang, S.T., and Huang, S.M. (2000). Prognostic value of vascular endothelial growth factor expression in colorectal cancer patients. *Eur J Cancer* 36, 748-753.

Lee, J.M., Kim, I.S., Kim, H., Lee, J.S., Kim, K., Yim, H.Y., Jeong, J., Kim, J.H., Kim, J.Y., Lee, H., *et al.* (2010). RORalpha attenuates Wnt/beta-catenin signaling by PKCalpha-dependent phosphorylation in colon cancer. *Mol Cell* 37, 183-195.

Lee, W.H., Murphree, A.L., and Benedict, W.F. (1984). Expression and amplification of the N-myc gene in primary retinoblastoma. *Nature* 309, 458-460.

Liang, P.S., Chen, T.Y., and Giovannucci, E. (2009). Cigarette smoking and colorectal

cancer incidence and mortality: systematic review and meta-analysis. *Int J Cancer* 124, 2406-2415.

Liang, W.C., Wu, X., Peale, F.V., Lee, C.V., Meng, Y.G., Gutierrez, J., Fu, L., Malik, A.K., Gerber, H.P., Ferrara, N., Fuh, G. (2006). Cross-species vascular endothelial growth factor (VEGF)-blocking antibodies completely inhibit the growth of human tumor xenografts and measure the contribution of stromal VEGF. *J Biol Chem* 281, 951-961.

Loupakis, F., Cremolini, C., Masi, G., Lonardi, S., Zagonel, V., Salvatore, L., Cortesi, E., Tomasello, G., Ronzoni, M., Spadi, R., *et al.* (2014). Initial therapy with FOLFOXIRI and bevacizumab for metastatic colorectal cancer. *N Engl J Med* 371, 1609-1618.

Lowrey, P.L., and Takahashi, J.S. (2004). Mammalian circadian biology: elucidating genome-wide levels of temporal organization. *Annu Rev Genomics Hum Genet* 5, 407-441.

Lowrey, P.L., and Takahashi, J.S. (2011). Genetics of circadian rhythms in Mammalian model organisms. *Adv Genet* 74, 175-230.

Luo, W., Cao, Y., Liao, C., and Gao, F. (2012). Diabetes mellitus and the incidence and mortality of colorectal cancer: a meta-analysis of 24 cohort studies. *Colorectal Dis* 14, 1307-1312.

Ma, Y., Yang, Y., Wang, F., Zhang, P., Shi, C., Zou, Y., and Qin, H. (2013). Obesity and risk of colorectal cancer: a systematic review of prospective studies. *PLoS One* 8, e53916.

Marvin, K.A., Reinking, J.L., Lee, A.J., Pardee, K., Krause, H.M., and Burstyn, J.N. (2009). Nuclear receptors homo sapiens Rev-erbbeta and *Drosophila melanogaster* E75 are thiolate-ligated heme proteins which undergo redox-mediated ligand

switching and bind CO and NO. *Biochemistry* 48, 7056-7071.

Miller, K.D., Siegel, R.L., Lin, C.C., Mariotto, A.B., Kramer, J.L., Rowland, J.H., Stein, K.D., Alteri, R., and Jemal, A. (2016). Cancer treatment and survivorship statistics, 2016. *CA Cancer J Clin* 66, 271-289.

Miyajima, N., Horiuchi, R., Shibuya, Y., Fukushige, S., Matsubara, K., Toyoshima, K., and Yamamoto, T. (1989). Two erbA homologs encoding proteins with different T3 binding capacities are transcribed from opposite DNA strands of the same genetic locus. *Cell* 57, 31-39.

Miyajima, N., Kadowaki, Y., Fukushige, S., Shimizu, S., Semba, K., Yamanashi, Y., Matsubara, K., Toyoshima, K., and Yamamoto, T. (1988). Identification of two novel members of erbA superfamily by molecular cloning: the gene products of the two are highly related to each other. *Nucleic Acids Res* 16, 11057-11074.

Mortality, G.B.D., and Causes of Death, C. (2015). Global, regional, and national age-sex specific all-cause and cause-specific mortality for 240 causes of death, 1990-2013: a systematic analysis for the Global Burden of Disease Study 2013. *Lancet* 385, 117-171.

Mullenders, J., Fabius, A.W., Madiredjo, M., Bernards, R., and Beijersbergen, R.L. (2009). A large scale shRNA barcode screen identifies the circadian clock component ARNTL as putative regulator of the p53 tumor suppressor pathway. *PLoS One* 4, e4798.

Pardee, K.I., Xu, X., Reinking, J., Schuetz, A., Dong, A., Liu, S., Zhang, R., Tiefenbach, J., Lajoie, G., Plotnikov, A.N., *et al.* (2009). The structural basis of gas-responsive transcription by the human nuclear hormone receptor REV-ERBbeta. *PLoS Biol* 7, e43.

Ranieri, G., Patruno, R., Ruggieri, E., Montemurro, S., Valerio, P., and Ribatti, D.

(2006). Vascular endothelial growth factor (VEGF) as a target of bevacizumab in cancer: from the biology to the clinic. *Curr Med Chem* 13, 1845-1857.

Reddy, P., Zehring, W.A., Wheeler, D.A., Pirrotta, V., Hadfield, C., Hall, J.C., and Rosbash, M. (1984). Molecular analysis of the period locus in *Drosophila melanogaster* and identification of a transcript involved in biological rhythms. *Cell* 38, 701-710.

Reppert, S.M., and Weaver, D.R. (2002). Coordination of circadian timing in mammals. *Nature* 418, 935-941.

Risau, W. (1997). Mechanisms of angiogenesis. *Nature* 386, 671-674.

Sahar, S., and Sassone-Corsi, P. (2007). Circadian clock and breast cancer: a molecular link. *Cell Cycle* 6, 1329-1331.

Sahar, S., and Sassone-Corsi, P. (2009). Metabolism and cancer: the circadian clock connection. *Nat Rev Cancer* 9, 886-896.

Saltz, L.B., Clarke, S., Diaz-Rubio, E., Scheithauer, W., Figer, A., Wong, R., Koski, S., Lichinitser, M., Yang, T.S., Rivera, F., *et al.* (2008). Bevacizumab in combination with oxaliplatin-based chemotherapy as first-line therapy in metastatic colorectal cancer: a randomized phase III study. *J Clin Oncol* 26, 2013-2019.

Sato, T.K., Panda, S., Miraglia, L.J., Reyes, T.M., Rudic, R.D., McNamara, P., Naik, K.A., FitzGerald, G.A., Kay, S.A., Hogenesch, J.B. (2004). A functional genomics strategy reveals *Rora* as a component of the mammalian circadian clock. *Neuron* 43, 527-537.

Schrader, M., Danielsson, C., Wiesenberg, I., and Carlberg, C. (1996). Identification of natural monomeric response elements of the nuclear receptor RZR/ROR. They also bind COUP-TF homodimers. *J Biol Chem* 271, 19732-19736.

Shin, D., Kim, I.S., Lee, J.M., Shin, S.Y., Lee, J.H., Baek, S.H., and Cho, K.H. (2014). The hidden switches underlying RORalpha-mediated circuits that critically regulate uncontrolled cell proliferation. *J Mol Cell Biol* 6, 338-348.

Siegel, R.L., Miller, K.D., and Jemal, A. (2018). Cancer statistics, 2018. *CA Cancer J Clin* 68, 7-30.

Smith, A.G., and Muscat, G.E. (2006). Orphan nuclear receptors: therapeutic opportunities in skeletal muscle. *Am J Physiol Cell Physiol* 291, C203-217.

Sun, Y., Yang, Z., Niu, Z., Peng, J., Li, Q., Xiong, W., Langnas, A.N., Ma, M.Y., and Zhao, Y. (2006). MOP3, a component of the molecular clock, regulates the development of B cells. *Immunology* 119, 451-460.

Takahashi, Y., Kitadai, Y., Bucana, C.D., Cleary, K.R., and Ellis, L.M. (1995). Expression of vascular endothelial growth factor and its receptor, KDR, correlates with vascularity, metastasis, and proliferation of human colon cancer. *Cancer Res* 55, 3964-3968.

Taniguchi, H., Fernandez, A.F., Setien, F., Ropero, S., Ballestar, E., Villanueva, A., Yamamoto, H., Imai, K., Shinomura, Y., and Esteller, M. (2009). Epigenetic inactivation of the circadian clock gene BMAL1 in hematologic malignancies. *Cancer Res* 69, 8447-8454.

Taylor, D.P., Burt, R.W., Williams, M.S., Haug, P.J., and Cannon-Albright, L.A. (2010). Population-based family history-specific risks for colorectal cancer: a constellation approach. *Gastroenterology* 138, 877-885.

Torre, L.A., Bray, F., Siegel, R.L., Ferlay, J., Lortet-Tieulent, J., and Jemal, A. (2015). Global cancer statistics, 2012. *CA Cancer J Clin* 65, 87-108.

Triqueneaux, G., Thenot, S., Kakizawa, T., Antoch, M.P., Safi, R., Takahashi, J.S.,

Delaunay, F., and Laudet, V. (2004). The orphan receptor Rev-erbalpha gene is a target of the circadian clock pacemaker. *J Mol Endocrinol* 33, 585-608.

Xiao, L., Wang, J., Li, J., Chen, X., Xu, P., Sun, S., He, D., Cong, Y., and Zhai, Y. (2015). RORalpha inhibits adipocyte-conditioned medium-induced colorectal cancer cell proliferation and migration and chick embryo chorioallantoic membrane angiogenesis. *Am J Physiol Cell Physiol* 308, C385-396.

Yang, G., Wright, C.J., Hinson, M.D., Fernando, A.P., Sengupta, S., Biswas, C., La, P., and Dennery, P.A. (2014). Oxidative stress and inflammation modulate Rev-erbalpha signaling in the neonatal lung and affect circadian rhythmicity. *Antioxid Redox Signal* 21, 17-32.

Yang, X., Downes, M., Yu, R.T., Bookout, A.L., He, W., Straume, M., Mangelsdorf, D.J., and Evans, R.M. (2006). Nuclear receptor expression links the circadian clock to metabolism. *Cell* 126, 801-810.

Yin, L., Wu, N., and Lazar, M.A. (2010). Nuclear receptor Rev-erbalpha: a heme receptor that coordinates circadian rhythm and metabolism. *Nucl Recept Signal* 8, e001.

Zeng, Z.L., Luo, H.Y., Yang, J., Wu, W.J., Chen, D.L., Huang, P., and Xu, R.H. (2014). Overexpression of the circadian clock gene BMAL1 increases sensitivity to oxaliplatin in colorectal cancer. *Clin Cancer Res* 20, 1042-1052.

Zeng, Z.L., Wu, M.W., Sun, J., Sun, Y.L., Cai, Y.C., Huang, Y.J., and Xian, L.J. (2010). Effects of the biological clock gene BMAL1 on tumour growth and anti-cancer drug activity. *J Biochem* 148, 319-326.

8 Curriculum Vitae

Personal Information

Name: Wen Wu

Place of Birth: Anhui, China

Date of Birth: 21,02,1988

Gender: Male

Nationality: China

Address: RongKeCheng 5-1806, Jingkai District, Hefei, 230000, P.R.China

Mobile: +86 157 5514 0125

Email: wuwen_ahmu@163.com

Education and Work Experience

Jul.2018 - present

Resident doctor of General Surgery Department

The First Affiliated Hospital of USTC, Division of Life Science and Medicine, University
of Science and Technology of China

China

Oct.2014 – present

PhD student of Dr. sc. hum. Program

Medical faculty Mannheim of University Heidelberg

Germany

Sep.2013 – Aug.2014

Master of Translational Medical Research

Medical faculty Mannheim of University Heidelberg

Germany

Sep.2006 - Jul.2013

Bachelor and Master Program of Clinical Medicine

Anhui Medical University
China

Published Paper

Elke Burgermeister, Francesca Battaglin, Fagr Eladly, **Wen Wu**, Frank Herweck, Nadine Schulte, Johannes Betge, Nicolai Härtel, Jakob N Kather, Cleo-Aron Weis, Timo Gaiser, Alexander Marx, Christel Weiss, Ralf Hofheinz, Ian S Miller, Fotios Loupakis, Heinz-Josef Lenz, Annette T Byrne, Matthias P Ebert. Aryl hydrocarbon receptor nuclear translocator-like (ARNTL/BMAL1) is associated with bevacizumab resistance in colorectal cancer via regulation of vascular endothelial growth factor A. *EBioMedicine*. 2019, 45:139-154.

Elke Burgermeister, Patrick Höde, Johannes Betge, Tobias Gutting, Andreas Merkel, **Wen Wu**, Marc Tänzer, Maximilian Mossner, Daniel Nowak, Julia Magdeburg, Felix Rückert, Carsten Sticht, Katja Breitkopf-Heinlein, Nadine Schulte, Nicolai Härtel, Sebastian Belle, Stefan Post, Timo Gaiser, Barbara Ingold Heppner, Hans-Michael Behrens, Christoph Röcken, and Matthias P.A. Ebert. Epigenetic silencing of tumor suppressor candidate 3 confers adverse prognosis in early colorectal cancer. *Oncotarget*. 2017, 8: 84714–84728.

Jiong Chen, **Wen Wu** (co-first author), Longjiang Chen, Hangcheng Zhou, Renbao Yang, Liwei Hu, Yue Zhao. Profiling the potential tumor markers of pancreatic ductal adenocarcinoma using 2D-DIGE and MALDI-TOF-MS: up-regulation of Complement C3 and alpha-2-HS-glycoprotein. *Pancreatology*. 2013, 13:290-297.

9 Acknowledgements

I would like to express my gratitude to all those who helped me during the writing of this thesis.

I want to thank Prof. Dr. Matthias Ebert, the Director of the Dept. of Internal Medicine II, for giving me the opportunity to perform the thesis in his laboratories, scientific discussion and the support for research reagents.

I would like to extend my sincere gratitude to my scientific supervisor, PD Dr. Elke Burgermeister, for her instructive advice regarding the conceptual and experimental design of the thesis research topic and useful suggestions and corrections on my thesis. I am deeply grateful of her scientific discussion, support and advice in the completion of this thesis.

I am also deeply indebted to my colleagues, Frank Herweck, Michaela Söhn, Isabel Hinsenkamp, Patrick Höde, who are warm-hearted and helpful with regard to to my thesis and life. They always supported my work patiently and nicely.

Especially, I am deeply grateful to the Translational Medical Research group, Prof. Sleeman and Ms. Kaeppele, whose professional arrangements and helps enabled me to solve the challenges and tasks I encountered in the study and life.

At last, I extremely appreciate everything my family has done for me. Without their supports, I could not get better and go further. I love them forever.